Acoustic attenuation by air bubbles in bad weather conditions; a comparison of hull- and keel-mounted transducers

Fannie Welcome Shabangu

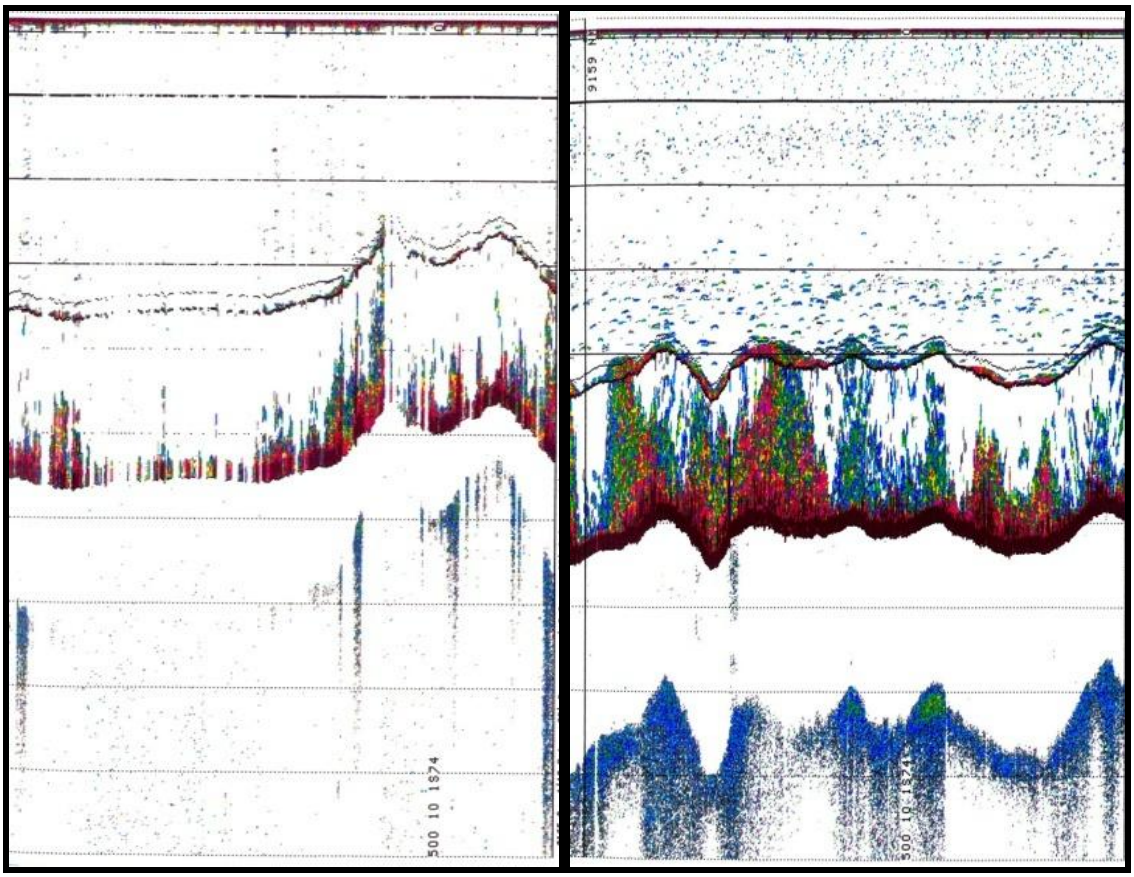

Master in Fisheries Biology and Management

Department of Biology
Faculty of Mathematics and Natural Sciences
University of Bergen, Norway
August 2009

Acoustic attenuation by air bubbles in bad weather conditions; a comparison of hull- and keel-mounted transducers

by

Fannie Welcome Shabangu

A thesis submitted in partial fulfilment of the requirements for the degree of

Master in Fisheries Biology and Management

Department of Biology

Faculty of Mathematics and Natural Sciences

University of Bergen, Norway

August 2009

ABSTRACT

Echo integration in bad weather conditions is problematic due to vessel- and wind-induced air bubble layer that is formed below the hull of a vessel, where acoustic transducers are mounted. The bubbles below the hull attenuate both the transmitted and received acoustic waves and may lead to an underestimation of the real fish abundance or density. A detailed understanding of the acoustic energy attenuation by the air bubble layer is crucial for establishing a correction factor for the recorded echo integrator measurements. The acoustic attenuation by the air bubble layer under different weather conditions were estimated by observing the ratio of the nautical area backscattering strength of the sea bed between two inter-calibrated Simrad EK60 38 kHz hull- and keel-mounted transducers. By integrating the sea bed as a reference target over distance in various weather conditions, the amount of acoustic signal attenuated by the air bubbles was estimated. A correction factor for the hull mounted system was further established from the data.

The consistency of the bottom backscattered ratio was investigated in various wind speeds, and the best consistency of the ratio was found in periods with calm wind speeds (0-10 m/s). The results indicated that the estimated ratio strongly increased with wind speeds (Beaufort force) but at a lower magnitude than earlier reported and expected at 38 kHz. This indicates that the necessary corrections are less than earlier reported at similar wind speeds. This is however vessel specific, and may be effected by the transducer mounting position and by the shape of the vessel hull. There was a significant difference between the echo integrator values of the hull- and keel-mounted transducers, with the keel-mounted transducer performing better in all various weather conditions. In very bad weather, however, the data indicated that also the keel mounded transducer experienced air bubble attenuation as well. A strong correlation between the bottom backscattering strength responses of the two-transducer mounting systems was found, while a rather low correlation between the vessel pitch/roll and bottom backscattering strength was found. In conclusion, a new and modern technique of estimating a correction factor for air bubble acoustic attenuation was tested and verified. Since the investigations were made as a secondary or third priority objective during the surveys, a better material can be collected if special surveys are conducted for air bubble estimation. Especially when using this method with the vessel running in several directions into the wind should then be considered.

ACKNOWLEDGEMENTS

Firstly, I would like to thank my supervisor Professor Egil Ona for granting me the opportunity to work with him as a master student. I am so grateful for his passionate and patient introduction to this interesting field of acoustics. He has always believed in me and encouraged me to become a better strategic researcher. His invaluable and astonishing guidance and propositions throughout the writing of this thesis are highly appreciated. I learned a lot from him.

My deepest gratitude goes to Hans Erstad, the coordinator of the Norway-South African cooperation at IMR, Bergen, for his great constant availability in solving my problems. He is thanked for his devoted and effortful means in arranging my finances and all materials needed while studying. My stay in Norway as student would not have been so admirable without your help.

All credits go to Atle Totland for designing the multiplexer used in this study and for his detailed description on how this equipment operated. The software he designed also made it possible to extract the necessary information from my data sets.

Dr. Lucio Calise is thanked for reading through my script and giving many valuable comments. His explanations of the technical terms in acoustics helped a lot during the writing of this thesis. I would also like to thank him for letting me read through with his PhD thesis and referring me to relevant literature.

Dr. Hector Peña is thanked for providing the useful and relevant literature related to my thesis problem. It was through his suggestions and discussions during the data post-processing that made it achievable to finish the data scrutiny. His advice and comments on the thesis problem are highly valued.

The data merging in R would have not been doable without the help of Dr. Espen Johnsen. I am thankful for him in devoting his time to help me find relevant commands to merge my data sets together.

Reidun Heggø Sørensen is highly thanked for the help with everyday facilities and for kind help in getting this thesis organized and ready on time.

Dr. Rolf Korneliussen and Dr. John Dalen are thanked for their contributed helpful discussions and suggestions during the writing of this thesis.

The Department of Biology at the University of Bergen and the Institute of Marine Research (IMR) are thanked for sponsoring my field trips.

My friend and former classmate Shale Rosen is thanked for reviewing the English grammar in this thesis and giving wonderful ideas and suggestions. And I also thank all my other friends for being friends with me.

Finally, I would like to give special thanks and adoration to my family; my mom and dad, brothers and sisters are thanked for their constant encouragement and support throughout my studies. It would have not been possible without you; hence I say I am who I am because of you. I am grateful to the almighty God for my family and everything he has blessed me with.

I dedicate this thesis to my family.

CONTENTS

1. INTRODUCTION

Fisheries acoustic techniques are adequate and dependable compared to the traditional trawl surveys, providing important biological information about fish spatial distribution, density and biomass, and behaviour. Acoustic fish abundance estimates are by comparison the easiest and fastest method for pelagic fish abundance estimation (Simmonds and MacLennan, 2005). However, there are some uncertainties associated with the technique in bad weather conditions and other unfavourable conditions. In fisheries acoustics, the echo intensity of a certain amount of underwater targets is usually assumed to be proportional to the density of the targets with the same acoustic characteristics (Dalen and Løvik, 1981; Foote, 1983; Simmonds and MacLennan, 2005). The above principle is called the linearity principle, and it is the basis of echo integration method (MacLennan, 1990; Simmonds and MacLennan, 2005). Acoustic methods estimate fish density or biomass by summing the acceptable returning fish echoes, and this process is therefore called echo integration (Dragesund and Olsen, 1965; Simmonds and MacLennan, 2005).

The echo integration procedure requires detailed background knowledge of the backscattering cross-section of the expected target (Foote, 1983; Simmonds and MacLennan, 2005). Echo integration in bad weather is one of the most challenging processes encountered during acoustic fish abundance estimation (Dalen and Løvik, 1981; Ona, 1991; Berg *et al*., 1983; Aglen, 1994). In bad weather conditions, an air bubble layer may be formed in the sea surface and extend below the hull of the vessel where transducers are typically mounted (Knudsen, 2006). This layer of bubbles attenuates both the transmitted and received acoustic signals (Ona and Mamylov, 1988; Simmonds and MacLennan, 2005). By estimating the air bubble acoustic attenuation, the level of the lost signals can be compensated during the post-processing stage. At a certain stage, the weather conditions may be such that more or less the entire signal is blocked by air bubbles. The stop conditions for a survey are generally set long before this condition occurs (Ona and Mamylov, 1988; Parker-Stetter *et al.*, 2009).

Air bubble acoustic attenuation associated error leads mostly to an underestimation of the fish density if not corrected for (Aglen 1989; ICES, 2007). Aglen (1989) estimated the probabilities for the underestimation to be around 90 % and 50 % for the overestimation. Due to air bubbles or due to all other errors it is of great importance that the fish abundance estimates are made to be as precise as possible; reducing the systematic errors to a possibly

low or negligible level. Systematic errors are generally considered difficult to correct; their estimation usually requires careful data scrutinizing.

Historically, there have been several attempts to solve the problem of air bubble attenuation in bad weather conditions; such as suspension of acoustic surveys above 30 % bubble attenuation correction (Ona and Mamylov, 1988), using towed bodies (Dalen and Løvik, 1981; Kloser, 1996; Dalen *et al.*, 2003), implementing bubble attenuation estimator (Dalen and Løvik, 1981; Berg *et al*., 1983) and lastly using drop keels (Ona and Traynor, 1990). However, only the drop keel was found to be an efficient technique in resolving the bad weather problem without drastically reducing the average vessel survey speed (Ona and Traynor, 1990), especially during combined trawl-acoustic surveys. The drop keel can be protruded down below the bubble layer and to some extend eliminate the air bubble attenuation (Ona and Traynor, 1990; Simmonds and MacLennan, 2005; ICES, 2007).

Most recently, there has been a shift by research institutions from using purpose-built research vessels equipped with the hull- and keel-mounted transducers to the use of the commercial fishing vessels (FVs) for fish abundance estimation (ICES, 2007). These commercial vessels are most often without drop keels or towed bodies to deploy in bad weather conditions (Ona, 1991; ICES, 2007), but only equipped with transducers directly to the vessels' hulls. The hull-mounted systems are generally most efficient when acoustic surveys are conducted simultaneously with other research investigations (Aglen, 1989; Ona, 1991), which is usually the case with fishing vessels (Godø, 2004; ICES, 2007). The use of fishing vessels for acoustic data collection has led to the reoccurrence of the air bubble acoustic attenuation problem once considered more or less resolved (ICES, 2007; E. Ona, IMR, pers. comm.), and direct comparison of vessels with and without drop keel has shown large differences (Peña, 2009).

A systematic stock underestimation indisputably comes with detrimental economic consequences to the fishing industry (Hillborn, 2007), and may also be misleading to the scientific community and the management by giving an impression that a particular fish stock may be under severe fishing pressure while it may not be (Francis and Shotton, 1997). Most fishing vessels noise levels are also not in accordance with the ICES 209 recommendations, since they produce noise levels that are well within the hearing range of fish (ICES, 2007), and may thus resulting in another problem of fish vessel avoidance (Fréon *et al*., 1993; Mitson, 1995; Mitson and Knutsen, 2003; Jørgensen *et al*., 2004; ICES, 2008). Moreover,

factors like echosounder calibration; vessel heave compensation, etc. are usually of less importance in fishing vessels while these are very crucial and determining factors in research vessels (RVs) (Simmonds and MacLennan, 2005). These platform limitations will in many instances lead to a compromise between collections of qualitative or quantitative data (ICES, 2007).

There are several valuable reasons why research institutions use fishing vessels for the collection of acoustic data (Hampton and Soule, 2003; Godø, 2004 and ICES, 2007):

- To obtain information for single-species stock assessment;
- To obtain information for ecosystem approach to fisheries management;
- Low research costs and more vessel time at sea;
- Fish stock migration and distribution over time;
- Acoustic data can be acquired without disrupting commercial trawling;
- Acoustic data can be collected without scientific personnel onboard.

Nowadays, fisheries scientists and the International Council for Exploration of the Sea (ICES) are devoting some effort to work closer together with fishing vessel owners in designing and constructing vessels that can be more suitable for both uses as fishing and research platforms (Godø, 2004). Not so long ago the Institute of Marine Research (IMR) in Norway cooperated with the vessel owner in the construction of a purse-seiner/trawler FV "Libas" (94 m, 8000 HP). This was the first fishing vessel to be built as a scientific vessel (Godø, 2004); it is equipped with most required scientific equipments such as a drop keel, multi-frequency acoustic instrumentations, laboratories and hydrological data collection equipments.

While many studies have shown that a transducer mounted on a drop keel performs better compared to a hull-mounted transducer in bad weather conditions (Ona and Traynor, 1990; Simmonds and MacLennan, 2005; Knudsen, 2006a; ICES, 2007). However, there has never been any correction factor established for air bubble attenuation by the direct comparisons of the hull- and keel-mounted systems. In the past, air bubbles induced acoustic attenuations were compensated by adding a certain value to the echo during echo integration based on the personal experience of operator (Dalen and Løvik, 1981). Also, an "air correction" algorithm was implemented in some post-processing systems for echo sounder data like the Bergen

Echo Integrator (Foote *et al.*, 1991) or in the newer Large Scale Survey System (LSSS) (Korneliussen *et al.*, 2006).

Apparently, this method was not ideal since it was operator dependent, and greatly depended upon the experience of the operator. Since the correction factor was also vessel dependent, it is therefore considered unsatisfactory and inefficient. Establishment of an appropriate correction factor for different weather conditions is therefore needed for the compensation of the signals lost due to air bubble attenuation in bad weather conditions. A well-designed experiment can also be used to demonstrate the effective gain in using a keel-mounted system as compared to the traditional transducer mountings.

Air bubble acoustic signal attenuation

Kinsler *et al*. (1982) define attenuation as "the lost of acoustic energy from a sound beam". They further categorized the acoustic attenuation into two folds: the first as the conversion of acoustic energy into thermal energy and, the second as the deflection or scattering of acoustic energy out of the beam. Air bubbles in the water column cause a considerable amount of acoustic attenuation either by viscous forces and/or heat conduction losses. The compression of air bubbles by the passing sound waves results in the energy attenuation of the sound waves. Scattering in all directions by the entrapped bubbles also results in the reduction of the acoustic energy in directed sonar beams.

Severe amounts of air bubbles in the water column, which can often happen when the vessel bow is pounding its way through the sea waves, also alter the density and compressibility of the medium through which sound is propagating; thus in turn leads to a reduction of the speed of sound. The air bubble induces change in density and compressibility of the medium results in enormous reflection and refraction of acoustic energy away from the main transmission source. Consequently, a beam of sound waves can be attenuated by reflection, refraction, absorption, and scattering as it propagates through the seawater containing a high concentration of air bubbles (Kinsler *et al*., 1982). Wind-induced bubbles are mainly produced by the breaking sea waves (Urick, 1983), and these occur right below the sea surface.

However, Knudsen (2006a) claimed that wind-induced bubbles are not the main actual attenuator of the fisheries acoustic signal but rather bubbles that are generated by the vessel

itself as it bounces up and down on the sea surface in stormy weather conditions. The air bubble acoustic attenuation problem mainly occurs when hull-mounted transducers are used (Dalen and Løvik, 1981; Ona, 1991). The bubbles below the vessel hull attenuate both transmitted and received signals (Figure 1) by the conversion of the sound energy into heat energy (Urick, 1983), this process is known as "thermal damping" (Dalen and Løvik, 1981). Figure 1 is a simplified exemplification of the attenuation process but not a realistic indication of the magnitude of signal attenuation.

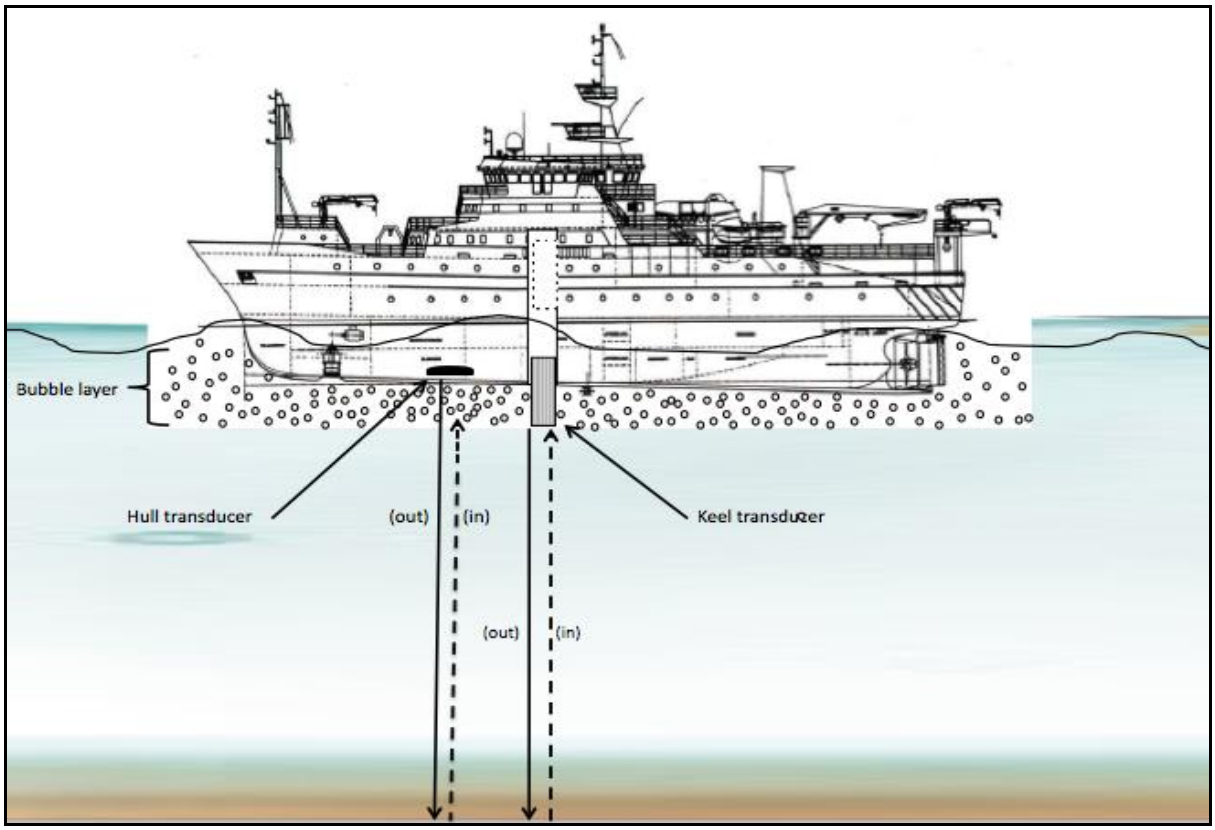

Figure 1. Schematic illustration of acoustic signal interference by air bubbles in bad weather conditions. Solid line refers to the transmitted signal (out) and the dashed lines refer to the returning signal (in) - indicating the reduced echo intensities.

In solving the air bubble acoustic attenuation problem, Berg *et al.* (1983) proposed that numerical "bubble attenuation estimator" software should be installed on research vessels to improve the bad weather acoustic performance of the hull-mounted transducers. The numerical attenuation estimator was empirically obtained by measuring the bubble density and bubble size distribution in relation to the resulting attenuation. Their method is not regularly used to compensate for the signal lost in bad weather conditions, as their bubble attenuation estimator was never realized and implemented. Later, after the drop keel was

introduced, the need for correction algorithms was reduced as the stop conditions for the survey was now more similar for both acoustic data collection and trawling.

The time varied gain (TVG) of scientific echosounders is used to automatically adjust for transmission loss, i.e. sound attenuation and geometric spreading (Aglen, 1989; Simmonds and MacLennan, 2005). Unfortunately, the compensation by this function cannot correct for the attenuation caused by air bubbles in bad weather conditions. The TVG compensation is target-transducer range and time delay dependent, while bubble attenuation is sea state and platform dependent.

The actual design of the hull is also proven to play a significant role in the attenuation of acoustic signals in bad weather conditions (Knudsen, 2006a). From his experience, vessels with a deeper and sharper raise angle of the hull in front of the transducer platforms had fewer problems with air bubble attenuation than vessels with a more flat bottom. On the first vessel type, the hull cut the air bubble layer and forced the bubble layer to the sides before hitting the transducer platforms. On flat-bottomed vessels, however, the air bubble layer is trapped under the bottom of the vessel, floating aft across the transducer face. In particular, a vessel with a large bulbous bow, flat on the bottom side, does not perform well in bad weather conditions. Knudsen (2006a) further explained that the hull shape in this way might determine the amount of air bubbles that may be present in front of the transducer on any vessel. Unfortunately, this study did not dissect the problem in detail, but it is still an interesting and controversial topic among manufacturers of commercial echo sounders. They all have their preferred mounting positions.

Further, Dalen and Løvik (1981) earlier examined the attenuation due to wind direction relative to the vessel heading direction, concluding that the astern encounter gave less attenuation compared to the forward and athwart encounters. Ona (1991) later demonstrated that vessel heave could be successfully used as an attenuation correction index by monitoring the integrated vessel heave in bad weather in relation to the attenuation observed. He further emphasised that most echo integration problems encountered in bad weather could be attributed to the attenuation of the transmitted signal by bubbles close to the hull, often created by the vessel itself. The hull shape and transducer mounting position are therefore considered to have unquestionable effects on the transmission of the sound waves in the water column. In his study a more constant aeration of the water column by the wave action gave more controllable mean signal attenuation.

In the present study, two 38 kHz Simrad EK60 scientific split beam transducers were used, one mounted on the hull in a standard blister and the other on the drop keel. The two transducers were alternately pinged using a multiplexer, which was consecutively internally steered by the ER60 system itself. With this system set-up, acoustic data were collected in various weather conditions in the Barents Sea. Simultaneously, the two ER60 raw data sets were obtained from the two different 38 kHz transducers that allowed a direct powerful comparison between the two systems. The sea bottom was used as the reference target. The two data sets were thereafter post-processed using the LSSS (Korneliussen *et al.*, 2006) software, which generated data base reports with the area backscattering coefficient from the two systems. From the resulting area backscattering strength data, ratios between the two measurement systems were established and compared both graphically and statistically.

The objectives of this study were therefore:

- To establish a correction factor for air bubble acoustic attenuation;
- To determine the effectiveness of the seabed as the reference target;
- To elucidate the benefits of using a drop keel-mounted transducer compared to a hull-mounted transducer.

2. NOMENCLATURES AND DEFINITIONS

2.1. Nomenclature

Symbol	Name	Unit
σ_{bs}	Backscattering cross-section	m^2
σ_e	Extinction cross-section	m^2
σ_a	Absorption cross-section	m^2
α	Acoustic absorption coefficient	dB m^{-1}
σ_e/σ_b	Attenuation coefficient ratio	-
s_a	Area backscattering coefficient	m^2 m^{-2}
s_A	Nautical area backscattering coefficient	m^2 nmi^{-2}
S_A	Nautical area backscattering strength [10 $\log_{10}$ (s_A)]	dB re 1 (m^2 nmi^{-2})
s_v	Volume backscattering coefficient	m^{-1}
S_v	(Mean) Volume backscattering strength [10 $\log_{10}$ (s_v)]	dB re 1 m^{-1}
TVG	Time Varied Gain (20 log R + 2αR)	dB

dB for decibels

2.2. Definitions

Term	Definition
Hull	is the basic structure of a vessel not including the masts, rigging, above board constructions or attachments of any kind. It is a central concept in floating vessels as it provides the buoyancy that keeps the vessel from sinking.
Drop keel	is the longitudinal structure along the centerline at the bottom of a vessel's hull, mainly for vessel stabilization but here in this study acoustic instrumentations are also housed. It can be protruded out and retracted in from the vessel hull to improve the quality of acoustic data.

3. THEORETICAL APPROACH

The measurement of the excess attenuation coefficient is based on a comparison of the bottom S_A response of a hull-mounted transducer with that of a keel-mounted transducer in bad weather conditions. The acoustic attenuation mainly depends on the extinction cross-section, the volume concentration and vertical distribution of the air bubbles in a vertical echo sounding system. The evaluation of attenuation as a function of depth is therefore a reliable way of precisely correcting the bubble problem with less variability, since this is the rate of acoustic energy attenuation per depth interval. Wind-induced bubble acoustic attenuation in various weather conditions was the primary concern of this study; hence fish related attenuations are not treated in all dimensions. Acoustic attenuations caused by any other biological sources are as well not considered because of their assumed negligible effect on the bottom echo (Foote, 1990). Therefore the bottom echo is considered to be mainly from the seabed, and no other factors are considered to contribute towards its overall intensity (Dalen and Løvik, 1981).

3.1 Basic assumptions

It is of utmost importance to note that the assumptions made below are based on the consideration of the time period for a master thesis completion, and they are a simplification. These assumptions are:

- There is a linear relationship between excess attenuation coefficient and wind speed;
- The bubble density (ρ_a) is constant throughout the water column, i.e. they are uniformly distributed in the insonified volume since this will not be estimated;
- Bubbles resonance and reverberation are considered negligible due to the high echo intensity of the seabed;
- All bubbles are of the equal size and radius; therefore the bubble size will not be measured;
- The echo intensity of the bottom is approximately constant between the two-transducer systems, i.e. they encounter the same target at the equivalent time thus $S_{A_1} = S_{A_2}$;
- Bubble reverberation effects are considered insignificant, since no small targets will be evaluated;

- The transducer mounting position does not have an effect on the backscattering coefficient in good weather conditions but it does have an effect in bad weather conditions;
- The seabed is not assumed to be flat due to the use of the two 38 kHz transducers that simultaneously sample the same target (the seabed) hence gives homogeneous backscattering coefficients.

3.2 Mathematical modelling

Initially, Løvik (1980), then later Furusawa *et al*. (1992) described air bubble spectrum estimate by backscattering cross-section (σ_{bs}), extinction cross-section (σ_e), and absorption cross-section (σ_a) of the air bubble layer. They both mathematically expressed the bubble spectrum as follows:

$$\sigma_e = \sigma_{bs} + \sigma_a \tag{1}$$

This study mainly considered two theoretical models introduced by Foote (1983) and Foote *et al.* (1992), which are applied in addressing the problem of echo extinction by fish shadowing or signal extinction. Since the blockage of the signal by the bubble is a similar principle to the shadowing or extinction by fish swimbladder in dense schools or shoals (Ye, 1996), hence these models were applied to bubble acoustic attenuation. The Foote's 1983 model states that there is linearity in the signal scattering and echo energy of the target fish, meaning that the total echo intensity (E_{tot}) from a volume containing a randomly distributed number of targets is on average the exact reflection of the echo capacity of the aggregated target fish. Foote (1983) therefore expressed the linearity principle mathematically as:

$$E_{tot} = \sum_{i=1}^{N} E_i \tag{2}$$

where E_i is the mean echo energy from the *i*th fish.

The above model (Equation 2) stands true for less dense fish schools or shoals, where a linear relationship between the target and the received echo energy is assumed (Dalen and Løvik, 1981; Foote, 1983). Therefore, this model cannot be applicable in dense fish aggregations where there is shadowing by fish on the upper layer (Armstrong *et al.*, 1989; MacLennan *et al.*, 1990; Toresen, 1990; Furasawa *et al.*, 1992; Zhao and Ona, 2003), and in the case of bad

weather conditions where wind-induced bubbles scatter and attenuate acoustic signal (Dalen and Løvik, 1981; Berg *et al*., 1983; Novarini and Bruno, 1982).

However, in instances with uniform number of fish that are uniformly distributed within a particular thick layer Δz, Foote (1983) recommended the use of Equation (3) which calculates the E_{tot} considering extinction effects at least in *ex situ* situations:

$$E_{tot} = \frac{1-\exp(-2v\Delta z\sigma_e)}{2v\Delta z\sigma_e}\sum_{i=1}^{N} E_i \qquad (3)$$

where: v is the bubble density;

σ_e is the expected mean extinction cross-section of the bubbles (Equation 1);

Δz is the vertical extent of the bubble layer;

E_i is the aforementioned mean echo energy from the *i*-th bubble.

The multiplication by two is due to the two way absorption of the signal.

Foote *et al.* (1992) used a different theorem (Equation 4) for evaluating the effect of signal extinction by fish schools (analogous to air bubbles in this study). Foote's model uses the sea bottom as the reference target for the extinction attributed to the large fish aggregation, it also assumes a flat sea bottom. In this instance, the bubble layer will be used as the scattering and extinction source within a defined depth channel. The model is expressed in terms of the mean volume backscattering coefficient (s_v) in m^{-1}:

$$s_v = \rho\frac{\sigma_{bs}}{4\pi}\frac{1-\exp(-2\rho\sigma_e\Delta z)}{2\rho\sigma_e\Delta z} \qquad (4)$$

Where: σ_{bs} is the expected average backscattering cross-section of the bubbles;

ρ is the bubble density, assumed to be constant;

σ_e is the average extinction cross-section of the bubbles.

The integration results of s_v over a certain depth channel does not rely on the random vertical extent, if it includes the bubble layer while it excludes the bottom. Then the expected area backscattering coefficient associated with the bubble layer can be expressed as:

$$s_{a,Bu} = (\sigma_b / 8\pi\sigma_e)[1 - \exp(-2\rho\sigma_e \Delta z)] \tag{5}$$

The area backscattering coefficient of the bottom without the bubble layer (s_{a,B_0}) is expressed as:

$$s_{a,B} = s_{a,B_0} \exp(-2\rho\sigma_e \Delta z) \tag{6}$$

Simultaneous solution of Equation (5) and (6) gives

$$s_{a,B} = s_{a,B_0}[1 - (8\pi\sigma_e / \sigma_b) s_{a,Bu}] \tag{7}$$

where $s_{a,Bu}$ and s_{a,B_o} are the estimated area backscattering coefficient of the air bubble layer and the seabed in the absence of bubbles respectively.

Equation (7) shows how the problem in calculating the σ_e can be solved by a pair wise evaluation of $s_{a,Bu}$ and $s_{a,B}$. The linear regression of the $s_{a,Bu}$ and $s_{a,B}$ determines the regression coefficients α and β:

$$s_{a,B} = \alpha + \beta s_{a,Bu} \tag{8}$$

Therefore, the attenuation coefficient ratio can be derived from Equation (7) as:

$$\sigma_e / \sigma_b = -\hat{\beta} / (8\pi\hat{\alpha}) \tag{9}$$

where $\hat{\beta}$ and $\hat{\alpha}$ are the determined regression coefficients.

The above regression in Equation 8 is heavily dependent on the thickness of the bubble layer. In the case of very low bubble concentration, the range in values of the $s_{a,Bu}$ may be quite low, resulting in erroneous regression estimates.

The volume backscattering coefficient (s_v) describes the density of targets per volume, but not the density per area which might as well reflect the amount of the signal attenuated over a

certain depth interval in a given fish school or bubble layer. The area backscattering coefficient (s_a) can be derived from the s_v (Knudsen, 1990), since the s_a is just an integral of the volume backscattering coefficient (s_v). The s_a is a dimensionless factor while s_v is one dimensional (MacLennan *et al.*, 2002).

To determine the range attenuation, the s_a could be used, which will give an estimate of how much signal is lost in good-to-bad weather condtions. The s_a ($m^2\ m^{-2}$) is defined by:

$$s_a = \int_{z_1}^{z_2} s_v dz \tag{10}$$

where z_1 and z_2 are the limits of the depth channel.

For many practical purposes, for example the Simrad EK500 echosounders, the nautical area backscattering coefficient (s_A) is used in many instances instead of the s_a (MacLennan *et al.*, 2002; Foote *et al.*, 1992). The relevance of the s_A is due to the inclusion of the precise scaling factor $4\pi(1852)^2$ as the mean cumulative backscattering cross-section:

$$s_A = 4\pi(1852)^2 \int_{z_1}^{z_2} s_v dz \tag{11}$$

where dz is the difference in depth between the depth channel limits. The units of s_A are square meter per square nautical mile ($m^2\ nmi^{-2}$).

The attenuation coefficient ratio (σ_e/σ_b) defined by Equation (9) was determined from both the hull- and keel-mounted transducers and used to set the correction factor. In good weather conditions the ratio between the two transducers should be approximately equal to unity, while in bad weather conditions the ratio should be in overall greater than one.

4. MATERIALS AND METHODS

4.1 Basis of the study

Extreme high survey costs and the high demand for more data for fisheries stock assessment purposes have led research institutions to take advantage of using fishing vessels as acoustic data collection platforms. Unfortunately, fishing vessels are generally not well equipped or suited to perform this kind of task as research vessels. Given that in the Norwegian Sea and many other seas around the world, the sea states are predominantly rough with stormy weather conditions occurring repeatedly in the main distribution area for oceanic fish stocks. Wind induced air bubbles can significantly reduce the quality of acoustic data collected by vessels with only hull-mounted transducers. This study was undertaken to calculate a correction factor for this frequently encountered systematic error and to thereby improve the quality of acoustic data collected.

4.2 Research platform

As a platform for acoustic data collection the research vessel "Johan Hjort" [64.4 m, 3264 HP (2400 KW)] (Figure A.4 in Appendix A) was used, principally because this vessel is equipped with both drop keel- and hull-mounted transducers. It was built in 1990 with a v-shaped hull, typical of older vessels. The v-shaped hull does to some extend "plough" water sideways of the transducer as the vessel moves forward, and in this way, improves the quality of acoustic data collected in such vessels by removing the bubbles in front of the transducer (Knudsen, 2006a). Thus, the RV "Johan Hjort" likely represents a best-case scenario for hull-mounted transducers.

In contrast, the hull shape of most modern vessels have a flat bow that tends to improve the vessel stability in bad weather conditions, but reduces the quality of acoustic data collected from hull-mounted transducers. The Institute of Marine Research (IMR), Norway, owns the vessel; it is fundamentally used in the conduction of both fisheries and environmental research. The keel- and hull-mounted transducer cables are both wired to the instrument room, from where the multiplexer (illustrated below) can be easily connected.

4.3 Acoustic instrumentations

Acoustic transducers were mounted in the hull and the drop keel respectively. The Simrad 38 kHz transducer characteristics and settings used are briefly summarized in Table 4.1.

Table 4.1. The parameters and settings of the two Simrad ES38B transducers used for the present study.

Parameter (unit)	Value
Beam type	Split
Transducer type	ES38B, 88 discrete elements
Central frequency (kHz)	38.095
Transducer depth (m)	5-8
Maximum transmitted power (W)	2000
Pulse duration (μs)	1024
Sample interval (μs)	256
Bandwidth (Hz)	2425
Two way beam angle (dB)	-20.6
GPT-SW version	070413
-3 dB beam width alongship (deg)	6.84
-3 dB beam width athwartships (deg)	6.78
Angle offset alongship (deg)	-0.09
Angle offset athwartships (deg)	-0.13
Angle sensitivity (deg)	21.90

The hull-mounted transducer was housed in a standard blister, with the 38 kHz transducer utilised in this study and the 120 kHz transducer was not used (Figure 4.1). The 38 kHz transducer was used for comparison due to its normal usage in fisheries acoustics, and also because it is the only available usable frequency in the hull-mounted transducer of this research vessel. The transducer was located at 5 meters depth below the sea surface, but assumed to fluctuate with wind- and wave-actions. The beam opening angles of the two Simrad ES38B transducers are the within the recommended opening angles for scientific echosounders (Simmonds and MacLennan, 2005; Parker-Stetter *et al.*, 2009).

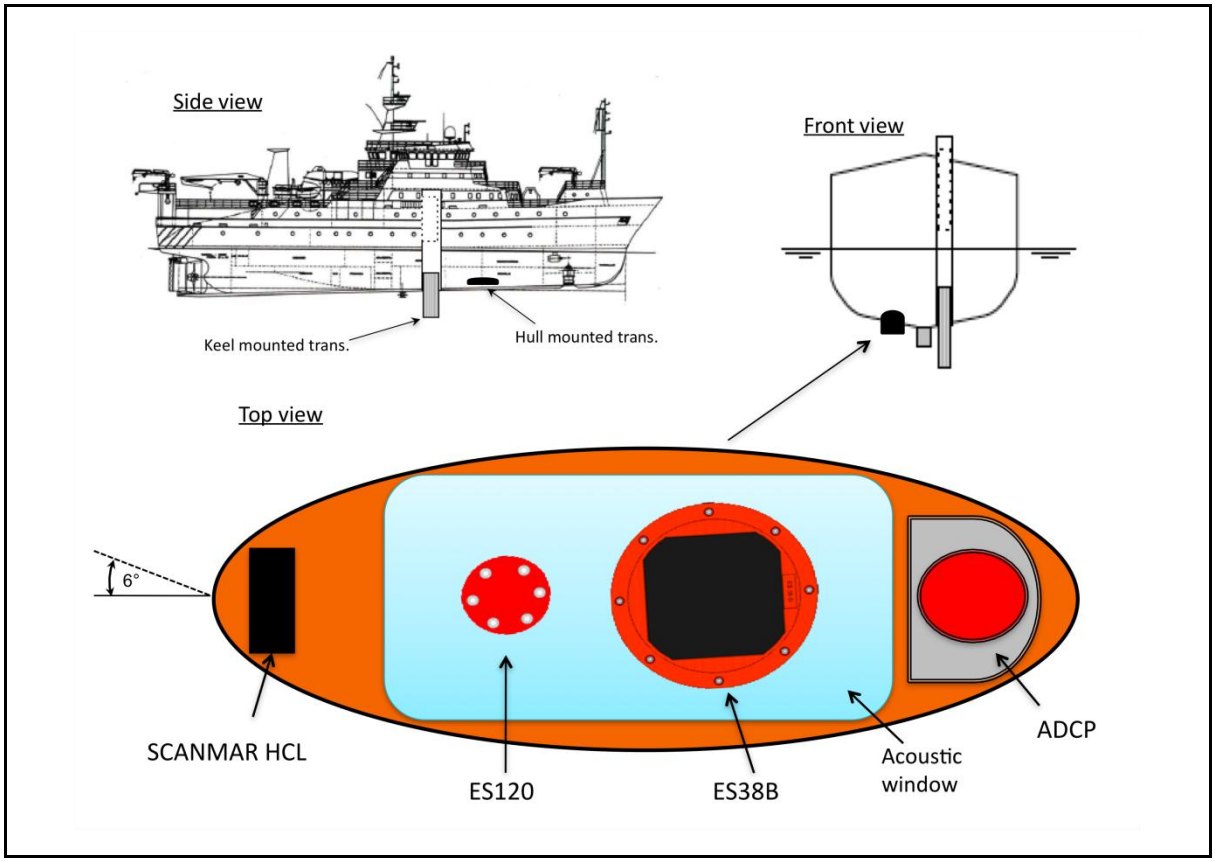

Figure 4.1. Schematic diagram of the 38 kHz transducer mounted on the hull of the RV "Johan Hjort". The 120 kHz transducer was not used in the surveys. (Drawing adopted from H.P. Knudsen, IMR, pers. comm.)

The 38 kHz transducer on the drop keel was installed close to three other transducers (Figure 4.2). These are the Simrad ES18, ES120 and ES200 transducers, operating at 18, 120 and 200 kHz, respectively. The transducers were placed at 8 meters below the sea surface when the keel was fully lowered. The Acoustic Doppler Current Profiler (ADCP) and Scanmar HCL (Hydroacoustic Communication Link) are also mounted in the drop keel but not used during the experiment. Throughout the use of the vertical echo sounding system, the sonar system of the vessel was then turned off to avoid potential interference (Peña, 2005; ICES, 2007; Peña, 2009).

Wind speed, wave height, wind direction, vessel speed and vessel heave movement data were logged simultaneously to the ER60 from an Octans III- Fiber-Optic Gyrocompass with Integral Motion Sensor (iXSea, Marly-le-Roi-France). The wind speed and direction were measured by the Thies Clima AMS 07 weather station on the vessel, and logged each second to the "Survey logger 'software'". Wave height and wave direction relative to the vessel were manually observed and entered to the survey logger by the navigator.

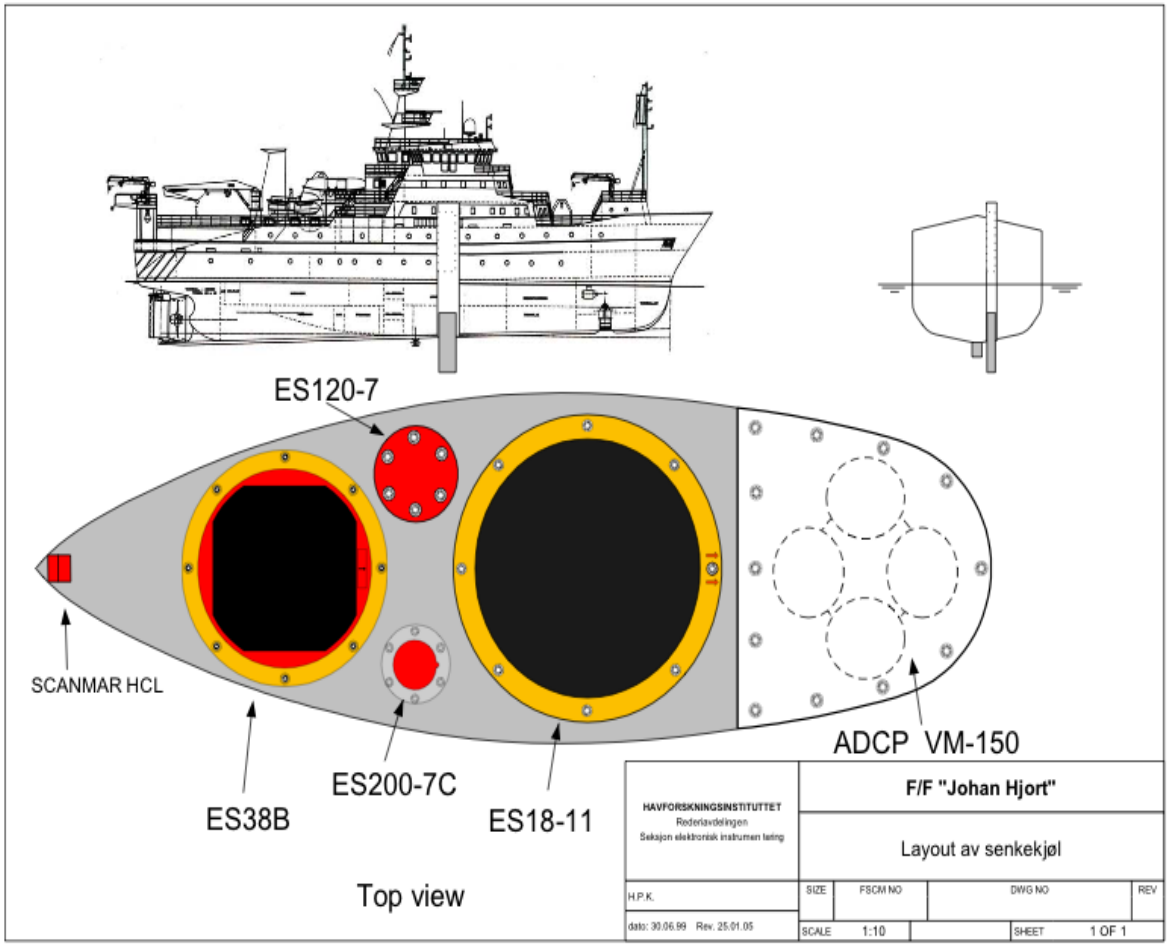

Figure 4.2. The layout of transducers in the drop keel of the RV "Johan Hjort". Only the 38 kHz ES38B transducer was used for the experiment. The Scanmar HCL and the ADCP are also incorporated in the keel.

4.4 Alternate pinging

The alternative pinging was performed between the hull- and keel-mounted transducers. This enabled different range sampling by the two-transducer mounting systems. The drop keel of the vessel was protruded to its maximum depth of 3 m below the hull while alternately pinging to the hull-mounted transducer. The multiplexer (MUX) system was connected to one EK60 General Purpose Transceiver (GPT) that served as a commander between the two transducers mountings (Figure 4.3).

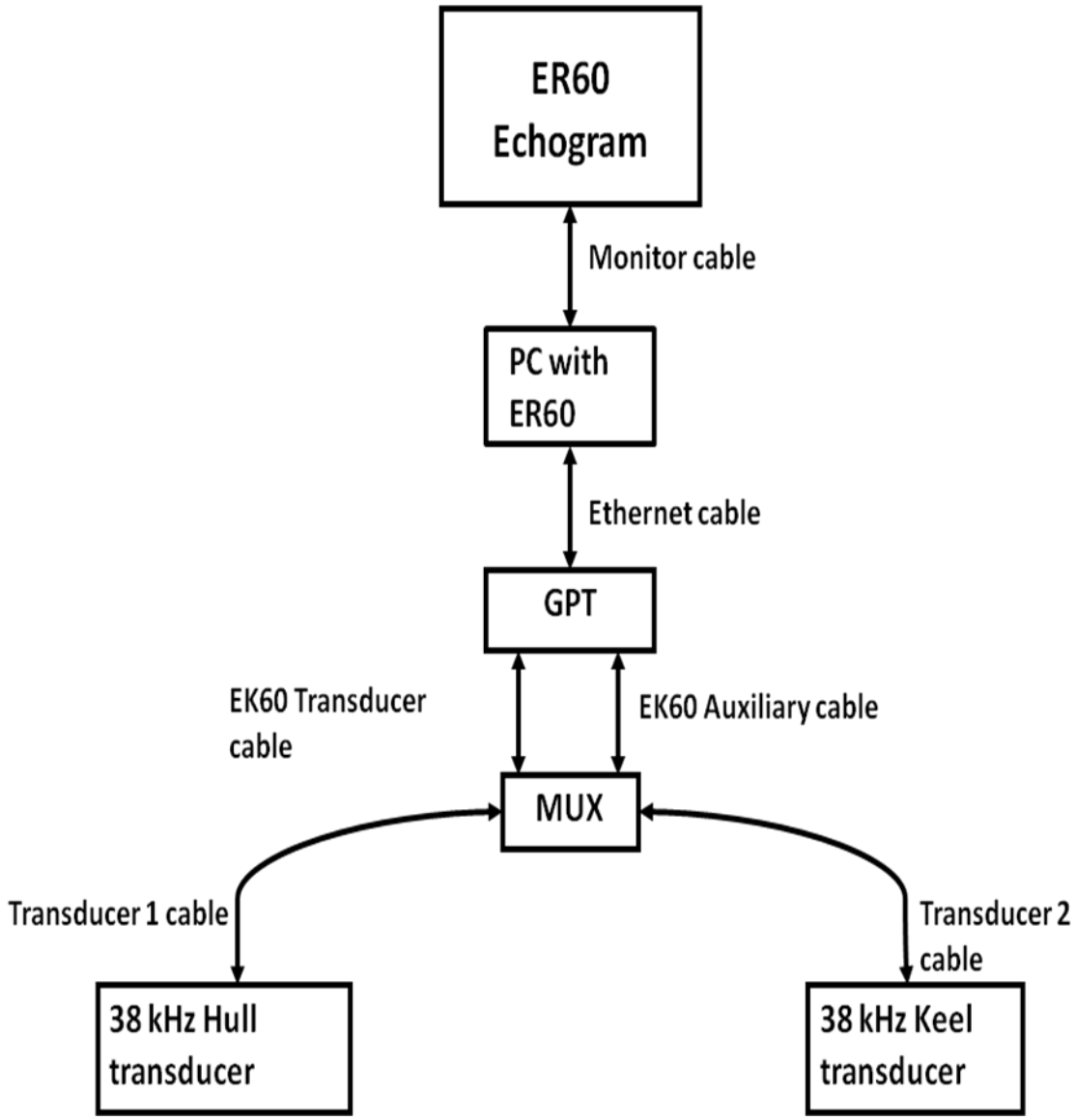

Figure 4.3. Schematic diagram of the communication set-up between the multiplexer (MUX) and the EK60 general-purpose transceiver (GPT). The MUX pinged alternately between the hull- and drop keel-mounted 38 kHz transducers. All data collected were stored in a personal computer (pc) that also ran the ER60.

The multiplexer system was remotely controlled by the GPT; the GPT transducer ports were connected to the MUX on two sides and MUX was directly plugged to the echo sounders. The photographic picture of the multiplexer showing all the ports is given in Figure A.1 in the Appendix A. Since it is a split beam technology system, each the transducer cables had 4 pairs or 8 wires (Figure 4.4).

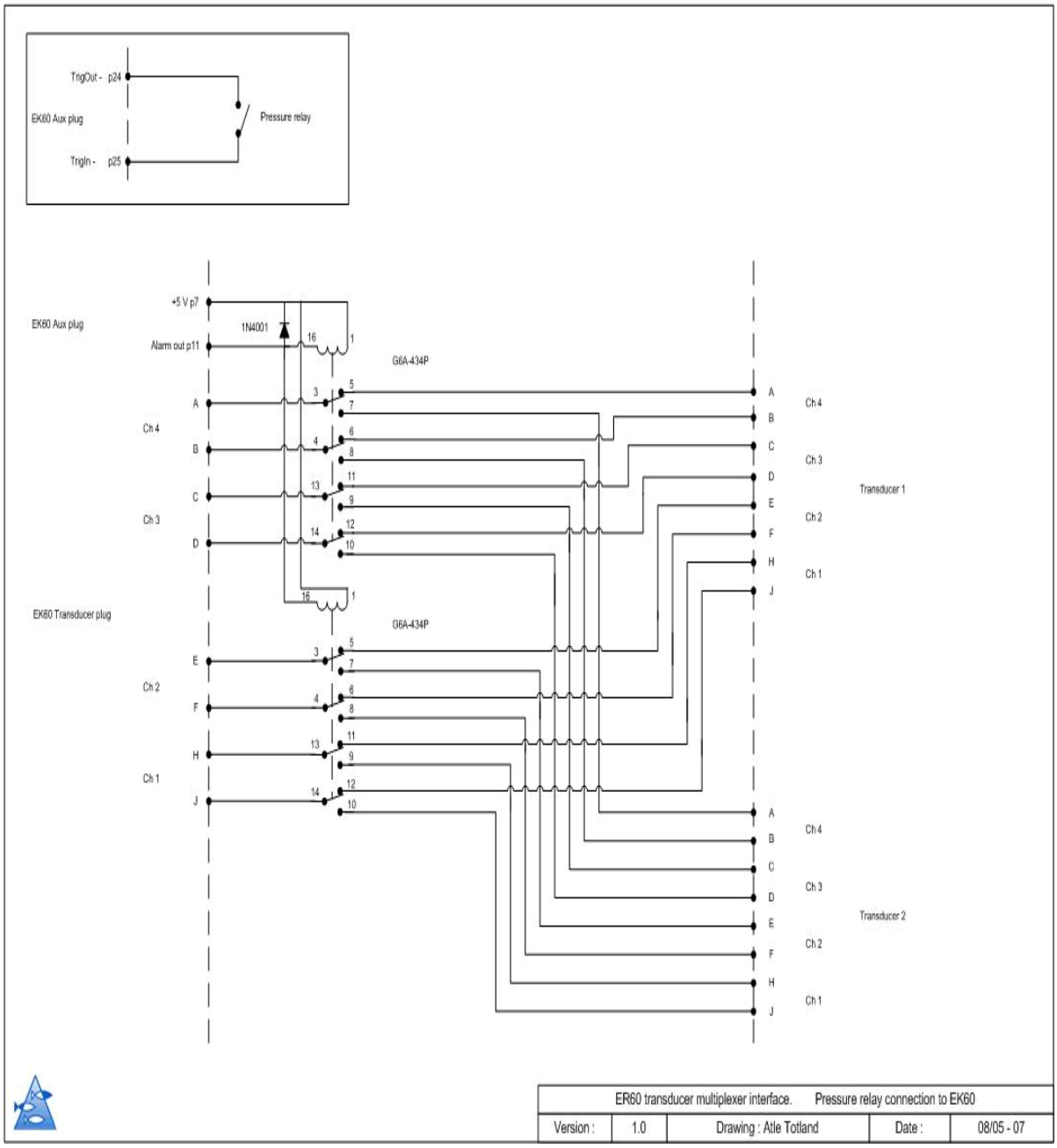

Figure 4.4. The detailed multiplexer circuit illustrating how the alternate pinging was executed by channel switching transmission between the two transducers. Ch and p, refer to channel and pin respectively. (Diagram by A. Totland, IMR, Norway.)

To switch the GPT (wires) to the two transducers (8*2 wires), the MUX uses 2 relays; these are controlled from the GPT AUX-port by the signal "Alarm out". If "Alarm out" was 5 volt for transducer 1, no current went through the relay coil (since there is also 5 volts on the other side of the relay), then allowing Transducer 1 to be connected to the GPT. If "Alarm out" is 5 volt for transducer 2, no current went through the relay coil and eventually the relays switched to transducer 2. The Simrad ER60 software controlled all the "Alarm out" signals,

as well as the transmission, and the storing of acoustic data to 2 separate portions of the data files in the pc (A. Totland, IMR, pers. comm., 2008).

4.5 Data collection

The Simrad EK60 38 kHz scientific echosounder data for the bottom backscattering coefficient comparison were collected onboard RV "Johan Hjort" in the Barents Sea under various weather conditions in three consecutive surveys (Figure 4.5). The vessel was steaming at various speeds in correspondence to the wind speeds. The first set of the data was acquired from the 17th to 27th of October 2008 in the Barents Sea. The time period chosen for the data collection was motivated by the fact that during this month of the year the weather conditions are generally considered rough in the Barents Sea, i.e. almost winter weather conditions.

It is generally reported that the Norwegian economic exclusion zone experiences high wind forces between 11-14 m/s and above in most parts of the year (Knudsen, 2006b). It is this kind of weather conditions that this study anticipated. The second set of data was conducted on the 4th and 5th of February 2009, when the weather conditions were also generally rough. The third set data collection was conducted on the 20th and 25th of February 2009 as a supplementary data set in very bad weather conditions. Acoustic data collections were by-products in all these surveys; the primary aim of the first survey was to test fish capture equipments while the aim of the second was to research the Barents Sea oceanography, and that of the third was during the winter abundance estimation survey for demersal fish. Unfortunately, the multiplexed data created some problems for the display of the LSSS system, putting one empty ping between each real transmission in each file, so it was decided not to use the multiplexer during standard survey work. This reduced the data collection for this study to periods when the data were not used for fish abundance estimation.

In all the events, the multiplexer was plugged to the GPT and acoustic attenuation data were extrapolated simultaneous. Ping averaging in rate was automatically done by the ER60 itself. Data were stored on a ping-by-ping logging. The MUX ping rate was set to 1 ping per 1 second for the two 38 kHz frequencies and the same for the other three frequencies. The switch occurred every ping; one ping was consecutively transmitted at a time to the hull-mounted transducer, and then switching to the keel-mounted transducer for a ping as well.

Altogether, this set-up ensured that the identical volume of targets were insonified by the two-transducer systems. Consequently, the double pinging also led to a time delay in the two 38 kHz echograms. Due to the time delay on the ER60 echogram display, a general agreement was made that the multiplexer should be disconnected before trawling to precisely locate the fish in the water column. As a result, a period of four days from ten was lost in the first survey to accommodate the needs of the fish capture researchers.

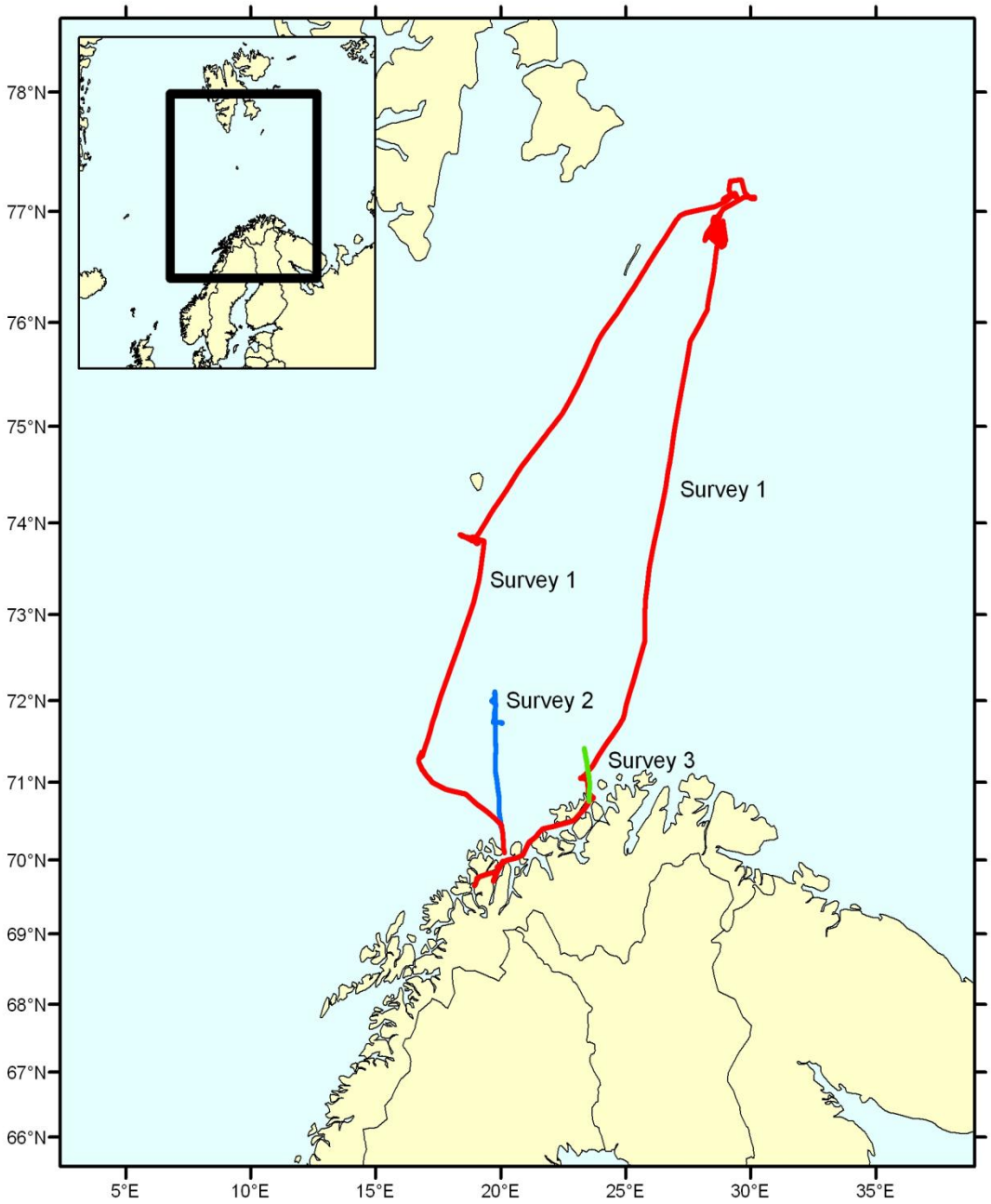

Figure 4.5. Vessel tracks geographical positions of the three surveys in the Barents Sea. (Map by Karen Gjertsen, IMR, Bergen, drawn using the ESRI ArcMap software.)

The acoustic personnel onboard constantly monitored the ER60 echogram to ensure that the alternative pinging was functioning as expected. The instrument chief strictly controlled the EK60 echosounder settings in the instrument room; the other users logged to the ER60 through the Ethernet LAN (Local Area Network) were only observers, hence could not make changes. The instrument chief mainly operated from 08:00 to 20:00 UTC. After this time the equipments were assumed to be working accordingly well until the following day. The data obtained were evaluated on everyday basis to check if the equipments were working well and that all the required data were being logged. However, the collected data were always found to be of relatively good quality.

4.6 Calibrations

Calibration is the process of establishing a relationship between a measuring device and the units of measure. In the case of scientific echosounders, this is accomplished by comparing the output of an instrument to a standard target having known acoustic scattering characteristics (Foote *et al.*, 1987). Calibration is an indispensible procedure to be performed in order to ensure the accuracy and precision of the acoustic data or measurements; therefore echosounders should be frequently calibrated, and preferably before important surveys for stock estimation (Knudsen, 2009). The RV "Johan Hjort" was calibrated in Skogsfjord, Ringvassøy, Norway, according to the standard target procedures described by Foote *et al*. (1987). The calibration was conducted after the first two surveys, but before conducting the third survey. The weather conditions on the calibration site were optimally calm. The vessel drop keel transducers are usually calibrated every four to six months to ensure the proper performance of the echosounders.

However, the hull-mounted transducer had not been calibrated during the ten years prior to this study, since it has not been used in surveys ever since the drop keel instrument package was installed. It now served as a backup transducer on this vessel. The exact acoustic performances of this transducer were not known beforehand, and the important gain settings were simply set to be the same as those of the keel-mounted transducer, since the transducers were otherwise identical. The vessel was initially rigged stagnant by anchors before the calibration began. The copper sphere with 60 mm diameter (CU60) was used as the standard target. Three 0.4 mm diameter monofilament lines supported by winches placed on three chosen point on the vessel held the copper standard sphere at the desired calibration depth

and location inside the acoustic beam. The drop keel was retracted to its original height below the hull; and the echosounders were therefore calibrated at this operational depth.

The standard sphere was moved inside the beams of the EK60 transducers until enough detections were acquired. Thereafter, the hull-mounted transducer was calibrated using the same procedure described above. The Conductivity, Temperature and Density (CTD) data were collected at all operational depths before and during the calibrations to determine the speed of sound in the water column between the transducer and the sphere.

The standard target calibration method was executed by running the built-in ER60 software "calibration.exe". The split beam on-axis sensitivity and the beam pattern were accomplished in one single beam mapping operation to determine the on axis gain (G) and the S_A correction (*SaCorr)* in decibels (dB). Beam models (polynomial and EK-Simrad) were then compared to the acquired data to determine the beam parameters used for the investigation of the point-beam compensation by the post-processing software. The calibration program harmonized the parameters in the beam model to minimize the root mean square error (rms-error) computed on the recorded data (Calise, 2009).

The rms deviations indicate how well the beam models fit the recorded data. Hence, they were utilized to evaluate the validity of the calibration, which can be declared satisfactory if the rms-value is less than 0.2 (Simrad, 2008). The G and the *SaCorr* are important for the volume backscattering strength (S_v), and hence the area backscattering coefficient (s_A) is determined from the 10 detections closest to the acoustic axis. The "calibration.exe" concludes the calibration by confirming and updating the transducer parameters inside the GPT of the echosounder (Simrad, 2008). A file in ASCII format containing information in a standard form on: calibration parameters, gain and *SaCorr*, beam parameters results, statistical comparison with beam models and target detections of the standard target involved in the analysis could also be stored (Tables C.1 and C.2 in Appendix C).

The calibration process aimed at evaluating the compensation for geometrical spreading or transmission loss and power gain. The target strength (TS) and the mean volume backscattering strength (S_v) of the sphere in the split beam echosounder were determined mathematically by:

$$TS = 10\log(P_r) + 10\log(r^4 10^{2\alpha r}) - 2G(\theta,\phi) - 10\log\left[\frac{P_t \lambda^2}{16\pi^2}\right] \qquad (12)$$

$$S_v = 10\log(P_r) + 10\log(r^2 10^{2\alpha r}) - 2G_0 - 2S_{aCorr} - 10\log\left[\frac{P_t \lambda^2 c \tau_{nom} \psi}{32\pi^2}\right] \quad (13)$$

where: P_r is the power of the received signal measured at the transducer terminal (W);

P_t is the power of the transmitted signal referred to the transducer terminal (W);

G is the transducer gain in the target direction (θ, ϕ) (dB);

G_0 is the on-axis transducer gain (dB);

r is the range of the target sensed by the transducer (m);

c is the sound speed (m/s);

α is the absorption coefficient of the medium (Bel/m);

λ is the wave length (m);

ψ is the equivalent beam angle (sr)

τ_{nom} is the nominal pulse duration (s); and

S_{aCorr} is the integration correction (dB).

Equations (12) and (13) require that several parameters should be measured, which makes the calibration output from such measurements to be more precise compared to earlier calibrations, with respect to the axis measurements.

The *TS* and S_v measurements from Equations (12) and (13) are applicable to both split beam and multi beam sonar respectively (Ona *et al.*, 2009).

4.6.1 Inter-calibration of the two 38 kHz echosounding systems

As a verification of the sphere calibrations, an inter-calibration was conducted between the two 38 kHz transducers on the LSSS post-processing system. The inter-calibration aimed to explicitly compare the hydro acoustical performance of the 38 kHz EK60 transducers in various weather conditions (Figures 4.6-4.7).

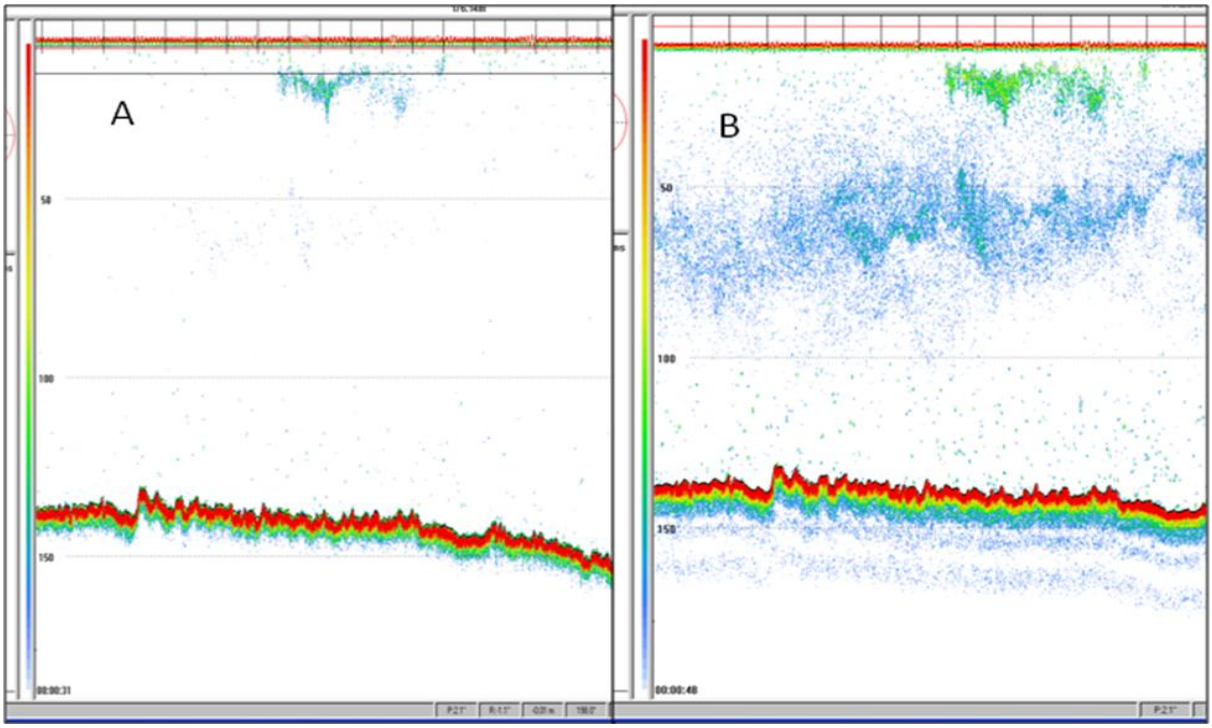

Figure 4.6. ER60 echogram from the 38 kHz hull-mounted transducer (A) with fish in the water column showing total acoustic attenuation and keel-mounted transducer (B) without attenuation in moderate weather conditions, wind speeds from 15 to 22 m/s.

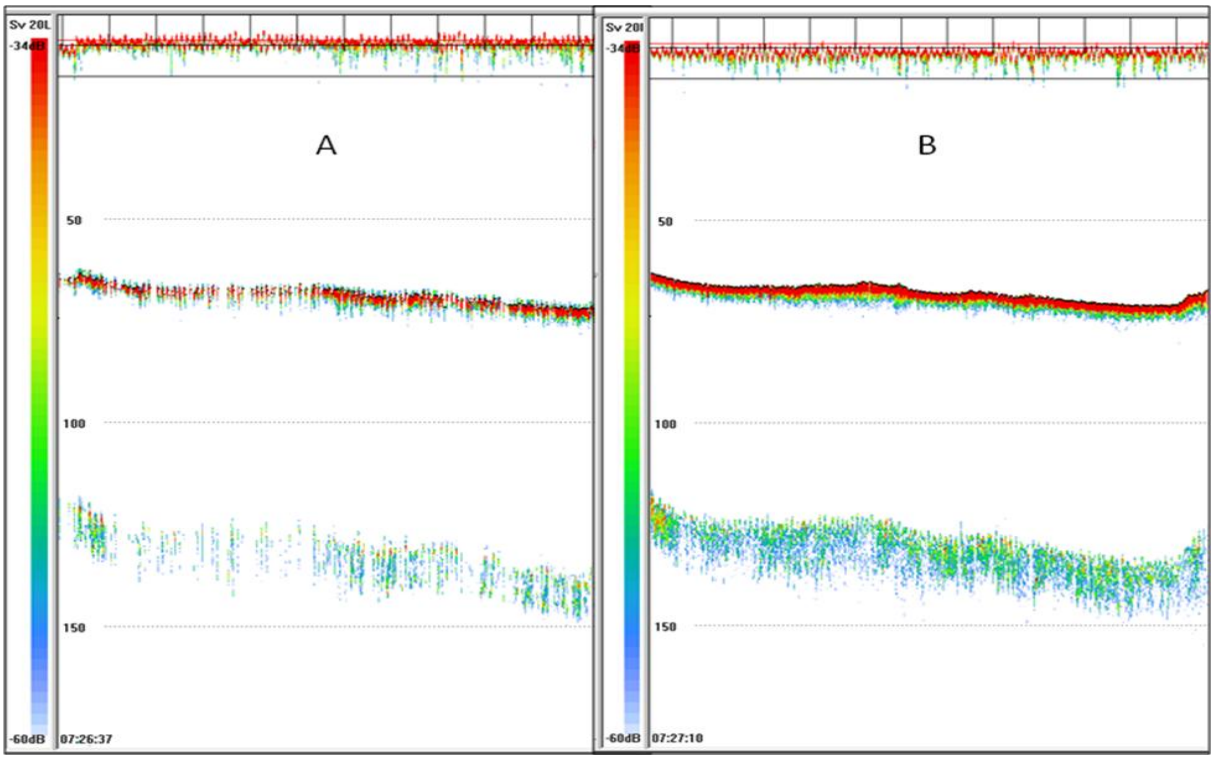

Figure 4.7. An exemplary ER60 echogram from the 38 kHz hull-mounted transducer (A) showing air bubble attenuation of the bottom signal and drop keel transducer (B) without attenuation. The blank or washed out stripes are due to complete acoustic signal attenuation in 23 m/s wind speed.

The data obtained by the multiplexer method were used for this inter-calibration purpose. The inter-calibration was accomplished by a comparison of the resultant nautical area backscattering coefficient (s_A) of the bottom echo at the two 38 kHz frequencies in relation to the prevailing wind speeds. The ratio (R) between the bottom s_A values of the 38 kHz of the two systems was computed as s_A keel (*K*) over s_A hull (*H*):

$$R = \frac{s_A(K)}{s_A(H)} \tag{14}$$

The above Equation (14) has no units, but by linearizing the two variables one can get the ratio in dB re 1 (m^2 nmi^2):

$$Log(\frac{S_{A,K}}{S_{A,H}}) = S_{A,K} - S_{A,H} \tag{15}$$

With the above equation the established correction factor can be relatively compared to previously established correction factors with easier. Under ideal conditions in good weather, and after calibrating the systems with a standard target, the ratio of the mean backscattering coefficients of the bottom echo should be very close to 1.0. The comparison gave a powerful verification of the desired and expected outcome, i.e. both transducers give similar bottom backscattering strengths, nautical mile by nautical mile. With this verification method, it was now possible to measure the effect of air bubble attenuation on the hull-mounted system, if we first assume that the keel mounted system is not affected by air bubble attenuation. Collection of data on wind speed, wind direction, wave height and vessel movement over the same time intervals as the bottom data were now the background data for the analysis.

The inter-calibrations were performed in both good and bad weather conditions; using the bottom echo as the reference target. The echo intensity of the bottom was integrated in a layer well covering the entire first echo of the bottom, and over a distance of 0.1 nautical mile. At a ping rate of 1 ping s^{-1} and a vessel speed of 10 knots, this represents an average over 36 pings. Using the alternate pinging on the two transducers, most of the data collected at 10 knots survey speed represents an average over 18 pings. At slower speed, the number of pings, say 5 knots may represent 36 pings again. The frequency response of the bottom signal at the other frequencies could also be monitored, but is not further studied here, since all of these were mounted on the keel, presumably unaffected by air bubble attenuation. The detailed inter-calibration results are given in the results section 5.4.

However, there were instances before the two transducers were calibrated where the frequency response between the two transducers was exceedingly deviating (Figure 4.8). The 38 kHz keel-mounted transducer had then a stronger frequency response than the 38 kHz hull-mounted transducer. Later, the calibration results were used to compute a correction factor for both 38 kHz transducers, which was implemented before the analysis of the bottom backscattering coefficient ratio was made. The s_A-values of the bottom signal generally decreased exponentially with increasing of the frequency. After this first scrutiny was completed, the collected data from the two transducers and the different frequencies were carefully analysed. The associated bottom s_A-values were evaluated carefully, with a resolution of 0.1 nmi by 0.1 nmi. Thereafter, bottom S_A plots were made between the two 38 kHz transducers.

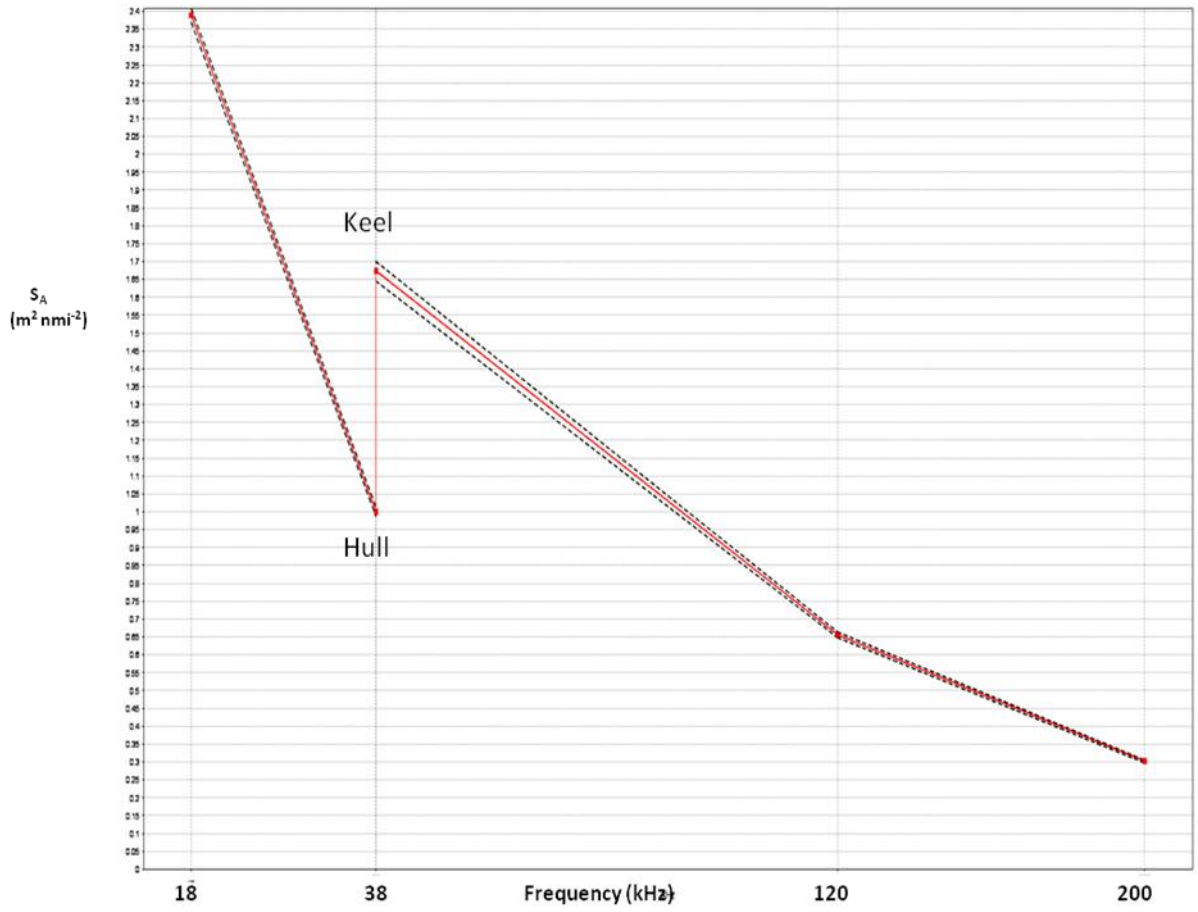

Figure 4.8. The frequency responses of the two transducers at 38 kHz, also included are the response at the three other frequencies 18, 120 and 200 kHz during survey 1 before calibration. Only the frequency response of the two systems at 38 kHz was of interest in this study. Graph from the LSSS post-processing analysis.

A linear regression analysis to determine the relationship between the data from the two 38 kHz transducers was performed mathematically:

$$s_A(H) = a + b.s_A(K) \quad (16)$$

where *a* and *b* are the regression coefficients, *H* and *K* refer to the hull- and keel-mounted transducers respectively.

The linear regression determined if the backscattering strength of the bottom from the two systems had a linear relationship. If not, it would have indicated that the systems were not performing correctly. In good weather conditions, i.e. without attenuation, ideally the slope should be close to 1.0 and the intercept close to 0. Since the bottom echo is quite variable due to changes in slope, roughness and hardness, large variability along the transects is expected, but since two identical transducers are measuring the same bottom with the alternate pinging, the expected mean ratio should be close to 1.0 if this method shall have any validation.

4.6.2 Actual calibration of the two systems

The actual calibration was done after the first two surveys and before the third survey. From the calibration results the actual transducer *G* and the *SaCorr* of the systems were derived. It was later realised during the data scrutiny with the LSSS and it was also confirmed by the ER60 replayed echograms that both systems had the same transducer gain, set by an experienced instrument operator after trying the old transducer in the hull. This implied that during the collection of data in the first two surveys, the hull-mounted transducer gain was set to be the same as the keel-mounted transducer seemingly because there were no previous calibration data available for use at the time. The transducer gain was therefore set to be 27.03 dB for both systems.

However, the later calibrations results indicated that the two systems had slightly different transducer gains. The actual transducer gain for the hull-mounted transducer obtained from calibration was 26.92 dB, while the 27.03 dB gain was confirmed by calibration output to be the correct setting for the keel-mounted transducer. So, for the computation of the gain to be used for post-correction, the transducer gain results determined by calibration were used with confidence.

The final gain used for the post-correction of the bottom area backscattering coefficient data for both systems were generally computed using the following formulations:

Total gain before calibration $T_b = G_0 - S_{A_0}$ (17)

Total gain after calibration $T_c = G_1 - S_{A_1}$ (18)

where the subscript *0* refers to the values before calibration, and the subscript *1* refers to the values after calibration.

From Equations (17) and (18), the actual transducer gain can be computed by revisiting Equation (13), after calibration it can be simplified into:

$$S_v(corrected) = S_v(observed) + 2\Delta G \quad (19)$$

where ΔG is the difference between the total gain before and after calibration.

From the above computation, all the other parameters in Equation (13) are known to become constants after calibration.

Then the final corrected bottom s_A will be computed as:

$$s_A(corrected) = s_A(observed) \cdot 10^{2\Delta G/10} \quad (20)$$

where the $10^{2\Delta G/10}$ term refers to the linear correction factor for the area backscattering coefficient.

The computed correction factor was therefore directly multiplied to all the integrated bottom data in the database output of each survey in Microsoft® Excel 2007. The correction factors based on calibration data for the three surveys are shown in Table 4.2.

Table 4.2. The applied corrections to the measured area backscattering coefficient for survey 1 and 2 (upper table) and survey 3 (lower table), based upon the calibration data obtained for the two transducers. TG is used for describing the total gain of the volume backscattering coefficient.

Hull-mounted system, survey 1 and 2				
	Gain(dB)	*SaCorr* (dB)	TG (dB)	
Gains before calibration	26.92	-0.59	26.33	
Gains after calibration	26.24	-0.83	25.41	
Gain difference (dB)				0.92
Correction factor, linear				1.527566
Gains set during the survey, (dB)	27.03	-0.61	26.42	
Gain difference, survey (dB)				1.01
Correction factor for survey, linear				1.592209
Keel-mounted system, Survey 1 and 2				
	Gain (dB)	*SaCorr* (dB)	TG (dB)	
Gains before calibration	27.03	-0.61	26.42	
Gains after calibration	26.92	-0.59	26.33	
Gain difference (dB)				0.09
Correction factor, linear				1.042317

Hull-mounted system, survey 3				
	Gain (dB)	*SaCorr* (dB)	TG (dB)	
Gains after calibration	26.24	-0.83	25.41	
Correction factor for survey, linear				1.000000
Keel-mounted system, survey 3				
	Gain (dB)	*SaCorr* (dB)	TG (dB)	
Gains after calibration	26.92	-0.59	26.33	
Correction factor, linear				1.000000

4.7 Data post-processing

The acquired ER60 raw data were initially scrutinized by means of the LSSS 1.2.4 post-processing software. The bottom echo scrutiny evaluated the variation of the bottom echo

intensity between the two 38 kHz transducers in various weather conditions. Data collected without the connection of the multiplexer were relatively easily distinguished from those collected with the multiplexer plugged on by their colours in the LSSS file selection menu. The files of data collected with the MUX plugged were mainly marked green, while those without the MUX were marked with a red marker and were not selected for the post-processing. This was vital in ensuring the right data sets were selected for the post-procession and analyses.

Firstly, the LSSS was configured to the administrator mode, and then categories were generated. It was anticipated that the scrutiny could be divided into two categories: the transmission pulse scrutiny and the bottom echo scrutiny. However, it was later realised that the transmission pulse part was difficult to evaluate because the vessel heave compensator was activated during all surveys. The compensation of the vessel movement is then incorporated and compensated for on the echogram by varying range of the start of the transmission pulse (Figure A.7 in Appendix A). The main advantage of doing this is that a flat bottom will appear flat on the echogram, even with the vessel moving up and down several meters in rough weather conditions. Two layers were set around the seabed echo with a height around 100 m as the bottom echo integration layer (Figure 4.9).

The bottom echo category had to be assigned to 100 % during the scrutiny since it was assumed to be the only contributing factor to the backscattered energy. Echoes from fish, zooplankton or any other scatterers were assumed not to contribute to this very large echo. Although fish species like cod (*Gadus morhua*), capelin (*Mallotus villosus*), and redfish (*Sebastes mentella*) were reported from trawl catches. The data were scrutinized in the pelagic mode with a noise threshold set to a high -60 dB, and the TVG of $20\log R + 2\alpha R$ for transmission loss compensation were applied. The ER60 vessel log raw data were logged at different vessel speed intervals, which made it difficult to evaluate and determine the actual distance travelled by the vessel over time.

During the data scrutiny the log distance was set to a high resolution of 0.1 nautical mile (nmi), which gave about 50 values per 5 nautical miles. The data were stored in a high quality marking interpretation. These were later pulled out as a different ASCII file; the database reports were generated as the compact scatter reports. The 0.1 nmi logged acoustic data gave bigger data files with date, time position and the area backscattering coefficient for the bottom signal. The files from the two transducers were later merged in excel, and

subsequently also merged with data files containing the information on wind speed and direction, vessel speed and course, as well as data on vessel movement. Some of these variables had to be computed and averaged before being merged with the acoustic data files.

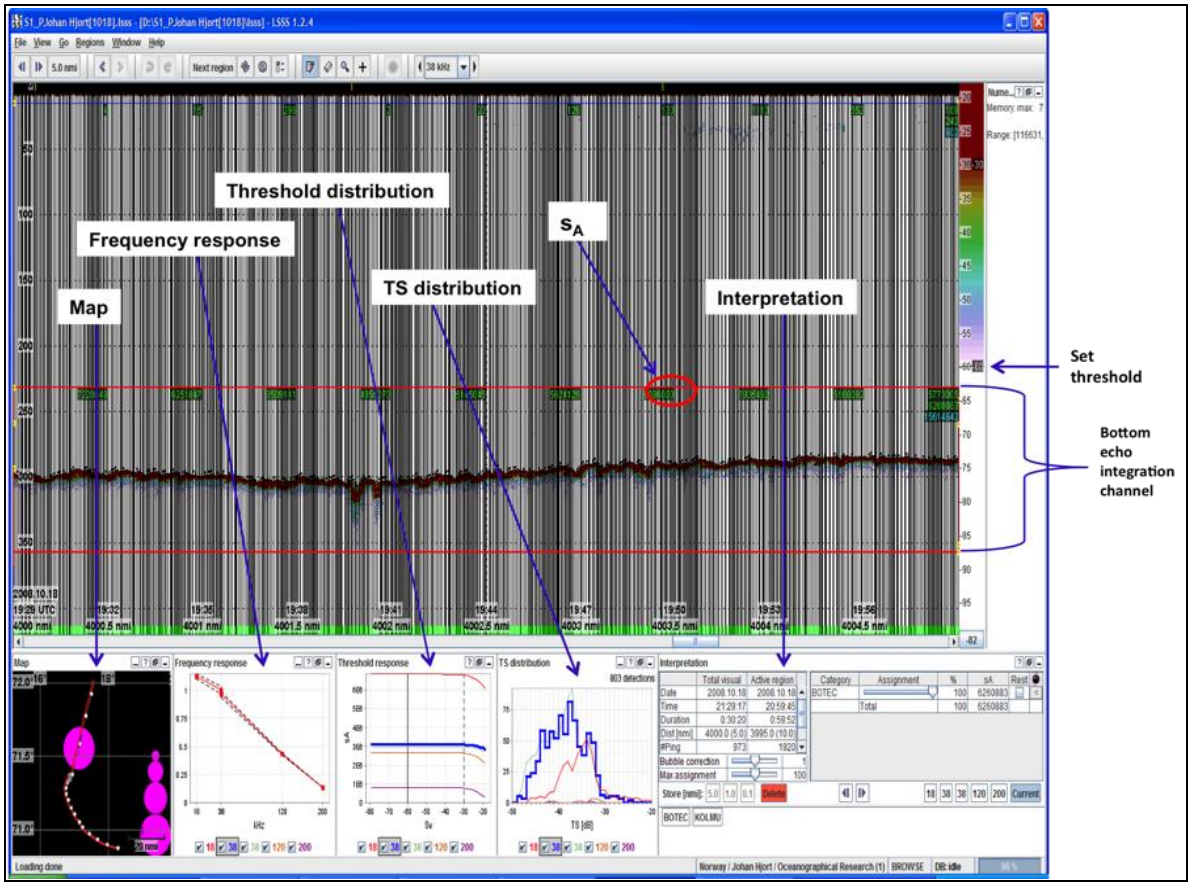

Figure 4.9. A LSSS screen snapshot showing the bottom echo integration channel and the resultant nautical area backscattering coefficients (s_A). The black stripes are the empty pings during the alternate pinging.

The whole data scrutiny gave in detail factors like the log, position, depth and importantly the bottom nautical area backscattering coefficient for the two EK60 38 kHz transducers. All s_A values for the bottom less than one million were not considered for use during the statistically comparisons, as most of these were collected on very sloping bottom. The typical nautical area backscattering coefficients for the bottom were between 1001443 - 67713527 m^2 nmi^{-2}. The bottom s_A ratio between the two systems was also later computed using Equation 14.

Thereafter, the bottom mean nautical area backscattering strength was computed:

$$S_A = 10\log_{10}(s_A) \qquad (21)$$

where s_A is the bottom nautical area backscattering coefficient (m^2 nmi^{-2}),

S_A is the bottom nautical area backscattering strength in dB re 1 (m^2 nmi^{-2}).

To obtain the wind speed and wind direction from this resultant acoustic data, the ER60 vessel raw data were statistically merged with the acoustic data. During the merging, only values of the wind speed and wind direction from the ER60 logging raw data that were closely equal to acoustic logging data were extracted. The combined acoustic data contained the wind direction and speed respectively. Due to the large size of the data set, a mean or average of the wind and bottom S_A had to be calculated for each 5 nmi. This averaging gave a much more presentable and readable graph of bottom S_A as a function of wind speed.

4.7.1 Vessel's heave, tilt and roll determination

The vessel heave movement had to be evaluated as an index of the air bubble acoustic attenuation in bad weather conditions, as earlier done by Ona (1991). Since it is well known that wind- and wave-actions affect the vessel movement, which will in turn influence the echo integral values form such recordings (Dalen and Løvik, 1981, Stanton, 1982). The research vessel-borne Octans gyrocompass and motion sensor were activated during the conduction of all surveys. The research vessel heave movements were logged in a datagram in the ER60 raw data, and data were derived by a specially designed software called the ER60LPHTR (Log, Position, Heave, Tilt and Roll). In these surveys, the vessel was headed into the wind and then turned and later sailed in the direction of the wind. Thereafter, data obtained from these surveys were replayed in the ER60 software with the ER60LPHTR running at the same time. The ER60 software was set to communicate with the ER60LPHTR in the internet broadcast mode during the replay. The ER60LPHTR read the output telegram from the ER60 and stored it to a file as an EK500 datagram output.

The EK500 datagram was set amongst other things to retrieve values of the following three parameters: vessel log, navigation and motion sensor data. These files contained information on the date, time, log, heave, tilt, roll, latitude, longitude and direction. Since the navigation data and vessel heave sensor were not chronological synchronized, the ER60LPHTR obtained the navigation data from the Global Positioning System (GPS). The timestamps in the output

files were unfortunately not in chronological order because the data were written in the file in the same sequence as they were received from the ER60 source (Atle Totland, per. comm.). The output files were therefore manually arranged in the appropriate chronological order.

4.7.2 Averaging the movement of the vessel

Computations were made to determine the instantaneous vessel heave movement in meters (m) for various weather conditions. Approximately 60 values per minute were obtained from the ER60LPHTR, being either positive or negative. Positive values indicated the upward movement of the heave while the negative values indicated the downward movement of the heave. To remove the point effects of negative or positive sign on the outcome, all values were squared. The horizontal and vertical heave movements were evaluated by integrating at the heave and roll. The heave movement or pitch (m) was integrated over distance using the formula:

$$AvH = \frac{1}{n}\int_{1}^{n_h} h_i^{\,2} \tag{22}$$

where: h_i is each individual heave reading;

n_h is the number of readings over the recorded distance travelled, in this case it was per 0.1 nautical mile.

The same procedure was applied to the vessel roll (degrees); also some values were negative or positive, negative indicated the roll to the port and positive roll to the starboard. Therefore, all values were squared to remove the movement angle effect and averaged per 0.1 nautical mile as *AvR*:

$$AvR = \frac{1}{n}\int_{1}^{n_h} r_i^{\,2} \tag{23}$$

where: r_i is each individual roll reading;

n_h is the number of readings recorded over the travelled 0.1 nautical mile.

Later, the variance and the standard deviation of the vessel heave and roll were also computed in order to remove the effect of the fixed offset and determine the probability distribution of the data. The statistical formulas used for computing the variance and standard deviations are given in Appendix D as Equations D.1-D.4. The vessel tilt was however of less interest in this instance since it indicated the vertical vessel movement, which is the same feature that is described by the heave and hence it was not scrutinized.

4.7.3 Weather data

The vessel heave movement is strongly influenced by the wind speed and sea state (Ona, 1991), for this reason weather data were collected. The sea state or wave height gives an indication of how the vessel was potentially moved sideways and vertically as the vessel headed towards a certain direction. The data of general wind speed (m/s), wind direction [angle (degrees)] and sea state (Beaufort force) were collected during the times of the surveys onboard the research vessel by the Thies Clima AMS 07 weather station at one minute intervals. The data was later retrieved in an excel file. After a careful scrutiny it was decided that the weather data sets should be treated separately according to the sea states. This would give a rightful correction factor in various weather conditions. Then the data was grouped into five groups according to prevailing wind conditions: 0-5; 5-10, 10-15, 15-20, and 20-25, all in units of meter per second (m/s). An example of a selected weather data set is given in Table C.3 in Appendix C.

4.7.4 Data merging

The data merging was performed in R-environment software version 2.8.1 (Vernables and Smith, 2002) installed with the RODBC package (see Appendix B for the commands used). The script editor Tinn R version 1.17.2.4 (2001-2005 rdm) was used for writing and saving the commands. The whole merging process is summarised in Figure 4.10. In order to determine the effect of wind speed on attenuation as a function of vessel movement, three data sets were linked together. Those were the weather data obtained from the vessel weather station, the acoustic data derived from the LSSS post-processing software and the ER60LPHTR derived vessel heave, tilt and roll data.

Firstly, the weather data were merged with the acoustic data using the logged distance as a merging reference point. Since the acoustic data were obtained using a high resolution of 0.1 nmi, they had many points compared to the weather data that were collected using a lower resolution. Due to the length differences between the two data sets, the logged distance points from the weather data that were very close to those in the acoustic data were merged together. Although this is not an absolute method, it gave an approximation of the wind speeds and wind directions at a given log distancing with the relative bottom s_A values. They were later pulled out as a different ASCII file called acoustic-weather data.

Thereafter, the acoustic-weather data were merged with the ER60LPHTR vessel heave, tilt and roll data. This was not an easy task; since the ER60LPHTR data was sampled each second in time, resulting in about 60 values or points per minute while the acoustic-weather data were sampled and averaged as one point per minute.

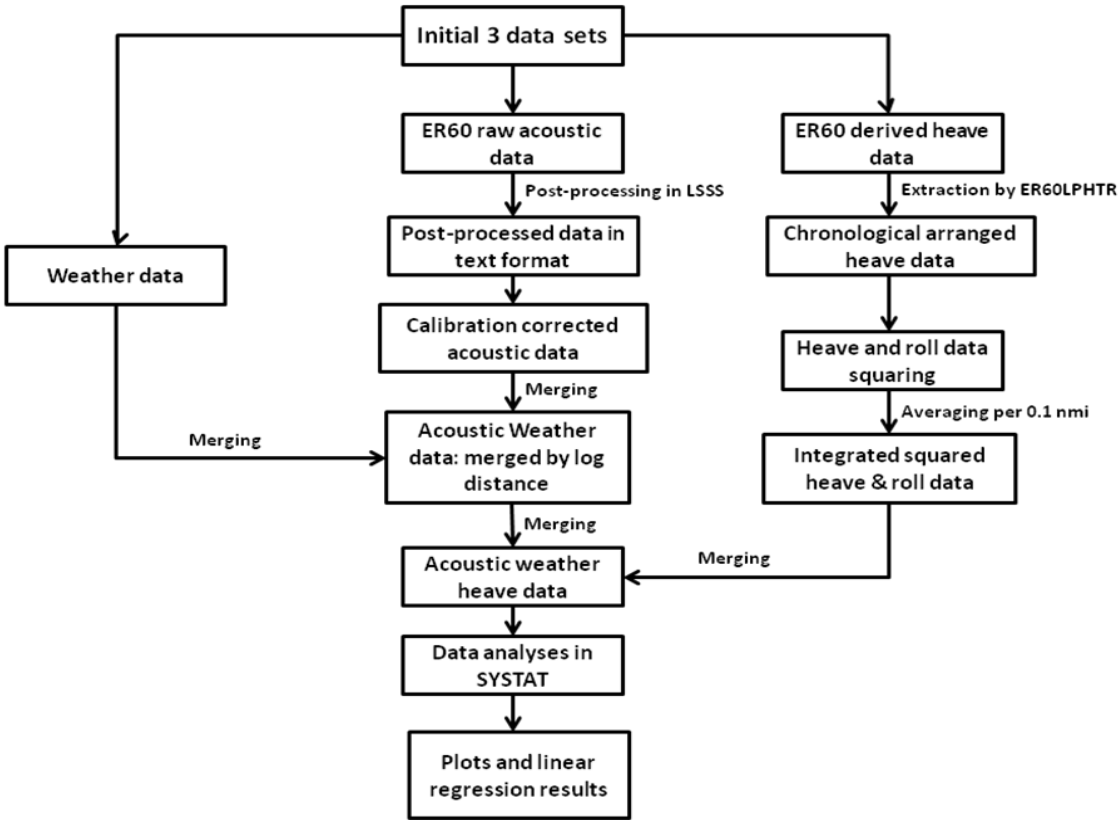

Figure 4.10. Diagram showing all the steps described during data merging and analyses.

In order to merge the two data sets, the ER60LPHTR 60 points per minute had to be averaged into one value per each 0.1 nmi. The exact log distancing between the two data sets were selected and merged accordingly. The exact log merging was used because it precisely merged the distance at which the vessel exactly tilted or pitched. After the merging, an excel file with s_A values, wind speeds and directions, vessel heave, tilt and roll was generated.

4.7.5 Linear regression lines at various wind speeds

The initial step of the data analysis was to obtain the linear regression between the hull- and keel-mounted transducers (Equation 16) to determine if there was linear relation between the two 38 kHz transducers at different wind speeds (m/s). Pings recorded at different wind speeds were treated separately according to their relative wind speeds. The correlation coefficient (*r*) indicated the optimal wind speeds where the two systems were still correlated to each other. The *r*-value ranges from -1 to +1, with a mean value around +1 indicating that there is a strong positive linear relationship between the two 38 kHz transducers, and a value close to -1 indicating that there is a negative relationship between the two transducers in question. Values close to zero indicated that there was no correlation between the two 38 kHz transducers. Linear regression plot were made in turn to confirm the correlation calculations. The plots were made with a zero intercept to check how the two data sets deviated from mean.

4.8 Data analyses

Acoustic data obtained from the LSSS post-processing software were manually sorted in excel spreadsheets prior to further analysed statistically. The sorting involved filtering out blank columns and taking out parameters that were not going to be considered. Since LSSS gave the bottom s_A values for the two transducer systems as separate files. These were also joined together in excel during the data sorting according to their time and logged distancing respectively. The mean echo intensity and standard deviation of the two systems at different wind groups were compared statistically. The attenuation curves at different wind speeds for the hull-mounted transducer were also plotted against the drop keel-mounted system. The SYSTAT 12 Version 12.00.08 (SYSTAT Software Inc., 2007) statistical programme was

used to perform the statistical comparisons and analyses of the mean attenuation coefficients and other variables of the two-transducer mounting systems (Figure 4.10).

4.9 Establishing the relative correction factor

It is a general theoretical expectation that the two-transducer systems should at least give a ratio (Equation 14) close to one in good weather i.e. without any air bubbles in front of the transducer face. The evaluation of the bottom s_A ratio can be done to either inter-calibrate the two systems or to establish a correction factor. The latter can be done before and after the multiplication by the correction factor obtained during calibration. It is highly expected that after the correction the two systems should give a ratio very close to one, since they are both compensated for total transducer gain. Fortunately, in this study the two systems did give the expected ratio. Therefore, they were not manually forced to give the desired ratio of one; this was a very crucial step since one of the systems was going to be used as reference to the other system in terms of attenuation. The establishment of this relationship between the two-transducer systems was therefore necessary, either relatively or absolutely as in this study.

After the verification of the ratio between the two systems, the air bubble acoustic attenuation correction factors were statistically established. First, one assumption or expectation should be made before the establishing the correction factor. That the keel-mounted transducer should be experience no air bubble attenuation since it was assumed to protrude beyond the bubble layer. With this assumption, the correction factor can be derived, once the ratio between the two-transducer systems has been verified to be close to one. Any changes in the ratio in bad weather conditions will be regarded as caused by air bubble attenuation. The keel-mounted transducer can be used as a reference to indicate how much echo intensity of the target is attenuated on the hull-mounted transducer. Since the echo intensity of the bottom on the hull-mounted transducer will be less than that in the drop keel. The established correction factor can later be used for correcting the measured integrator data on fish, as suggested and used in the literature.

For a comparison of this study established correction factor to the method implemented by Novarini and Bruno (1982) of evaluating the vertical attenuation as function of transducer depth at different wind speeds. They calculated the correction factor in dB:

$$A_v = (0.9754 - 0.08597w + 0.002367w^2) \times f^{1.32} \exp\left[-X(w)z_t\right] \qquad (24)$$

where $X(w) = 1616.77 w^{-2.36}$,

f is the frequency (kHz) used,

w is the wind speed (knots) and

z_t is the transducer depth (meters).

The equation holds in the range 8 kHz $\leq f \leq$ 60 kHz, 6 knots $\leq w \leq$ 30 knots, and $z_t \geq$ 1 m.

5. RESULTS

5.1 Wind conditions

Wind stresses on the sea surface form air bubbles close to the surface that may increase the attenuation of sound waves of the sound transmitted from transducer located above or inside the bubble layer. Vessel movement also in turn induces some air bubbles below the hull of the vessel (Figure A.3 in Appendix A). Weather conditions (i.e. wind speed, wind direction and sea state) are therefore the main factors determining the amount of the acoustic signal that will be attenuated. Data collections were conducted in separate surveys in order to obtain data covering the full variability within the regular fishery acoustic survey areas. Weather conditions varied considerably between each survey of this study. The average Beaufort wind force recorded in the first survey was on average calm at force 3 in the first period (Figure 5.1) (Figure A.2 in Appendix A shows the typical condition of the sea surface.). During the second period, however, the Beaufort force increased by one level to average force 4, due to high wind speeds in the middle of the survey (Figure 5.2). The sea state during the second survey was twice (at force 6) the first, and remained rough throughout the whole survey period (Figure 5.3). The Beaufort force in the third survey was at force 4 in the first period and then later dropped to 3 in the second period (Figure 5.4 and 5.5). Details and description of the Beaufort force categorization are given in Table C.9 in Appendix C.

The minimum and maximum wind speeds encountered in survey 1 were 1.0 and 22.4 m/s (Figure 5.1 and 5.2). For survey 2, whereas wind speeds less than 5 m/s were not encountered, the minimum and maximum wind speeds were 5.4 and 22.9 m/s respectively (Figure 5.3). In survey 3, the lowest wind speed observed was 10.7 m/s and maximum of 22.8 m/s (Figure 5.4 and 5.5).

It is apparently clear that there was a difference in wind speeds distribution between the three surveys that can be attributed to the seasonal difference in which these surveys were conducted. From the above comparisons it can be supposed that survey 1 weather conditions were generally calm since it was dominated by wind speeds below 10 m/s (Figure 5.6). In contrast, survey 2 and 3 are considered as rough weather conditions since they were dominated with occurrences of wind speeds above 10 m/s (Figure 5.6). Although it is previously reported in many studies that these wind speeds that wind-induced air bubbles are

already produced at these wind speeds (Dalen and Løvik, 1981; Berg *et al.*, 1983; Ona and Mamylov, 1988), there were low insignificant acoustic energy attenuations observed in this study.

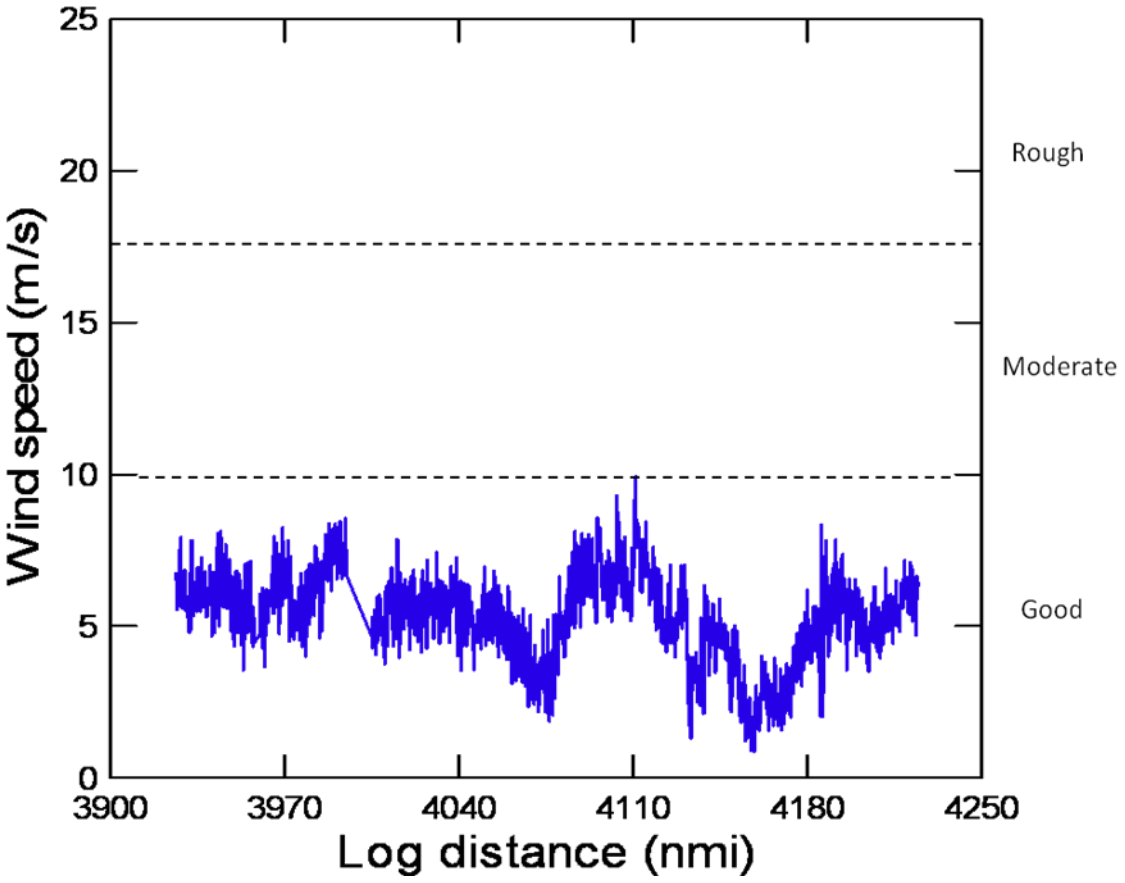

Figure 5.1. Prevailing wind speeds encountered during the period 1 of survey 1 data collection over the survey distance of 310 nmi. Also shown on the right of this graph is categorization scale of the weather conditions from good to rough weather conditions.

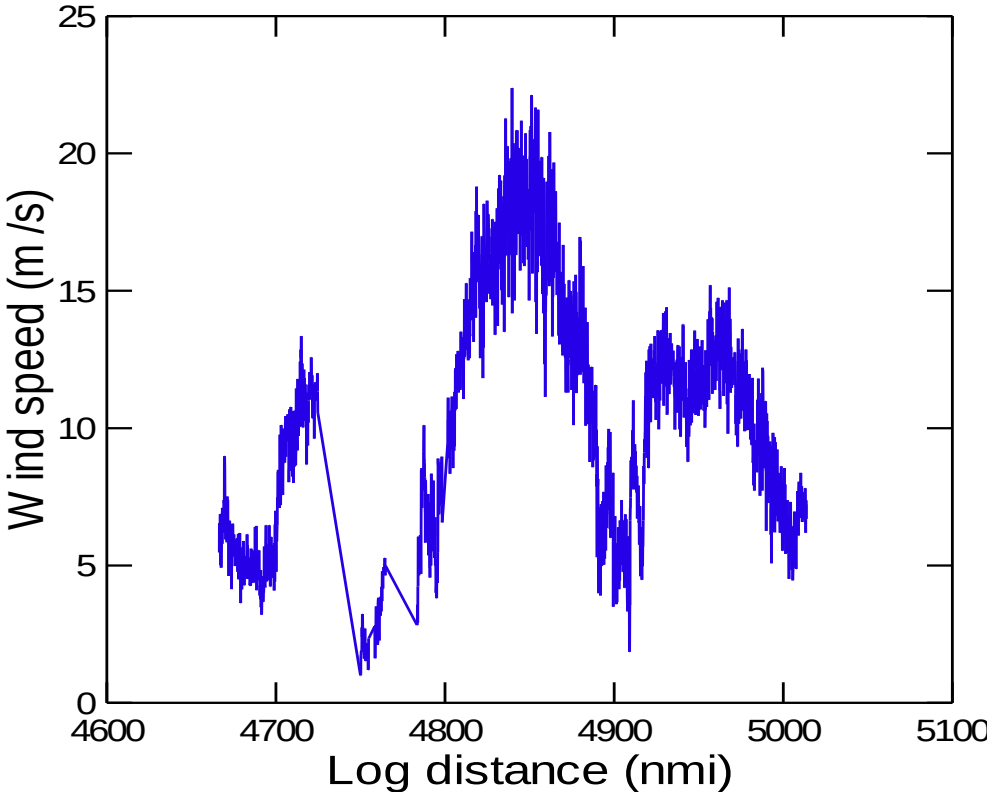

Figure 5.2. Encountered wind speeds during the period 2 of survey 1 data collection over a cruised distance of 365 nmi. The long lines are periods when acoustic data collections were ceased.

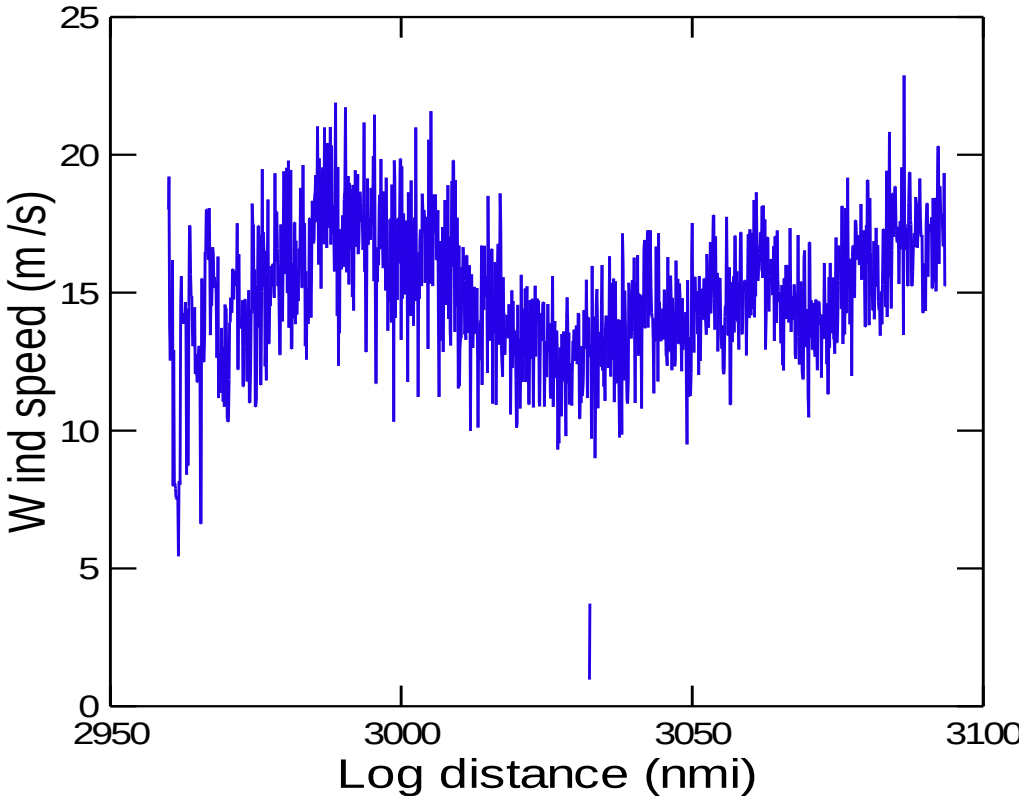

Figure 5.3. High wind speeds encountered during the conduction of survey 2 over a cruised distance of 149 nmi.

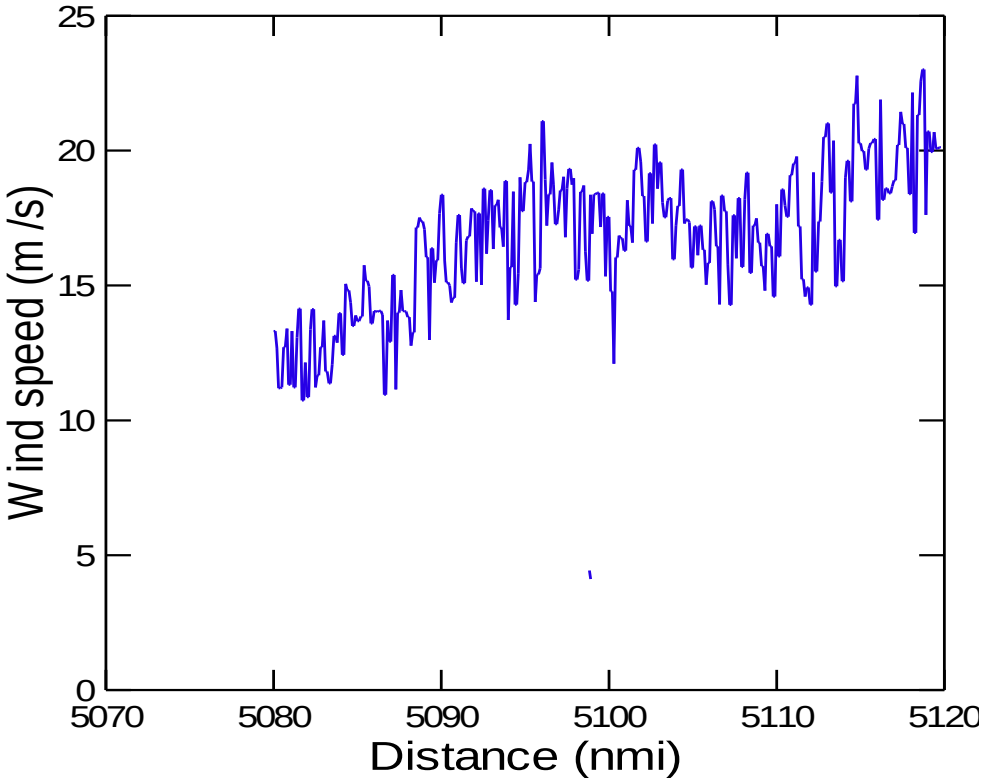

Figure 5.4. Prevailing wind speeds encountered during the first period of survey 3 data collection over a travelled distance of 100 nmi.

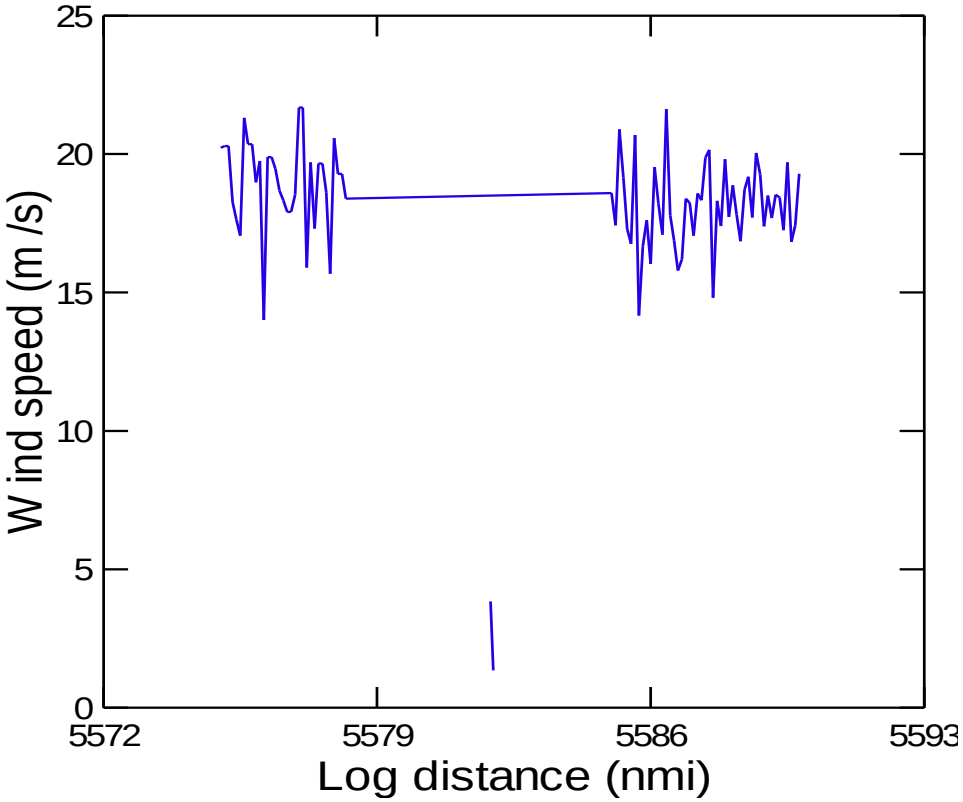

Figure 5.5. Prevailing wind speeds during the second period of survey 3 data collection over a short cruised distance of 8 nmi.

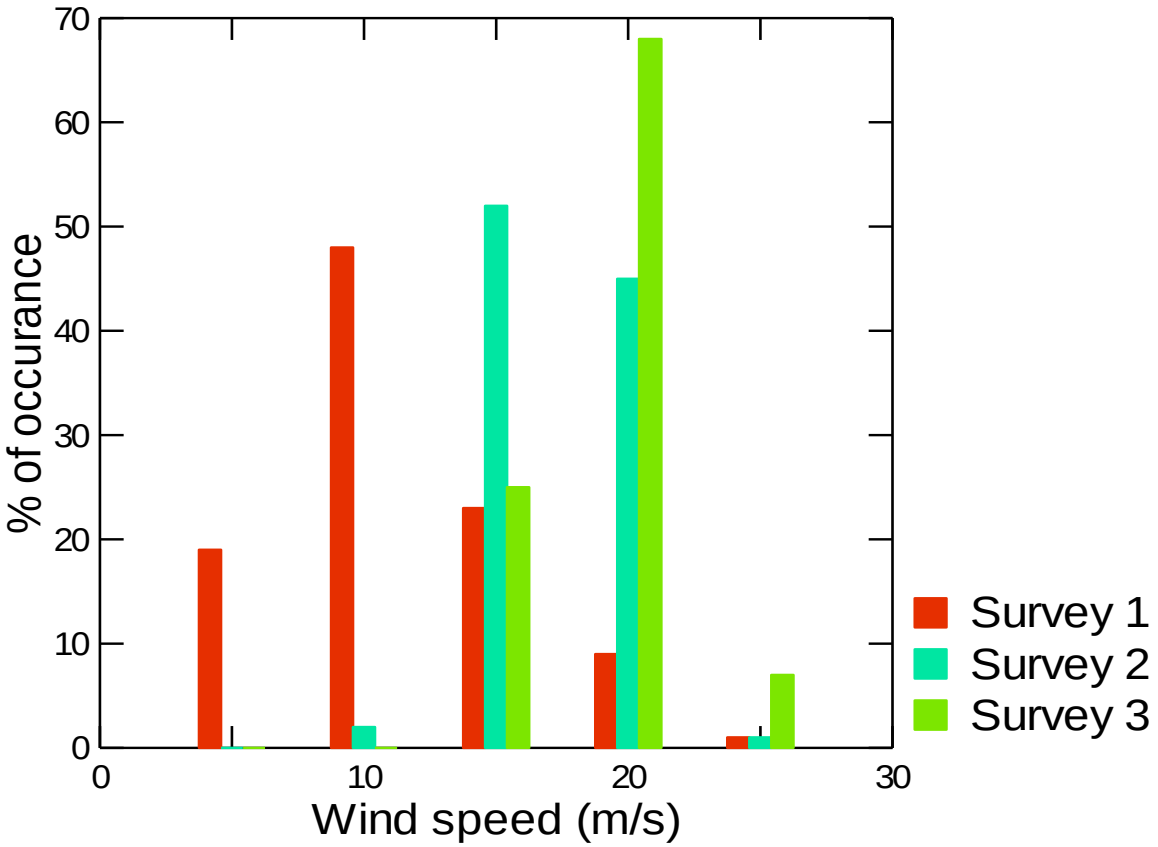

Figure 5.6. The overall frequency distribution of the wind speeds for all surveys conducted in this study.

5.2 Hydrographic conditions

Temperature, salinity and depth are the most important environmental factors that are well known for their effect on underwater acoustic sound propagation by absorbing sound waves (Johannesson and Mitson, 1983; Medwin and Clay, 1998; Simmonds and MacLennan, 2005). The absorption coefficient is usual expressed as the energy lost in dB over a given range (e.g. dB/m). Water temperature varied considerably with depth, with the shallower layers having higher temperatures and the deeper layers having lower temperatures [Figure 5.8 (A)]. The recorded lowest surface temperature was -1 ℃ and the highest was 11 ℃ in the survey area (Figure 5.7). The surface temperatures were observed to be warmer in area around the coast and colder in the open sea. The maximum depth measured by the CTD instrument was 350 m. The temperatures observed in this study are well suited for temperate regions. The salinity values ranged between 34.3-35.1 parts per thousand (ppt). The salinity did not vary with depth [Figure 5.8 (B)]. The analytical combination of salinity and temperature per unit distance give a good reflection of the absorption of sound (Johannesson and Mitson, 1983; Simmonds and MacLennan, 2005). The weather conditions were assumed and believed not to have changed from survey to survey; hence only results from last year's oceanography are presented.

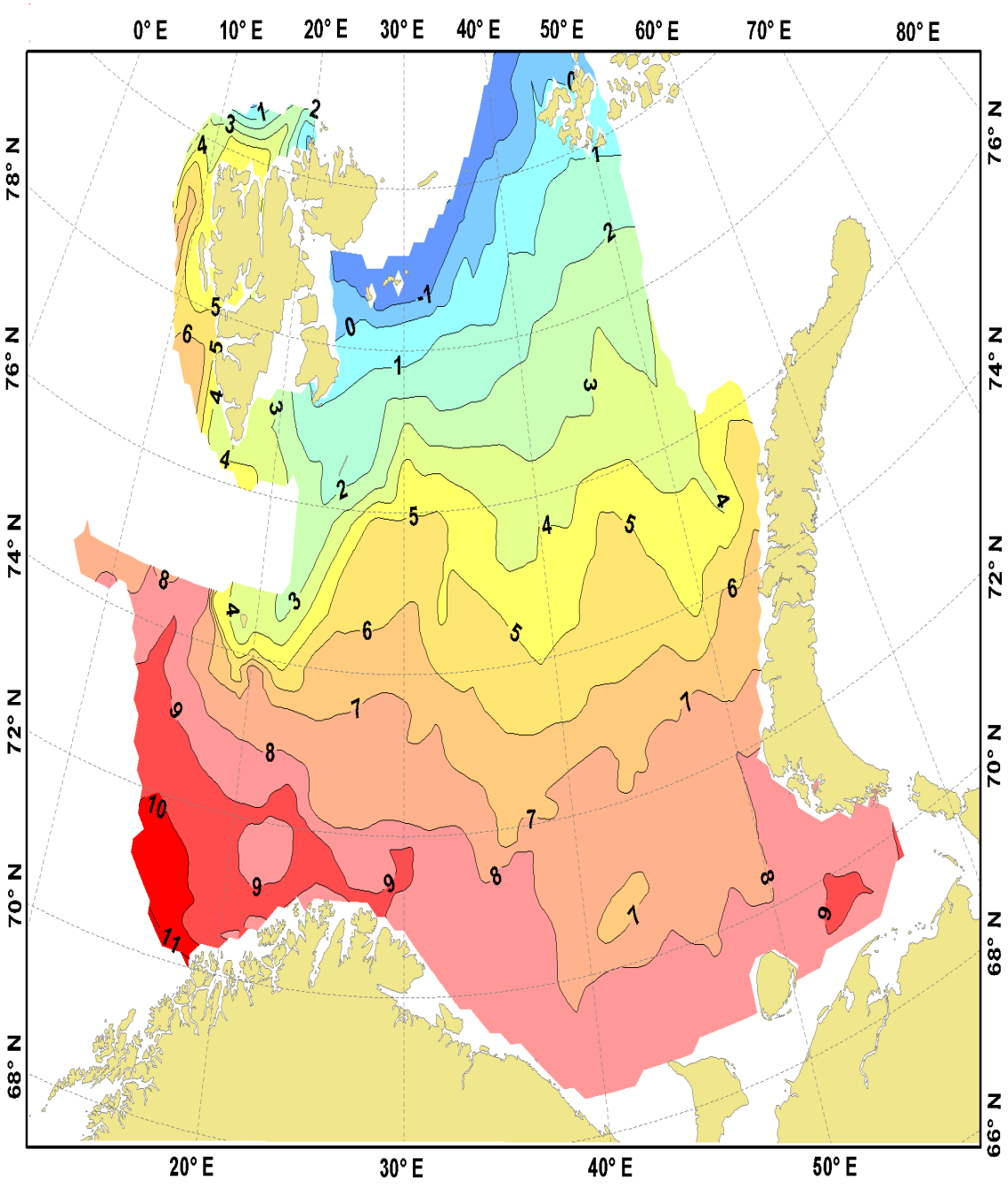

Figure 5.7. Surface temperature of the whole survey area in August-October 2008. (Graph from Barents Sea Ecosystem Survey 2008 report, unpublished.)

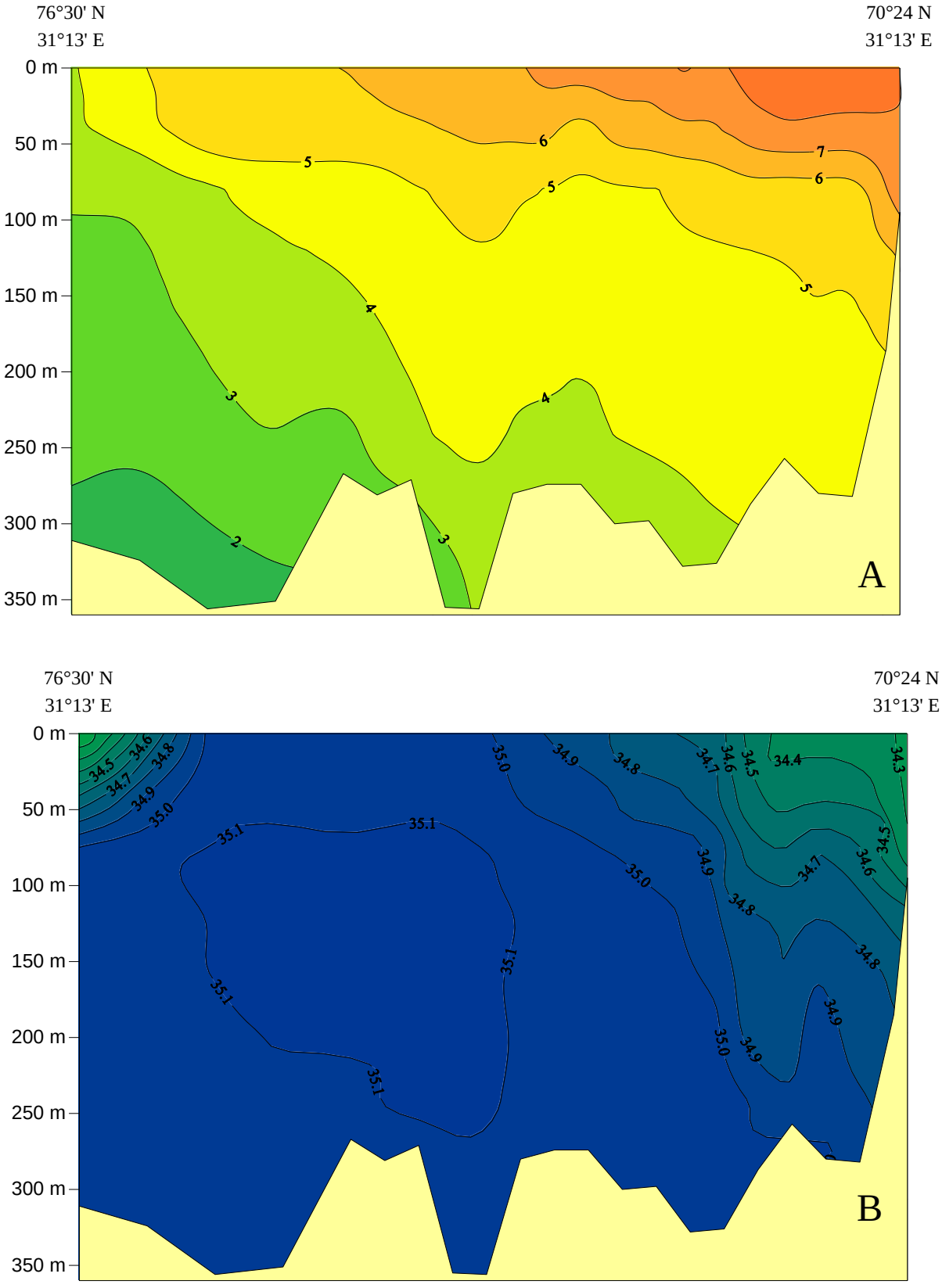

Figure 5.8. Temperature (A) and salinity (B) as a function of depth in the Vardø-North section August – October 2008, an area where most data was collected from. (Graphs from Barents Sea Ecosystem Survey 2008 report, unpublished.)

5.3 Standard target calibration

Accurate calibration is fundamental to the overall accuracy of the results when estimating the abundance size of a fish stock. The calibration of the entire echosounder system by a copper sphere under the two transducer systems was performed at 5 m transducer depth without encountering any technical problem. Although the hull-mounted transducer was not calibrated for many years, the calibration gain indicated that the two-transducer systems performed both exceedingly well. The root mean square (rms) value of the calibration results from the beam model for the hull-mounted was 0.11 dB and 0.14 dB for the keel was, the wind speed in the calibration site was 6.2 m/s in both instances (Table C.1 and C.2 in Appendix C). The above rms values are unquestionably well below the recommended Simrad value of 0.2 for the calibration to be considered good and successful (Simrad, 2008).

Based upon the sphere calibration results, in Survey 1 and 2, a correction factor of 1.59 dB was used for the data collected using the hull-mounted transducer and a correction factor of 1.04 dB for data collected using the keel-mounted transducer (Table 4.2). The corrected s_A ratios of the measured area backscattering coefficient of the two systems were significantly different (paired samples t-test, p-value < 0.05) from those before calibration (Figure 5.9 and 5.10). The pattern of bars in the graphs follows a normal distribution. For Survey 3 that was conducted after the sphere calibration where the whole system was updated according to the calibration output, the bottom s_A ratio distribution is shown in Figure 5.11. The distribution of the ratio in this survey more resembled a Poisson distribution. The ratio is above the expected one, which indicates that there was a high sound attenuation experienced in the hull system since this third survey was conducted in high wind speeds ranging from 15 to 25 m/s.

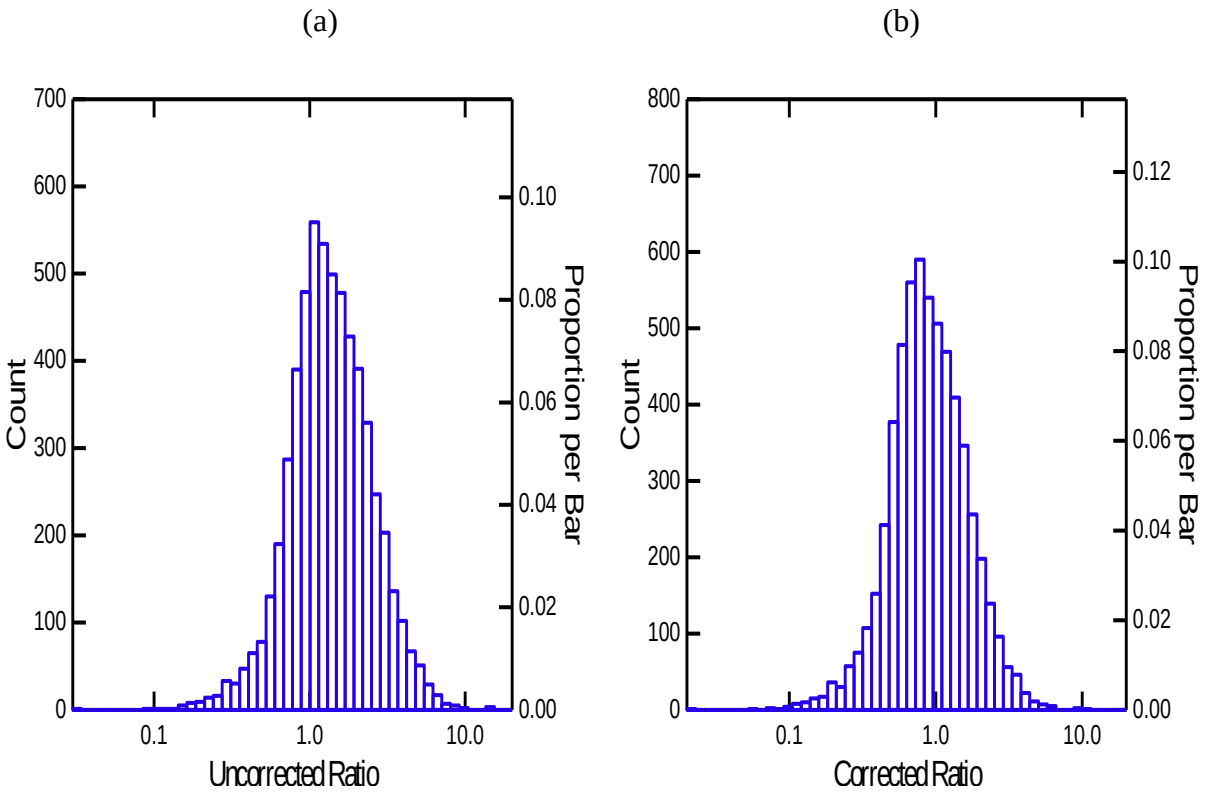

Figure 5.9. The frequency distribution bottom s_A ratios from Survey 1 indicating an improvement from the backscattering coefficient ratios before (a) to after (b) correction.

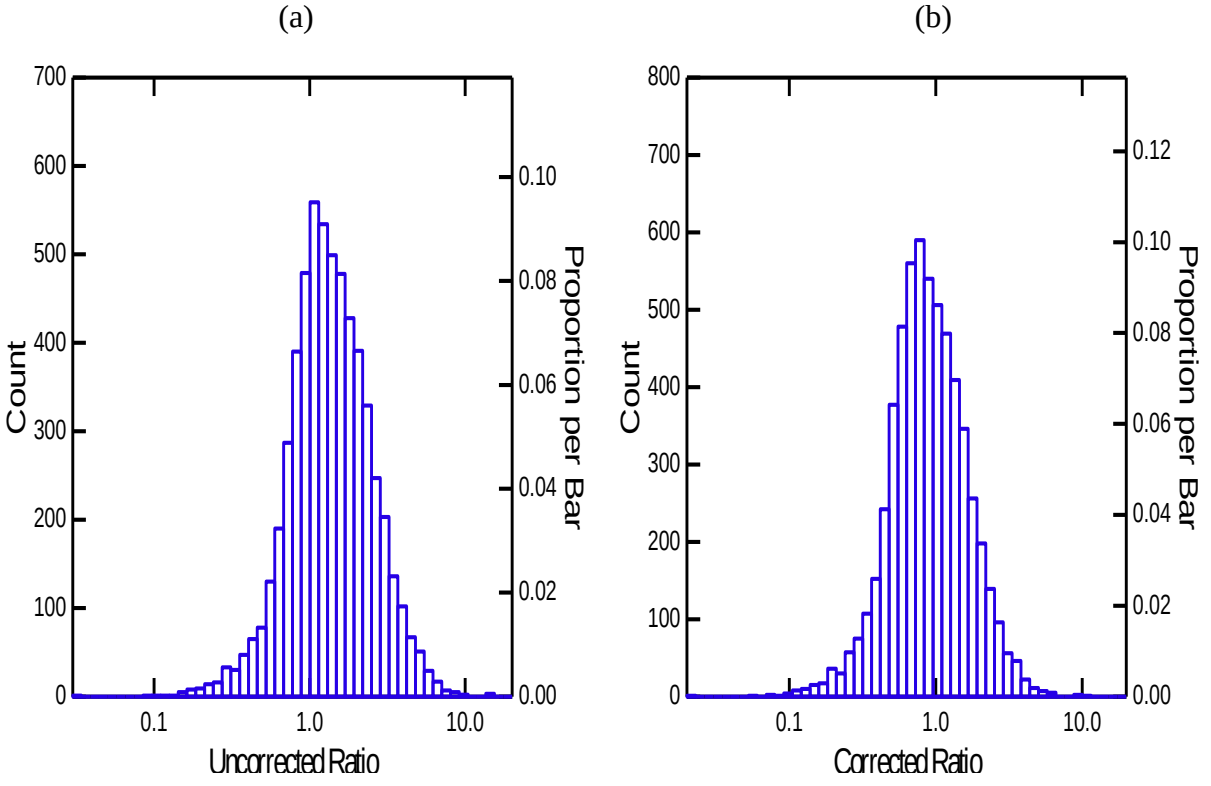

Figure 5.10. Histograms of the mean bottom s_A ratios frequency distribution for survey 2 before (a) and after (b) backscattering coefficient correction.

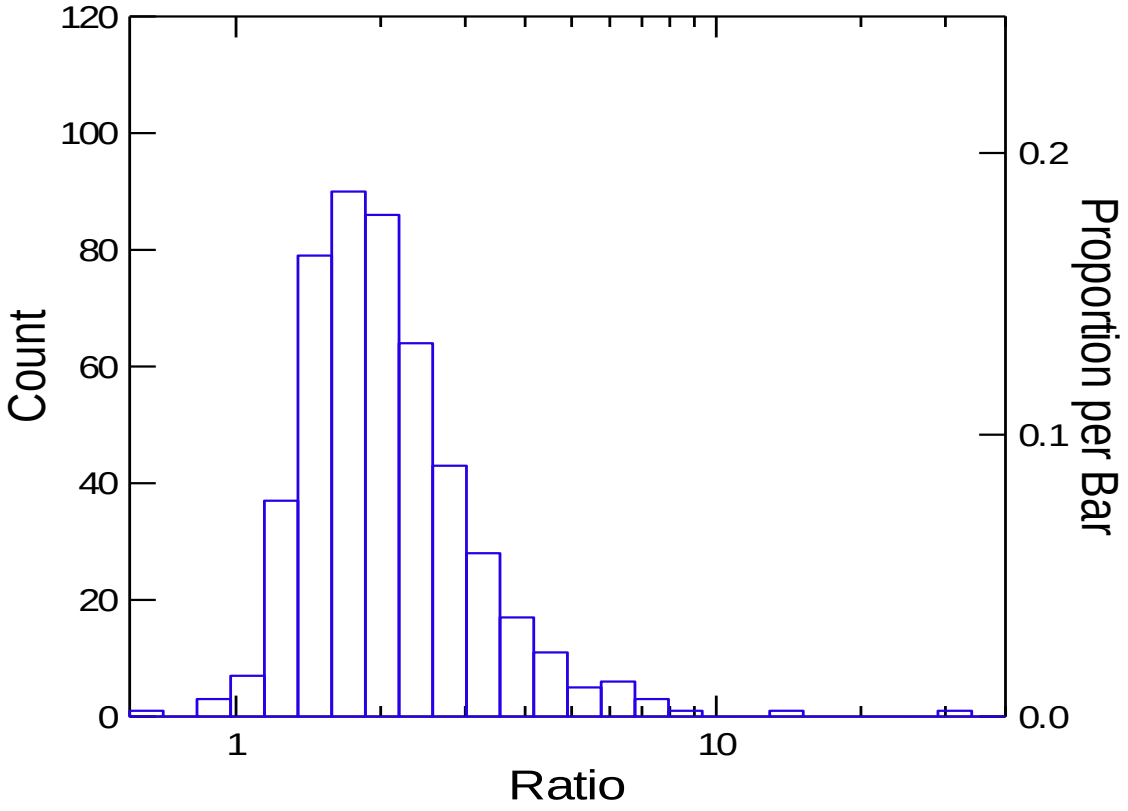

Figure 5.11. Histogram of the uncorrected bottom s_A ratios frequency distribution plotted by data directly obtained from sea measurements during Survey 3.

5.4 Intersystem acoustic calibration

Now that the electronic units are stable and the standard targets of high accuracy were available for the on-axis calibration, it should be possible in theory to obtain very close agreement between the two transducer mounting systems. The primary assumption of inter-calibration is that the two-transducer mounting systems of interest will on average give equal bottom echo intensity. The two systems should have the same number of samples, for pair-wise comparison. The sample sizes are well correlated to the cruised distance of the surveys. The first survey had the biggest paired sample size of 5872, followed by the second survey with a paired sample size of 1336; and the third survey had the smallest paired sample size of 483. These pair's results from the LSSS showed that the sample sizes from the two systems were as expected when using a multiplexer. The bottom s_A mean ratios between the two systems per wind speed group are also well approximately one at least in good to moderate weather conditions (0-15 m/s wind speeds). The ratio close to one positively confirms that the two systems were performing relative well and that the calibration process was a successful one (Table 5.1). However, in instances with high wind speeds above 15 m/s the ratio deviated from one to above two. Since the bottom s_A ratio is a quotient of two variables with the same dimension, it is expressed here as a numerical value without any unit. The above figures (Figures 5.9-5.11) also prove the good performance of the two systems in most cases with the ratio revolving around one.

Table 5.1. The main results of the basic analysis of the mean ratio (μ ratio) as function of wind speeds, including the Standard Deviation (SD), Standard Error of the Arithmetic Mean (SEAM), 95% Lower and Upper Confidence Limit (LCL and UCL), Coefficient of Variation (CV), the minimum (Min.) and maximum (Max.) values for each survey.

Survey no.	WS	μ ratio	SD	SEAM	95 % LCL	95 % UCL	CV	Min.	Max.
1	0-5	0.954	0.578	0.019	0.918	0.991	0.606	0.105	5.792
1	5-10	1.039	0.827	0.016	1.007	1.071	0.777	0.071	9.785
2	5-10	1.055	0.271	0.059	0.932	1.178	0.257	0.484	1.635
1	10-15	1.278	0.748	0.022	1.234	1.321	0.586	0.292	10.105
2	10-15	1.257	0.359	0.015	1.229	1.286	0.285	0.403	3.496
3	10-15	1.806	0.591	0.058	1.691	1.921	0.327	1.011	4.556
1	15-20	1.483	0.523	0.025	1.434	1.532	0.353	0.495	3.926
2	15-20	1.341	0.400	0.018	1.306	1.375	0.298	0.599	3.652
3	15-20	2.433	2.184	0.130	2.178	2.688	0.898	0.617	33.375
1	20-25	1.537	0.511	0.084	1.367	1.708	0.322	0.788	2.627
2	20-25	1.433	0.414	0.138	1.115	1.751	0.289	0.848	2.305
3	20-25	2.347	1.015	0.192	1.953	2.741	0.433	1.204	5.530

5.5 Bottom backscattering strengths

5.5.1 Backscattering strengths of the two systems

All the nautical area backscattering strengths of the bottom echo discussed here are the corrected using the calibration correction factor. The uncorrected were not considered except for survey 3 (where calibrated systems were used). The nautical backscattering coefficients of the two systems are highly suitable for the linear regression; the correlation coefficients were high in all surveys. In survey 1, the bottom S_A values from the two systems were highly correlated with an r-value of 0.759 (Figure 5.12). The response in survey 2 was better as well with the r-value of 0.805. It is evident in Figure 5.13 that some points are shooting beyond the low confidence limit; those can be said to be pings that were highly attenuated by air bubbles hence there are outliers. In survey 3, the response of the two systems was highly correlated (r = 0.941). The deviation of the data from the mean was generally narrow (Figure 5.14), which also indicates that the responses of the two systems were closely related. The linear regression slope is also close to one as in all other surveys.

The legends LCL, UCL, LPL and UPL in the Figures 5.13-5.15 refer to the 95 % Lower and Upper Confidence Limit, Lower Prediction Limit and Upper Prediction Limit respectively. Further regression results for all surveys are shown in Table C.4 in Appendix C.

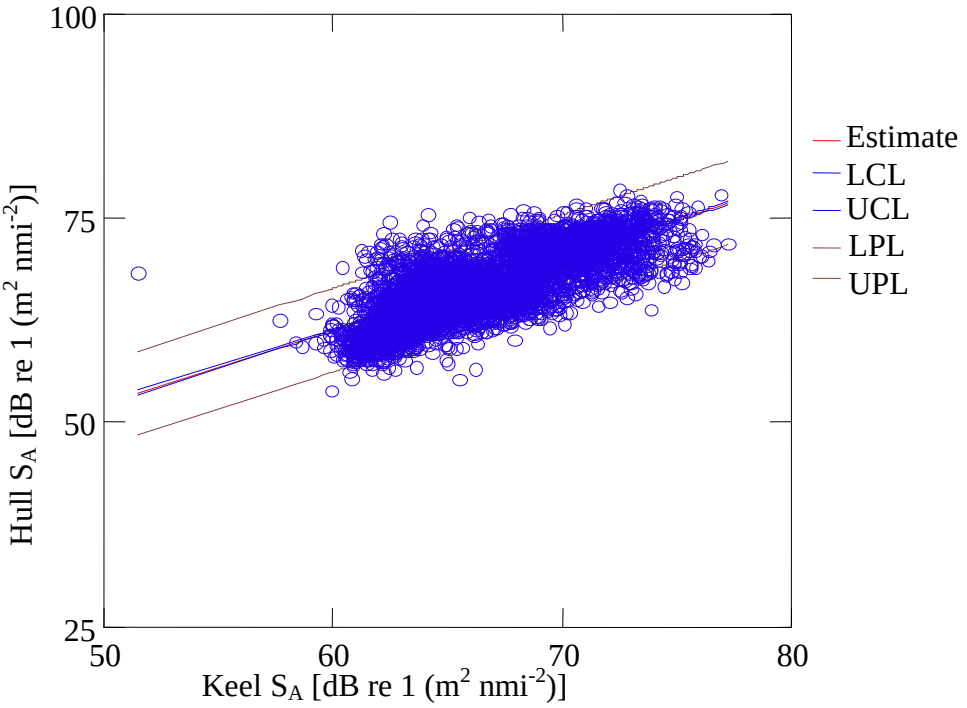

Figure 5.12. The relationship between the nautical area backscattering strength of the bottom echo from the two systems during survey 1. The estimated regression slope between the two systems is 0.902 and the Pearson correlation coefficient of 0.759.

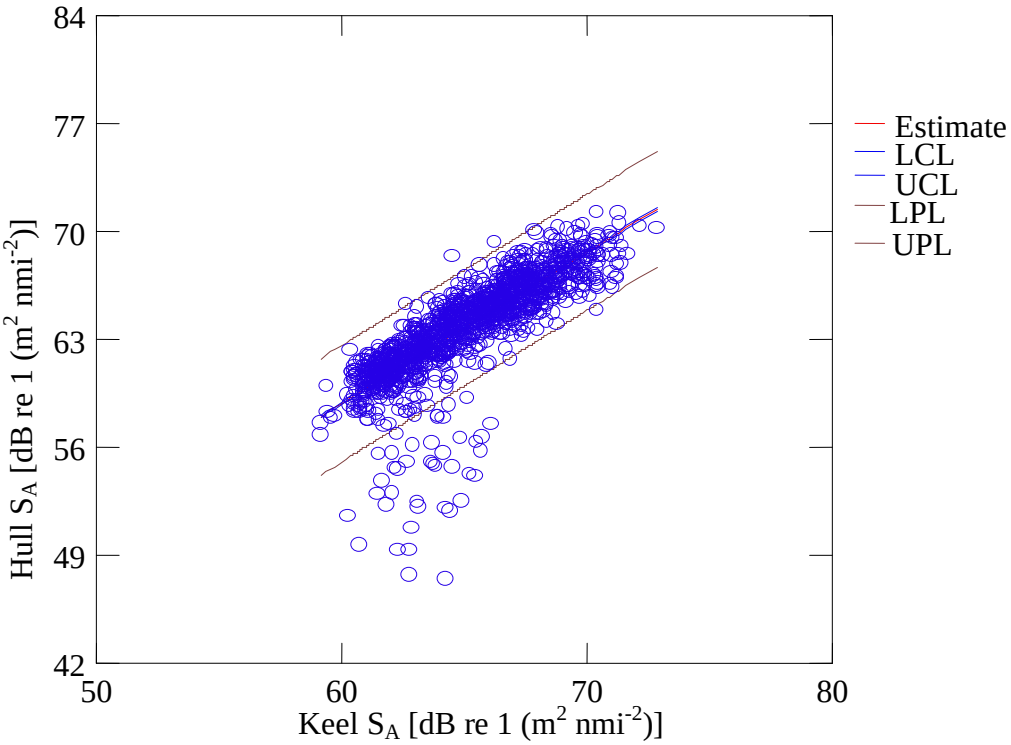

Figure 5.13. The relationship between the bottom nautical area backscattering strength of the keel-mounted transducer versus hull-mounted transducer from survey 2. The estimated regression slope was found to be 0.959 and a Pearson correlation coefficient of 0.805.

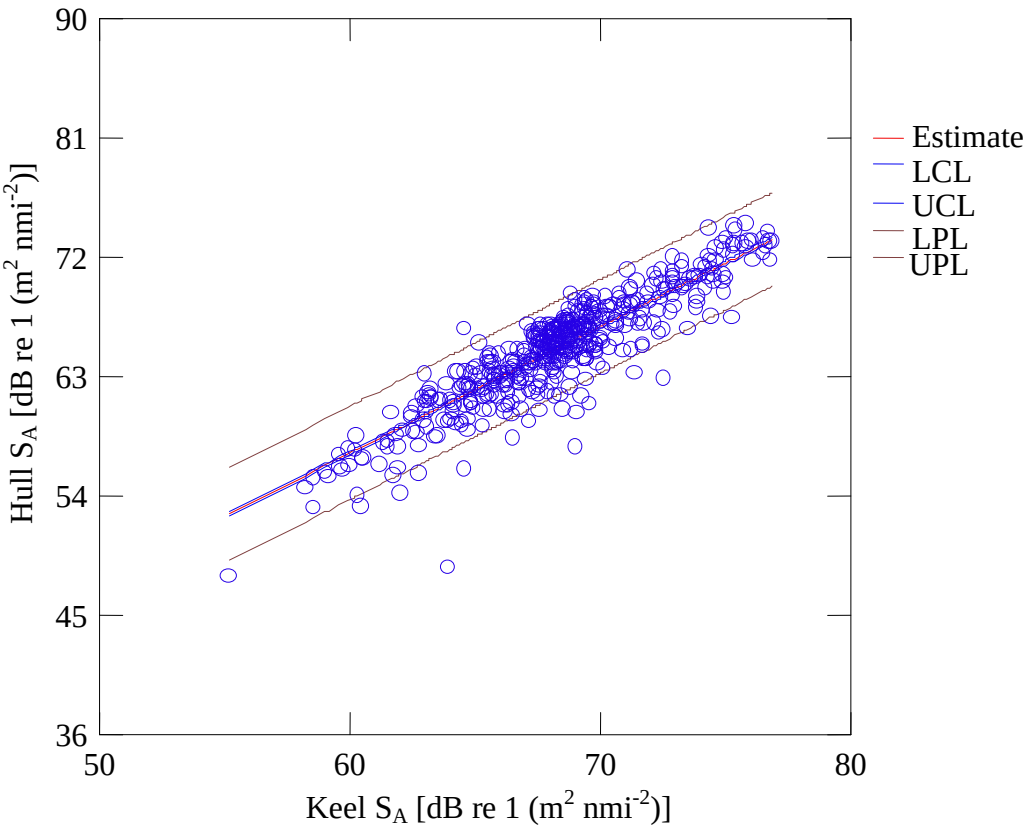

Figure 5.14. The nautical area backscattering strength response during survey 3 for the two-transducer systems in wind speeds 10-25 m/s. The estimated regression slope between the two systems is 0.989 and the Pearson correlation coefficient is 0.941.

5.5.2 Nautical area backscattering strength (S_A) according to wind speed groups

The nautical area backscattering strengths from each survey were treated separately according to different prevailing wind speeds. The comparison of the mean area backscattering strengths per wind group from all surveys indicates that there is a significant difference between the S_A values of the hull- and keel-mounted transducer (paired t-test, $p < 0.05$). The hull-mounted transducer had higher bottom S_A values than the keel-mounted transducer in wind speed groups between 0 and 10 m/s (Figure 5.15), but from wind speeds above 15 m/s the bottom S_A values of the hull-mounted transducer generally decreased more rapidly than that of the keel mounted transducer (Figure 5.15, 5.16 and 5.17). From the plots below it is evident that the bottom S_A values of both systems gradual decrease together with increasing wind speeds. The bottom S_A responses of the two-transducer systems were highly correlated at all wind speeds with a correlation coefficient (r) of 0.999. The bottom S_A is used here due to its compression impact on high area backscattering coefficient values which made it easy to handle the data in logarithmic mode.

In survey 1, the difference in percentage between the bottom mean S_A values of the two systems grouped according to wind speeds ranged from 0.8 - 2.6 %. In this survey at 10 - 15 m/s the bottom S_A decreased gradually with increased wind speeds (Figure 5.15). In Survey 2, there were little percentage differences between the means of the two systems; the range was 0.1 - 2 .3 % (Figure 5.16). Surprisingly, the bottom S_A means of Survey 3 which was conducted after calibration had a widest range in difference of 3.6 - 5.4 % (Figure 5.17). The hull-mounted transducer appears to have low bottom S_A values at a given wind speed above 15 m/s compared to the keel-mounted system. The general reduction of the bottom S_A on both systems is expected where wind speeds increase since the transducer is mostly measuring the bottom at a non-normal incidence, and this is not attenuation but purely an effect of vessel roll. There was no analysis of the day and night attenuation differences since in this instance attenuation is dependent on the wind speed.

There was a variation in the bottom echo nautical area backscattering strengths of the two systems over the cruised log distance (Figures A.8-A.12 in Appendix A). The hull-mounted transducer compared to the keel-mounted transducer had the lowest bottom S_A values over a given distance. The regression lines of the hull system versus the keel system grouped according to wind speeds are plotted in Figure A.16 - A.18 in Appendix A. The regression results of the S_A regressed per wind speeds are given in Table C.5 - C.8 in Appendix C.

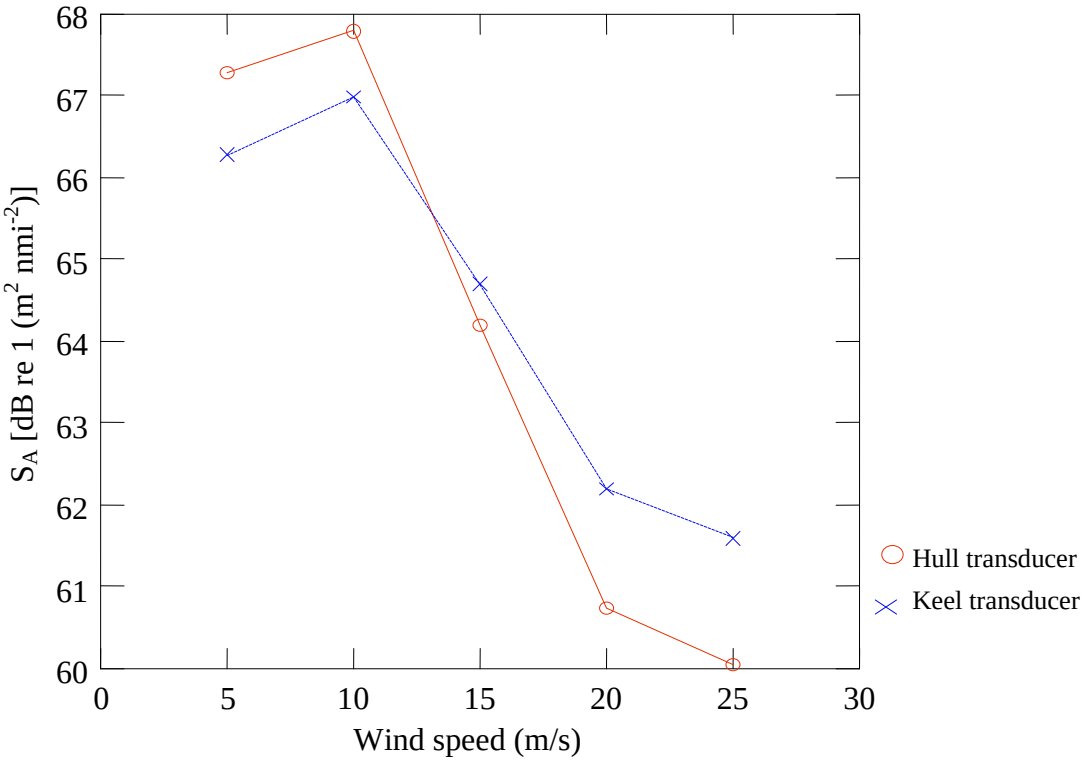

Figure 5.15. The corrected S_A- values for the hull and the keel transducers versus wind speeds for survey 1. The o and the x symbols represent the S_A mean values at a particular wind speed.

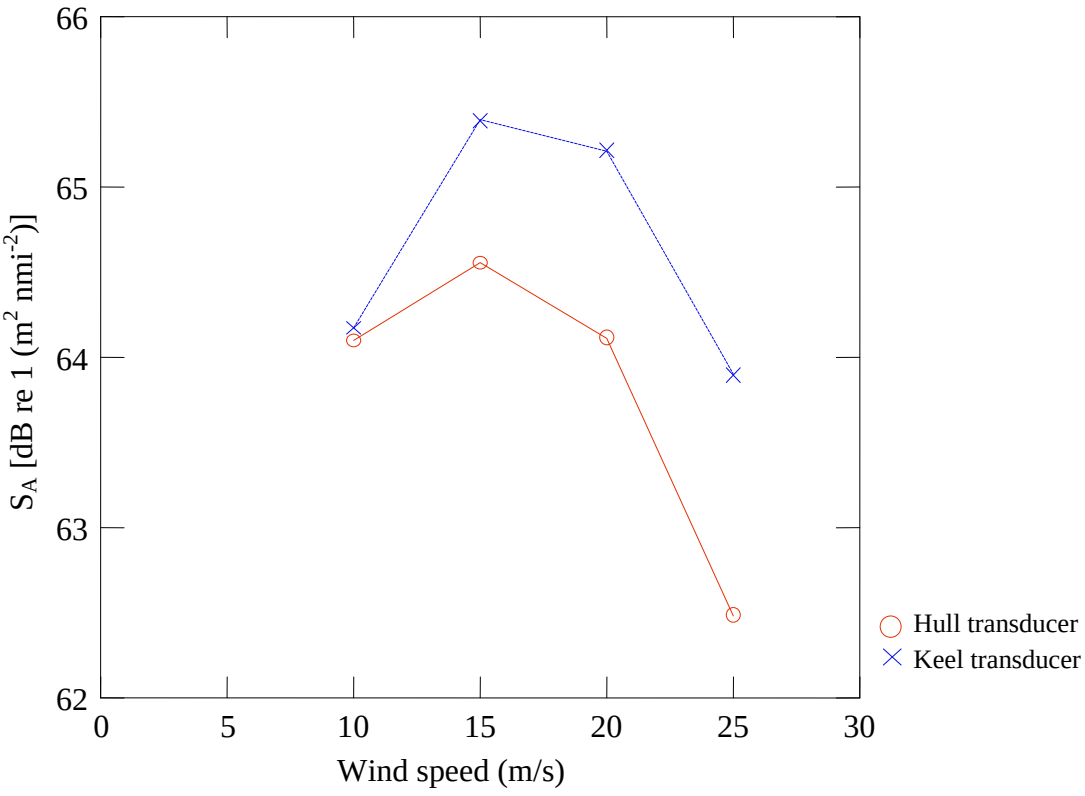

Figure 5.16. The observed S_A- values of the hull and keel transducers versus wind speed in survey 2.

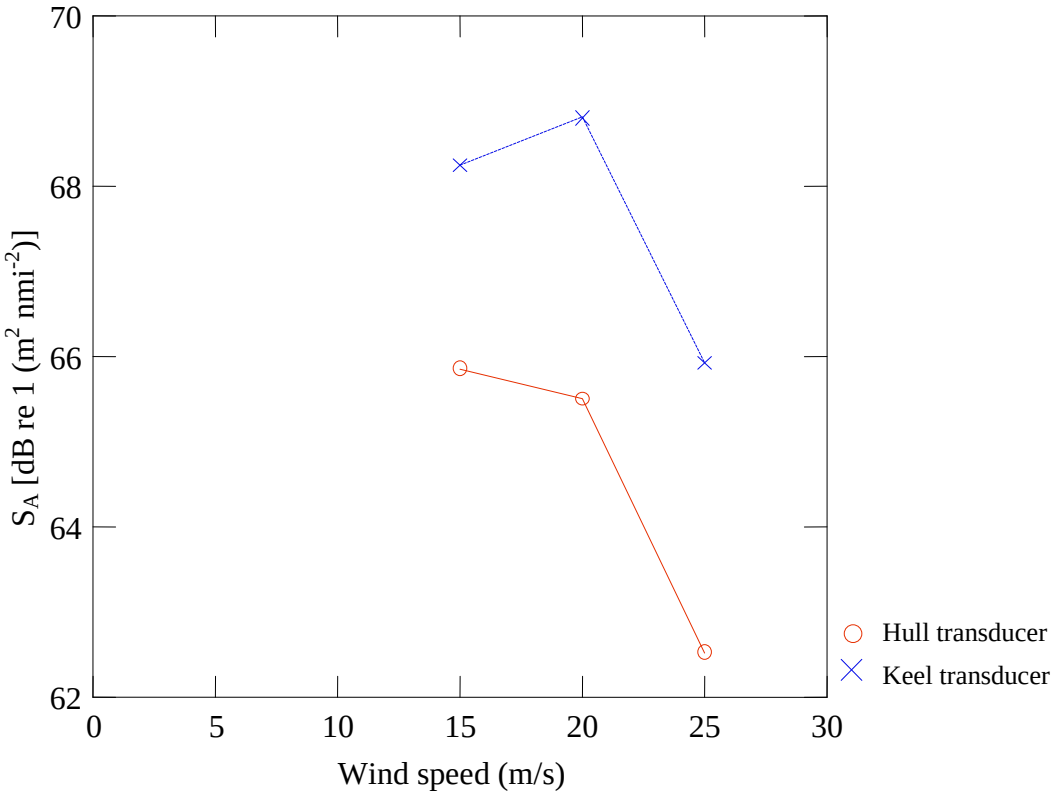

Figure 5.17. The S_A- values of the hull and keel transducers recorded in survey 3 at various wind speeds.

5.6 Vessel heave and roll as an index of attenuation

5.6.1 Heave movement relative to distance travelled

The vertical and horizontal movement of the vessel is here addressed by evaluating the heave and roll movements of the vessel. The integrated squared heave (ISH) and integrated squared roll (ISR) per 0.1 nautical mile (nmi) varied considerable over the travelled logged distances in each survey. In the first period of survey 1, the vessel heave mean and range were 0.202 and 1.233 m respectively [Figure 5.18 (a)]; the mean of the roll was 1.405° and a range of 10.729° [Figure 5.18 (b)]. In this first period, the two variables were not correlated at all, with an r-value of 0.303. In the second period of Survey 1 the observed heave mean was 0.290 m and the range was 1.939 m [Figure 5.19 (a)], the roll was highly variable with a mean of 4.791° and range of 31.201° [Figure 5.19 (b)]. In this second period, the two variables were not correlated as a result with an r-value of 0.180. The integrated square heave and roll movement in the above survey appeared to correspond positively to the distance travelled away from the coast, as the survey began in the fjord surrounded by mountains, the heave and roll were low but as the survey progressed towards the open sea the heave movement significantly increased.

The ISH in the beginning of survey 2 was high; it picked up in the middle of the survey but gradually decreasing towards the end [Figure 5.20 (a)]. While the ISR responded in an inverse way, as heave movement increased the roll decreased and vice versa [Figure 5.20 (b)]. The ISH mean was 0.805 m and the range was 3.199 m, the ISR mean was 13.727° and the range of 40.695°. The correlation coefficient of the heave and roll in this survey was low and equal to 0.330. The responses of these two parameters are also related to the cruising direction relative to the waves or wind direction. Surveys 2 and 3 cannot be linked to the distance away from the shore since they were both conducted in the open sea.

Though a short-period survey, in the first period of Survey 3 the ISH had a mean of 0.276 m and a range of 1.725 m. The ISH in the first 25 nmi was less than 0.5 m and then increased in the last 15 nmi above 0.5 m [Figure 5.21 (a)]. The mean ISR was 6.453° and range of 37.024° [Figure 5.21 (b)]. The ISR in this first period followed the same response as that of the ISH, the correlation coefficient is 0.709. The ISH mean of the Survey 3 second period was 0.328 m and a range of 0.730 m, all values were generally less than one [Figure 5.22 (a)]. The ISR mean in this second period was 29.286° and range of 13.958°, the response is shown in Figure 5.22 (b). The correlation between the two variables in this period was low, equal to

0.120. Apparently Survey 2 had the highest ISH and ISR compared to the other two surveys. From the above results it becomes clear that the vessel either moves more vertically or more horizontally in relation the wave or wind direction, but not in both directions at same time.

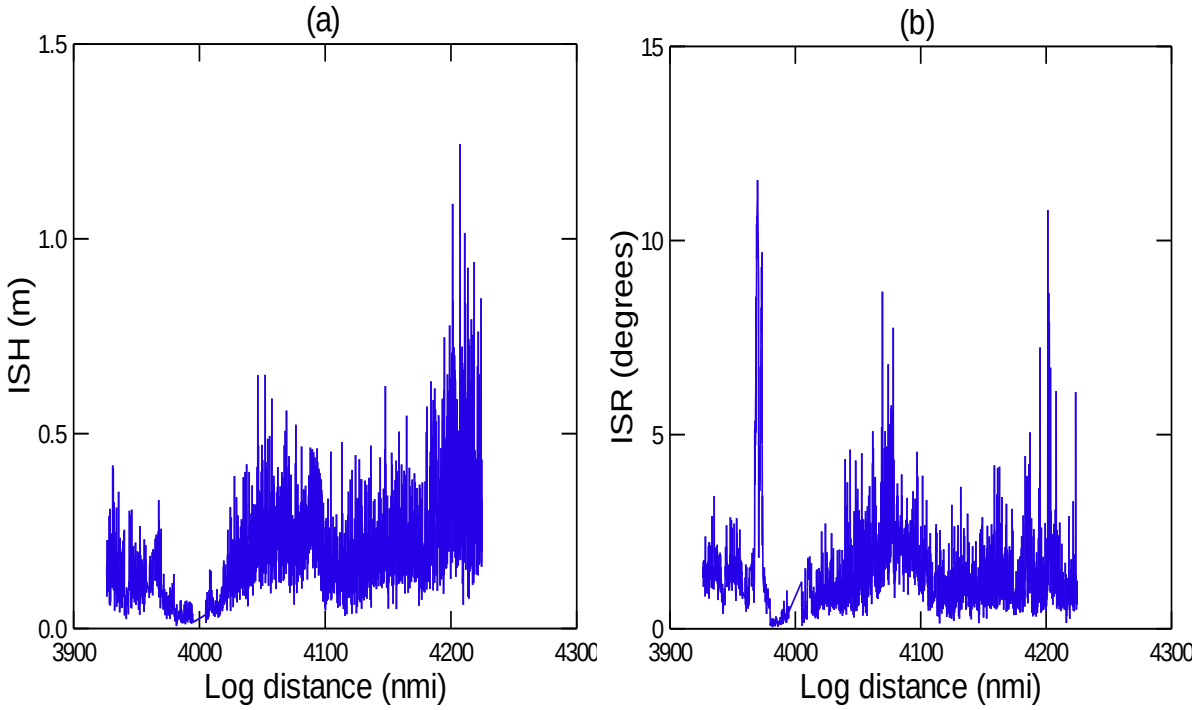

Figure 5.18. Integrated squared heave (ISH) (a) and integrated square roll (ISR) (b) over a cruised distance of 310 nautical miles in the first period of survey 1.

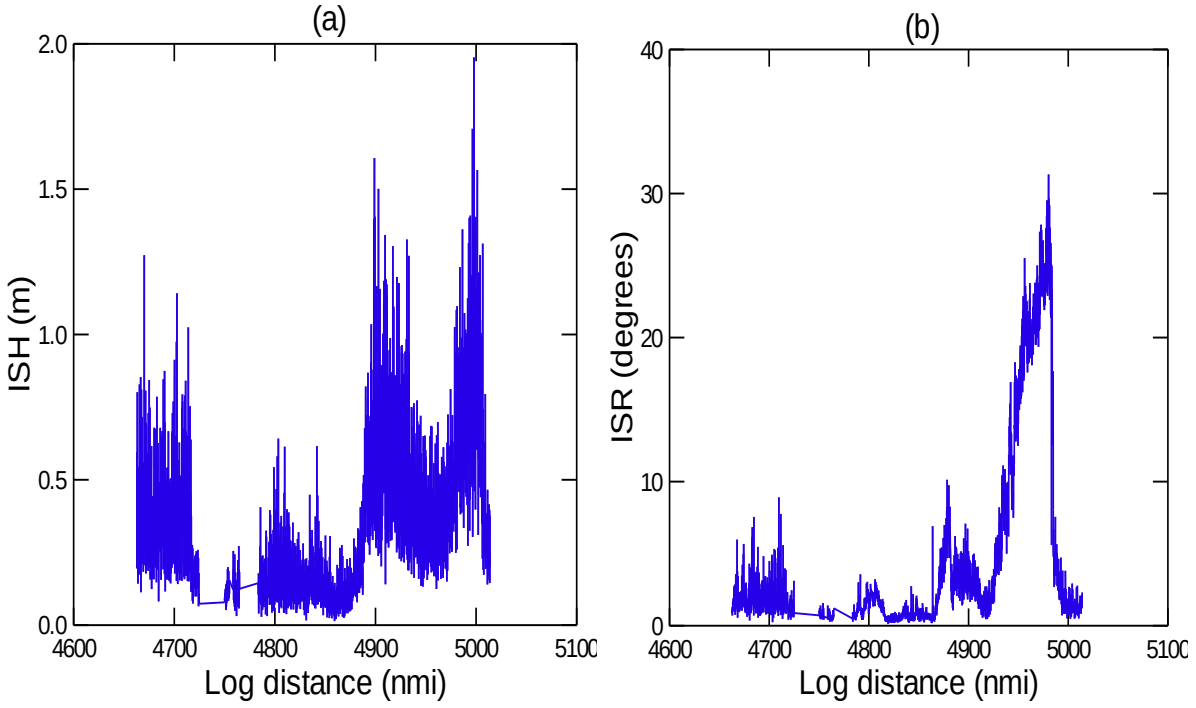

Figure 5.19. Integrated squared heave (a) and roll (b) over a cruised distance of 365 nmi in the second period of survey 1.

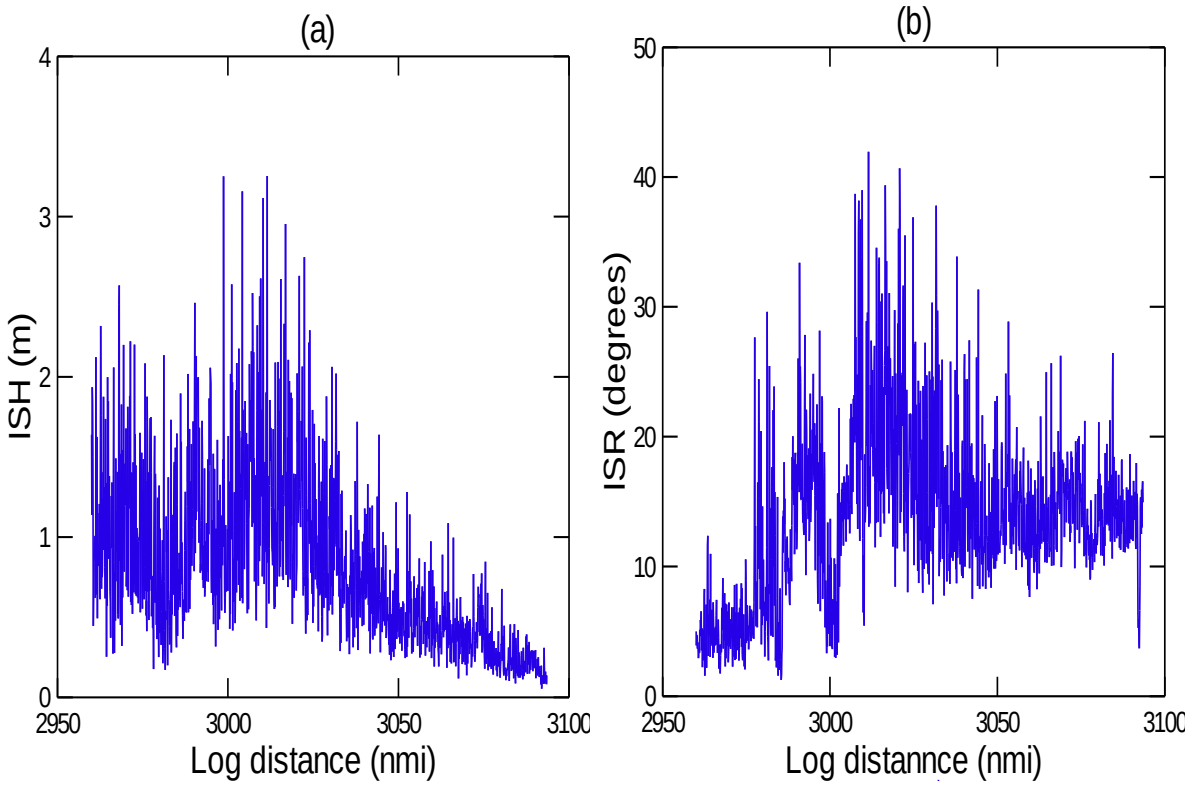

Figure 5.20. The overall ISH (a) and ISR (b) for survey 2 over sailed distance of 149 nmi.

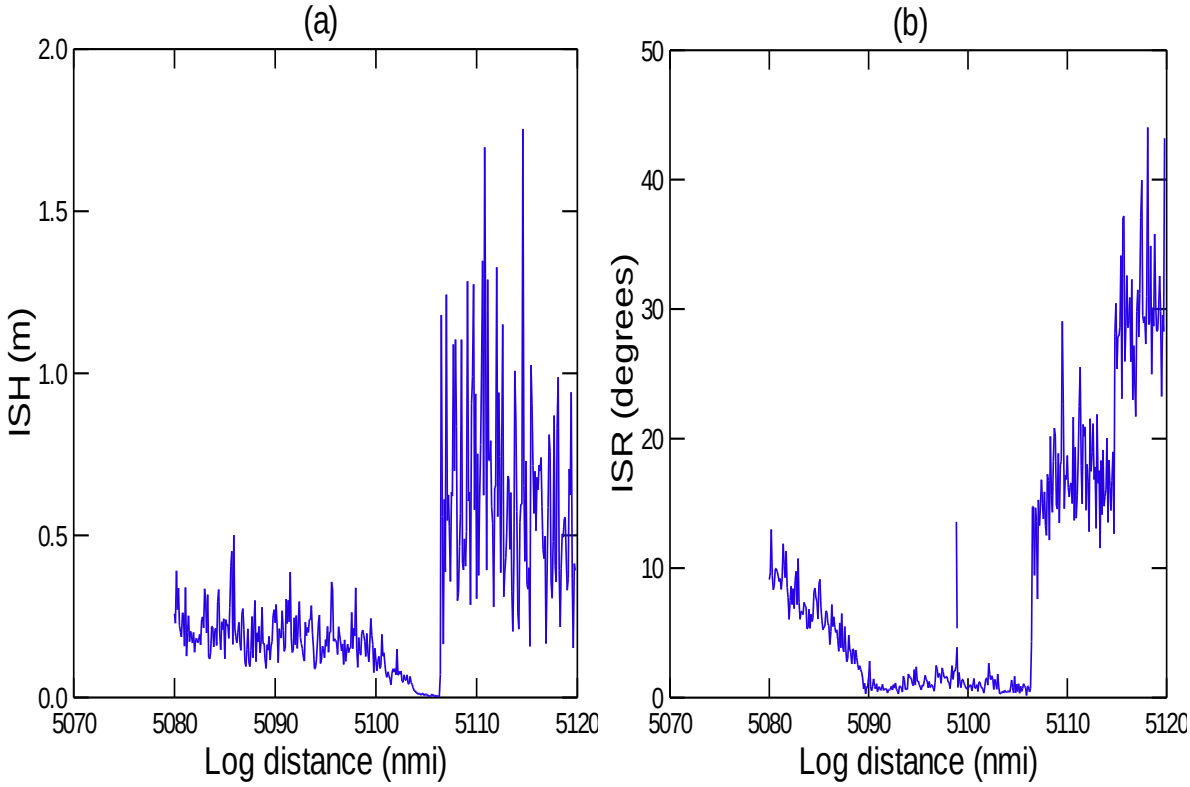

Figure 5.21. ISH (a) and ISR (b) over a cruised distance of 100 nmi in the first period of survey 3.

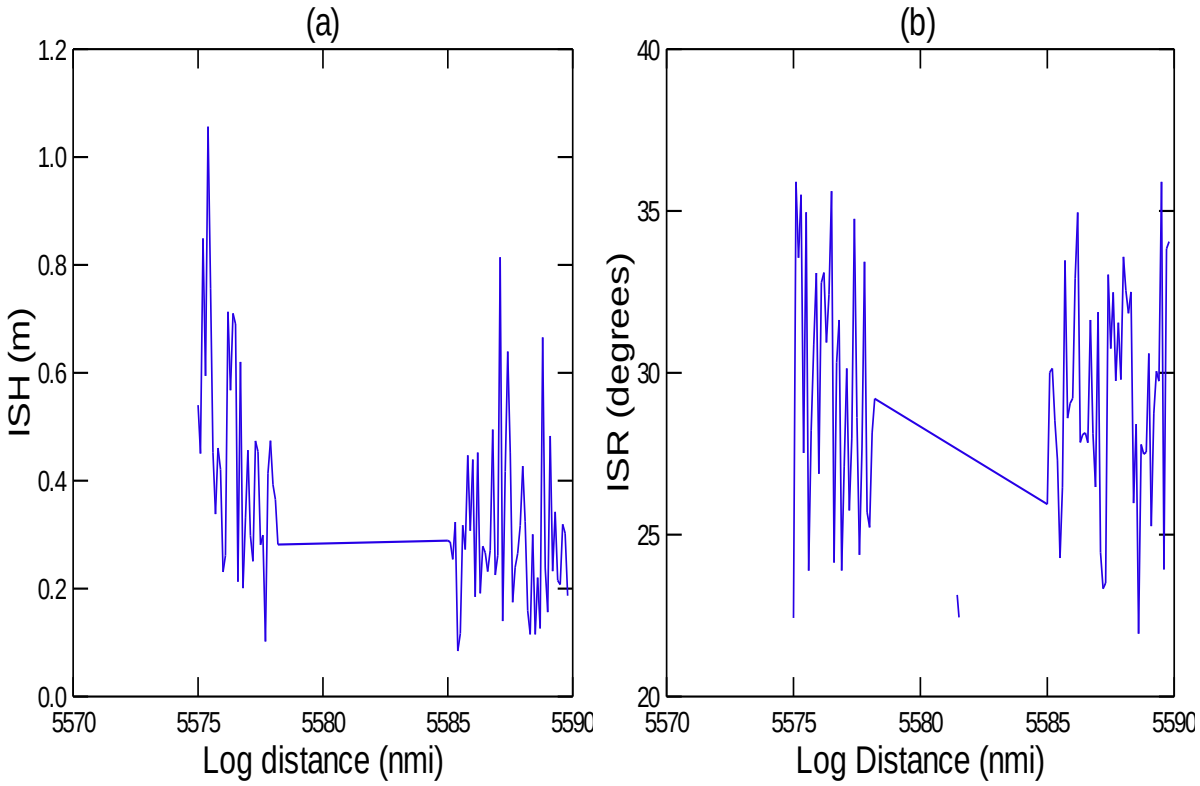

Figure 5.22. The ISH observed over a short cruised distance of 8 nmi in the survey 3 period 2. The straight line in the cruised distance between 5578 and 5586 nmi refers to periods where acoustic data collection was ceased.

5.6.2 Heave movement relative to wind speeds

Wind speed is an influential factor on the overall vessel movement both vertically and horizontal. The heave movement in the first survey was observed to show a rather weak response to the wind speeds, first increasing with the increasing wind speed then later decreasing [Figure 5.23 (a)]. The coefficient of determination (r^2) between the wind speed and ISH for this survey was weak, found to be 0.487. The vessel roll, however, showed a different pattern of response with its values remaining almost uniform in all other wind speeds but picking up at 15 m/s [Figure 5.23 (b)]. The r^2 of the roll versus wind speed was therefore very low at 0.019, showing no determinacy or linearity in the response of the roll. In survey 2 the occurrences were different with the heave appearing to decrease gradually with the increase in wind speed [Figure 5.24 (a)]. There was a high coefficient of determination between the ISH and prevailing wind speeds ($r^2 = 0.996$). The response of the roll in this survey increased in wind speeds between 10 and 15 m/s but decreased at wind speeds above 15 m/s [Figure 5.24 (b)]. The correlation between the roll movement and the wind speed was low; the r^2-value was 0.358.

The vessel heave in the third survey closely responded to the prevailing wind speeds [Figure 5.25 (a)], as a result there was a strong correlation (r^2-value = 0.738). As in the previous first two surveys the roll did not respond to the prevailing wind speeds [Figure 5.25 (b)], with the r^2 value as a result equal to 0.394. The ISH can be claimed here to respond positive in relation to prevailing wind speeds, but the ISR response does not seem to be influenced by the wind speed in the same way. The wind direction and the vessel heading are the determining factors of the vessel pitch/roll (Figure A.5 and A.6 in Appendix A). The size of the vessel is also another important contributing component. Since it was the heave movement which was correlated to the wind speed, it was reasonable to investigate the correlation between the backscattering strength and the heave movement. The comparisons showed that there were correlations between the heave movement and the bottom S_A values from both hull- and keel-mounted transducers (Figure A.19 - A.21 in the Appendix A). Figures A.13 - A.14 indicate the recorded roll and pitch plotted with standard deviations in various wind speeds. In good weather conditions, like in survey 1, it is normally expected that there should be no correlation between the bottom S_A values and heave movement since the vessel is assumed to be at its best stable environment. However, in bad weather conditions like in surveys 2 and 3 it is generally expected that there should be a correlation between the two parameters. Unexpectedly, there were very low correlations between the bottom S_A-values and heave

from the linear regression computations, although a weaker bottom echo is recorded at high heave positions. The dots in the figures below designate the mean while the whiskers designate the standard deviation. The standard error would have given better impression how the precise was the mean measured, it is used here since the data were found to be auto correlated hence the standard error could be computed.

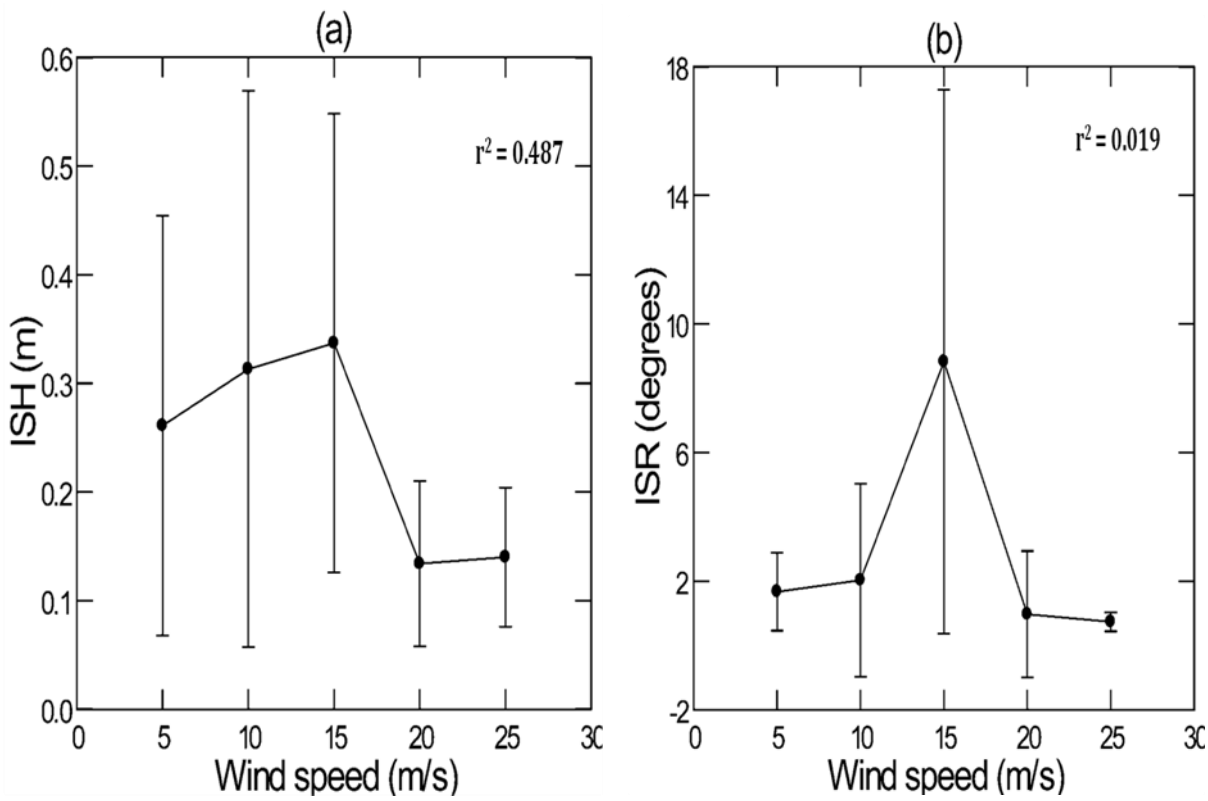

Figure 5.23. The mean ISH (a) and mean ISR (b) with standard deviations as function of the wind speeds in survey 1.

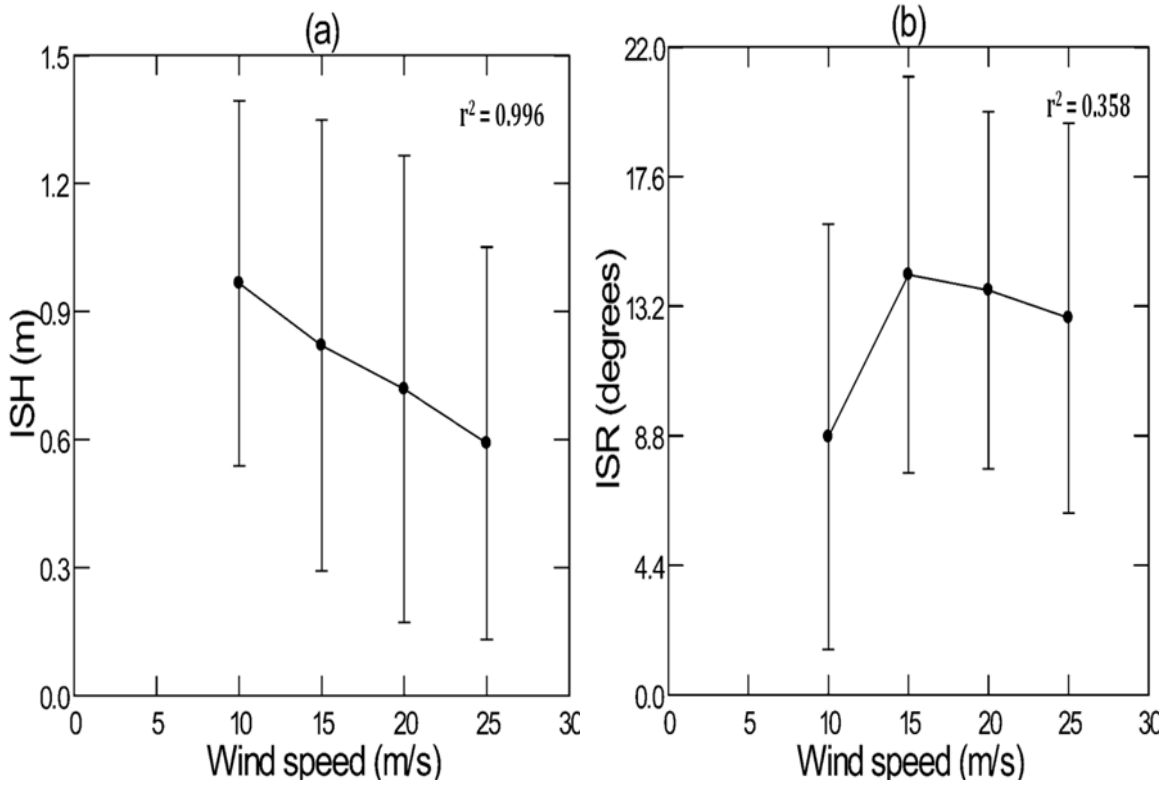

Figure 5.24. The mean ISH (a) and mean ISR (b) per wind speed observed in wind speeds 5 - 25 m/s plotted with standard deviations for survey 2.

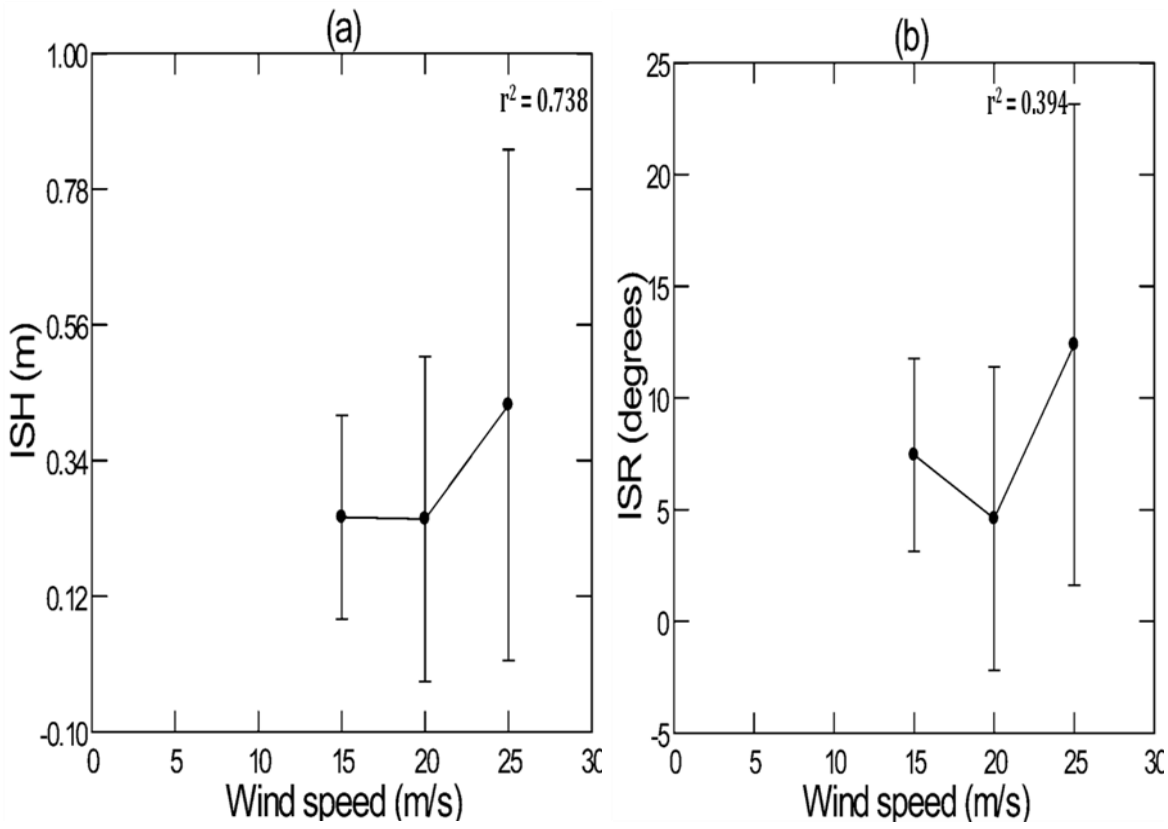

Figure 5.25. The observed mean ISH (a) and mean ISR (b) per wind speed groups at 15-25 m/s during survey 3.

5.7 Model applicability [Foote (1983) vs. Foote et al. (1992)]

After detailed and careful analyses of the acquired data from all surveys it became apparent that only one model could be applicable in this study at least in good weather conditions, the Foote (1983) linearity principle. The model of Foote *et al.* (1992) was not applicable since it requires the measurement of the non-computed extinction cross-section. It was planned to measure the extinction cross-section through the bubble layer by measuring the area backscattering coefficient of the bubble layer with simultaneous measurement of the bottom echo. Unfortunately, it was hard to define the upper layer limit for the bubble layer since the vessel heave compensation was activated in the echo sounder. Software must be made to remove this effect, and this was not available before the completion of this thesis. This part of the investigation was therefore omitted in the analysis.

5.8 Absolute correction factor establishment

There were two possible ways of establishing the absolute correction factor. The first was the use of the bottom s_A ratio of the 38 kHz two-transducer systems in various wind speeds. The second method was the use of heave movement as an index of the observed attenuation. The second method was not applied in this study due its complexity and lack of validation data. The bottom s_A ratio was here a very practical and robust method since all the required factors were well established, the mean bottom s_A ratio is the correction factor. Since the data in this study were treated separately according to surveys, they are here below reported in that manner. In survey 1, there was a high estimated r^2-value of 0.962 between the wind speed and mean bottom s_A ratio. The mean ratio per wind speed was generally less than 2 (Figure 5.26), and the overall mean bottom s_A ratio for this survey was 1.258. There was no significant difference between the mean ratios per wind speed category (one sample t-test, $p > 0.05$), although the mean ratio showed to increase with wind speed up 20 m/s where after it stabilized. Looking at the standard deviations in Figure 5.26, it is evident that there was a high deviation of the data around the mean for wind speed between 10 and 15 m/s. There was a special low attenuation in wind speed between 0 and 10 m/s for Survey 1 and 2, with the bottom s_A ratio (correction factor) close to one.

In survey 2, there was strong correlation between the wind speed and the mean bottom s_A ratio with an r^2-value of 0.951. The mean bottom s_A ratios were less than 2 as well; the overall bottom s_A mean ratio of the survey was 1.272. There was no significant difference observed between the mean ratios per wind speed category (one sample t-test, $p > 0.05$). In this second survey, it is evident in Figure 5.27 that the standard deviation spread slowly away from the mean values as the wind speed increases. Survey 3, which was conducted under high wind speeds above 15 m/s, the resultant r^2-value was lower at 0.634 compared to other previous surveys. Another important factor that was pointed out in this survey was the high standard deviation per wind group; the deviation was high especially at 20 m/s (Figure 5.28). The mean survey bottom s_A ratio was higher than that of previous two surveys at 2.195. The dashed lines at 1 in the correction axis in all the plots below represent the low limit of one whereby below it there will be low negligible error induced without correction.

For survey 1 and 2, a low numerical wind-determined correct factor was multiplied to the estimated backscattering coefficient, since their bottom s_A ratios are well below 2 (Figure 5.26 and 5.27). As a correction factor the observed integrator values at an average wind speed

of 20 m/s in survey 1, a 1.483 correction factor should be applied. For survey 3, the correction factor should be higher since mean bottom s_A ratios per wind speed are right above two (Figure 5.28). In a normal survey situation, a separate correction factor for each elementary sampling unit should be applied, for example per 1 nmi.

The overall correction factor is therefore established by averaging mean bottom s_A ratios and the standard deviations per wind speed for all three surveys (Figure 5.29). The correction factor increases exponentially with increasing wind speed until wind speeds reach 20 m/s where the correction factor stabilizes. The established correction factor can be applied to all surveys of this study or any other similar studies where the same or equivalent platform is used for data collection.

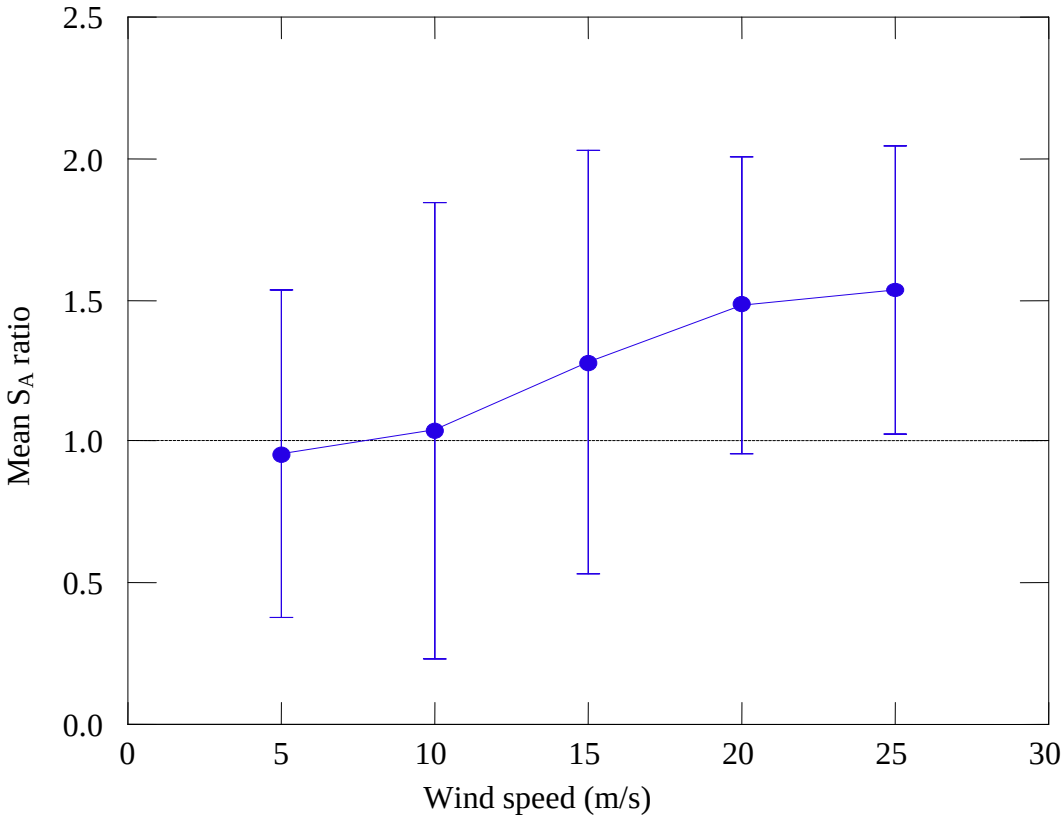

Figure 5.26. Mean backscattering coefficient ratio plotted with standard deviations in various wind speeds for survey 1 at 38 kHz.

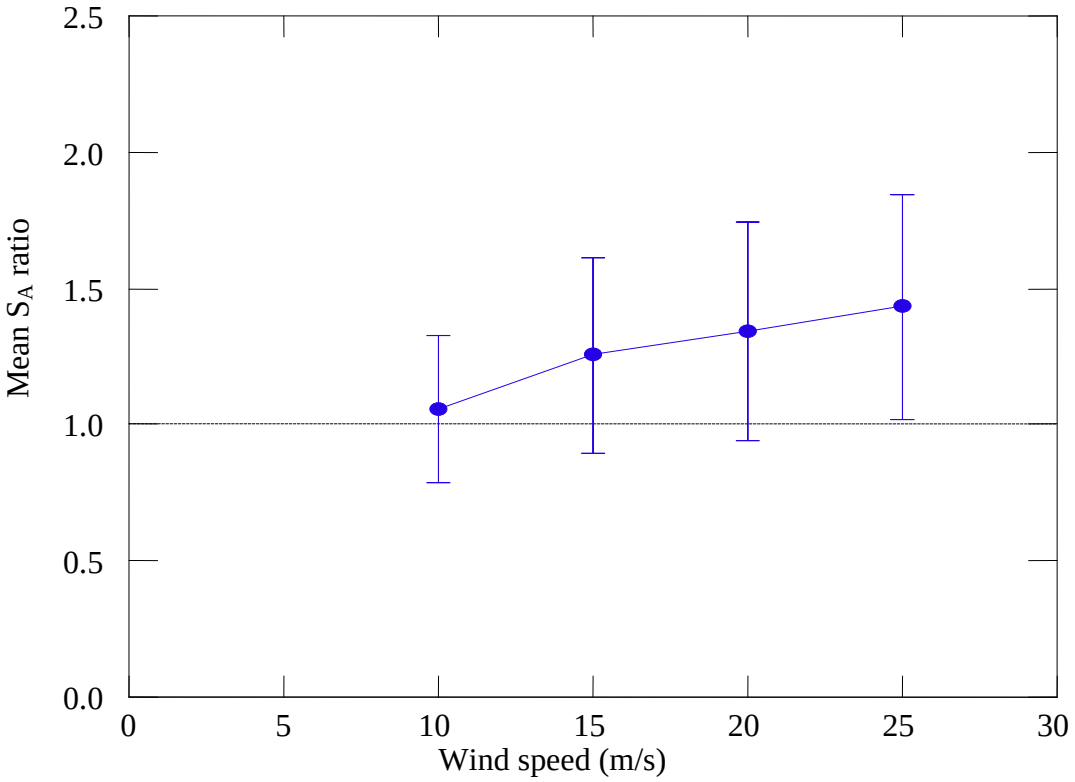

Figure 5.27. The mean bottom backscattering coefficient ratio in survey 2 in relation to the prevailing wind speeds at 38 kHz.

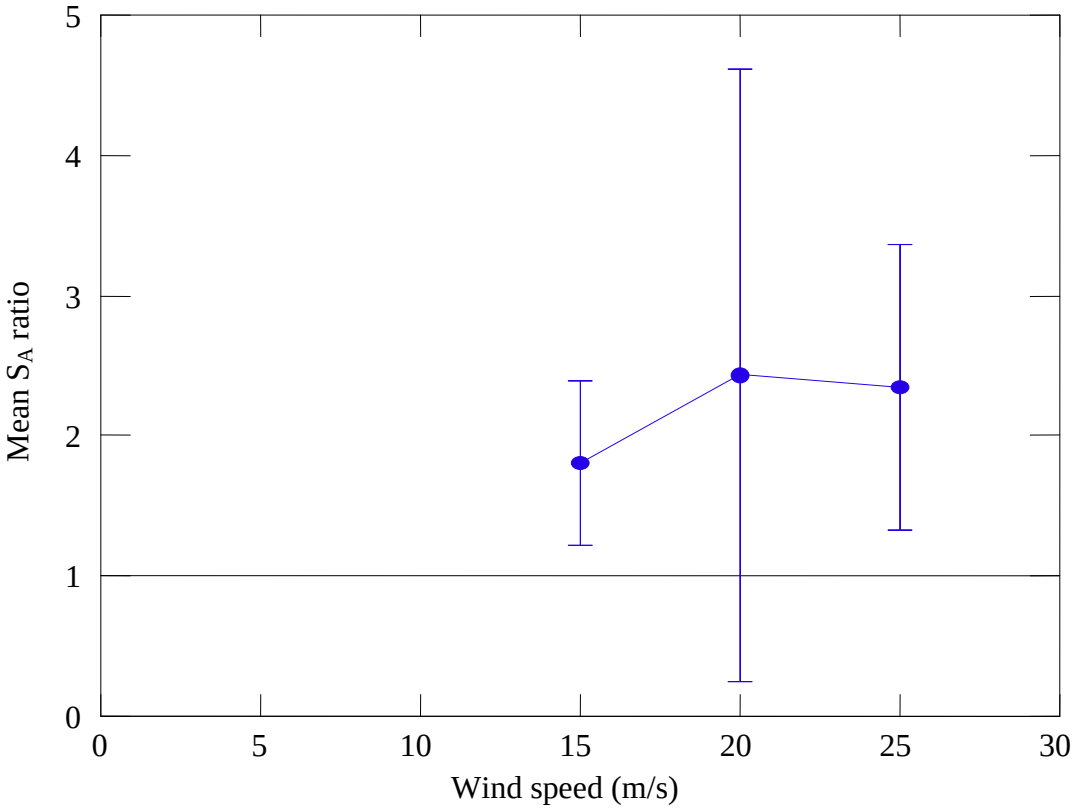

Figure 5.28. The mean backscattering coefficient ratio versus wind speed at 38 kHz observed in survey 3.

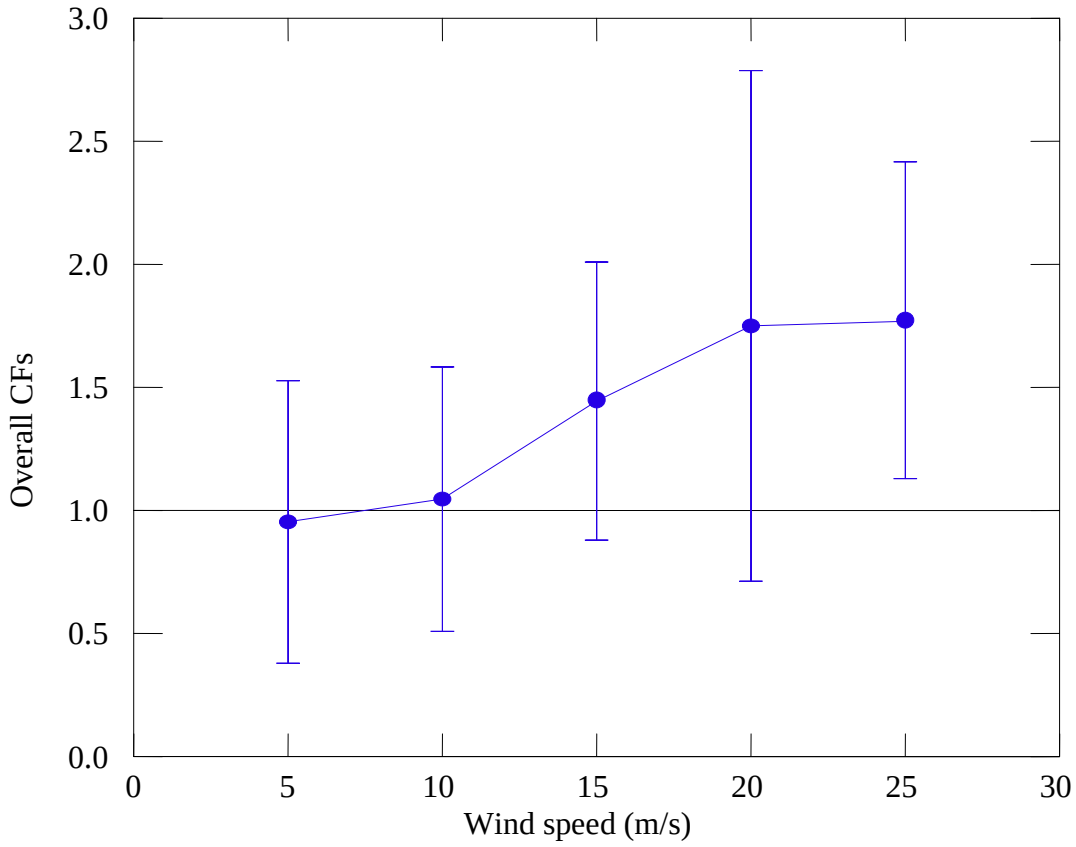

Figure 5.29. The overall correction factors (CFs) for all surveys in this study at different wind speeds.

6. DISCUSSION

6.1 Alternate pinging

The alternate pinging between the hull- and keel-mounted transducers was successful achieved through the specially built multiplexer system. This allowed the collection of data using the same ping rate and investigations of the same bubble layer with the two-transducer systems. The double coverage by the two transducers significantly saved significant survey time, which reduced greatly the survey costs and the bias introduced when sampling different air bubble layers, which would be the case in serial operation. The technique seemed to work well in general except for two discrepancies that were discovered during initial use; first a longer time delay than usual expected for survey work in the two 38 kHz ER60 echograms. Secondly, there were empty pings between each ping stored to the ER60 data. These deviations, which could not be removed at this stage with the post-processing system. Although these did not affect the echo integration, it prevented us to use the system under regular survey work.

Only a fraction of the otherwise available data was therefore collected now, mainly within time periods in the surveys that were not used for abundance estimation. Therefore, it is suggested that data is collected in areas where a ping rate of 0.5 sec^{-1} can be used in the survey, ensuring a normal ping rate of 1 sec^{-1} on the used keel transducer. With special attention, this can be achieved at depths of about 350 m with the EK60, if data storage is limited to the same range. Also, in order to improve the analysis of the bubble layer, the recordings should be made with no heave compensation. There is to our knowledge no recently published literature on the measurement technique for of attenuation correction purposes. The collected material is also not optimal since the investigations reported here was made during surveys with other main objectives. Especially the vessel should have been run in several directions relative to the wind and wave direction to evaluate the real vessel effect on the correction factor.

6.2 Vessel heave movements at various wind speeds

The effect of wind speed vessel heave movements was investigated in this study to evaluate its influence on how much signal is lost out of the beam during these movements. Narrow

beams (around 7°) are pronounced to be significantly affected by the vessel motion resulting in up to 64% error induced if not corrected (Stanton, 1982). Due to vessel motion, the transmitted signal may be received by the side lobe of the beam, which is half the strength on the acoustic axis (Simmonds and MacLennan, 2005). Unfortunately, wind direction relative to vessel heading was not determined since it was not the main focus of the study though it is known to contribute on signal loss. The correlation between the vessel heave movement and the integrated bottom backscattering strengths indicates that there is high potential for the heave to be used as a correction index for air bubble acoustic attenuation. This was also indicated by Ona, (1991), using a slightly different measurement of the heave. Since the heave can carry other information than wind speed, for example wave information and the effect of wind direction, it is important to evaluate these parameters in addition to the pure wind speed. It was observed that there more higher heave movements on the vessel at wind speed between 10 and 15 m/s than in all other wind speeds encountered during surveys. These movements can be attributed to the specific vessel heading direction relative to the direction of the wind and waves as observed by Ona (1991).

Before wind speed exceeds 15 m/s vessels are usually still headed against the prevailing wind direction if surveying in this specific direction. This may then cause high heave movements. But when wind speeds exceed 15 m/s, there is a tendency by vessel captains to change the normal heading direction into a safe or more comfortable direction that will impose less vessel movements. As a result, at wind speed above 15 m/s the heading direction is usually more or less the same direction as that of the wind, i.e. the skipper has turned the vessel with the wind and waves. It can be assumed that low vessel heave movements observed at high wind speed were by the time the vessel encountered winds from astern. With this assumption it can be claimed that results obtained in this study are in agreement with the results of Dalen and Løvik (1981); they found less vessel heave and roll movements when the vessel encountered winds from the astern direction. Winds from astern are also pronounced to push the vessel forward, which can be said to be a "free ride" since the vessel is more drifting with no or little fuel used for cruising at this point in time.

One other factor to be considered is the vessel cruising speed. During bad weather conditions the cruising speed is usually reduced from the normal 10 knots to around six knots. The reduction of the cruising speed gives a more comfortable situation onboard and the vessel can "shock" absorb the impact from rough waves. In addition, in some vessels, the vessel ballast tanks can be filled with sea water to increase the gross total weight of the vessel that helps in

the reduction of the vertical movement of the vessel (Peña, 2009). The hull of the vessel also traps water on its sides as it penetrates the sea waves that may assist in horizontally stabilising the vessel. The above mentioned factors do to some extend improve the stability of the vessel. These can be of pivotal help in understanding the observed decline in vessel pitch and roll at increased wind speeds. Since there are very few published literatures addressing this issue, it is therefore recommended that more effort should be devoted in solving and understanding how these factors may affect the air bubble attenuation, and how variable the ship-effect is.

Knudsen (2006a) claims that the old v-shaped kind of vessel hull design leads to high heave and roll movement compared the modern flat hull design due to the increased hull surface area. Surely many engineers, scientists and other personnel who have been onboard both vessels with either design will agree with the logic of this claim. One vessel with the v-shaped hull was used in this study; it is highly recommended for future studies that will investigate this problem to use two or more platforms with different hull designs. Unfortunately, to the best of our acquaintance there have never been any scientific research directed in investigating this problem in fisheries acoustics; therefore more studies to investigate the influence of this feature are advised.

Based on the general knowledge that small vessels are more affected by the wind-wave actions than bigger ones, hence small vessels experience higher attenuation than big ones. Therefore the heave and roll movement can be evaluated as a function of wind speed to determine the attenuation, since it is heave movements that induces air bubble layer below the hull that cover the face of transducer (Ona and Traynor, 1990; Knudsen, 2006a; Knudsen, 2009). It can be beneficial in the future if trials can be conducted with different vessel sizes to establish correction factors that can be more suitable to different vessel sizes. The effects of propeller cavitations on air bubble production and attenuation also needs to be evaluated.

6.3 Nautical area backscattering strength variability

The results indicated that the 38 kHz hull-mounted transducer was performing fairly well in terms of the resultant bottom S_A in good to moderate weather conditions. At times in good weather conditions the hull system had a higher bottom S_A values than the keel mounted system. Based on the theoretical assumption that the two systems should give equivalent

backscattering strengths, it was expected that the two systems should give more or less identical backscattering. The results section 5.5.2 revealed that this was only achieved in good to moderate weather conditions before attenuation became a problem. It was observed in the results that at wind speed above 15 m/s, the backscattering from the hull-mounted system were significantly reduced compared to those of the keel-mounted transducer.

The variability in the bottom S_A values between two-transducer systems is usually considered to be induced by calibration error and air bubble acoustic energy attenuation. Based on the results from the two confirmation ways, first by the sphere calibration and later inter-calibrated by the bottom s_A ratio, it can be said that the two-transducer systems used in this study were well calibrated. The results can be used to confirm the calibration since the hull- and keel-mounted transducers were observed to be both performing well in good to moderate weather conditions. Therefore the observed variability in bottom backscattering cannot be attributed to calibration errors. The observed difference in the bottom S_A can be associated to the surveyed difference types of the sea bottom, since different bottom types have different acoustic scattering properties (Foote, 1999).

It was generally observed from the results in both systems that the bottom S_A varied from area to area. The bottom depth can also affect the backscattering values of the bottom, since the transmitted intensity is expected to decrease exponential with distance away from the transducer (MacLennan *et al.*, 1990). But since there are no concrete evidence for the variation in properties and slopes of the sea bed (Foote, 1999); hence it is convenient to consider the overlaying bubble layer to influence the bottom echo in both systems. Nevertheless, when associating the variability of the bottom S_A per distance to the wind speed at particular distance it was seen that there was an indirect relationship between the wind speeds and bottom backscattering strength. Since a one level increase in wind speed will result in a cube increase in the bubble layer. Therefore the bottom S_A variability observed here can only be evidently associated to prevailing wind speeds.

From a pilot study by Ona and Traynor (1990) where an American RV "Miller Freeman" was used to investigate the benefits of using the drop keel in improving the quality of the acoustic data in bad weather conditions. The vessel used in their study had an equivalent length size to the vessel used in this study. Ona and Traynor (1990) reported similar variations in the bottom S_A values. Although they simulated the hull by retracting the drop keel its highest position, their study was conducted at various wind speeds with the drop keel in different

positions. They also associated the significant bottom S_A variations observed in wind speeds above 15 m/s to be caused by the bubble layer that is formed in the face of the transducer. No further errors can be attributed to the threshold used by the instrument chief and/or cruise leader during the data post-analyses, since the threshold used was the recommended -100 dB (Parker-Stetter *et al.*, 2009).

6.4 Validity of the correction factor

From the comparison of results of this study to previous studies it was revealed that the correction factors established in this study are relatively low compared to the ones created in the past by Dalen and Løvik (1981) from sea measurements and by Berg *et al.* (1983) from empirically calculations using the bubble estimator. In fact, the correction factors obtain here are even very low compared to the other previous studies even though they were established at high wind speeds. According to our up-to-date best knowledge, there have never been correction factors established in wind speeds exceeding 15 m/s (30 knots). This is the first exploratory study to establish a correction factor at wind speeds above 15 m/s.

Though Dalen and Løvik (1981) and Berg *et al.* (1983) did both collect data in wind speeds exceeding 15 m/s, they did not establish a correction factor at wind speeds above 15 m/s due to the tediousness of the correction factor establishment process at the time of publication (J. Dalen, IMR, pers. comm.). The corrections factors established in this study were established based on a modern and new technique, by using a multiplexer to alternate ping between the hull- and keel-mounted transducers. However, this technique may also be questionable when the weather conditions are really bad, and air bubble attenuation also occur on the keel transducer. In this case, repeated measures of the same bottom under different conditions might be helpful.

The *in situ* correction factors established in this study are in agreement up to a certain level with the theoretical expectation that the correction factor should exponentially increase of the with increase in wind speeds (Dalen and Løvik, 1981; Berg *et al.*, 1983, Ona, 1991). The establishment of the correction factor was based on the assumption that the keel-mounted transducer was not affected by air bubble acoustic attenuation in all weather conditions. However, at high wind speeds like above 17 - 20 m/s the established correction factor was stable and not increasing exponentially. Consequently, it can be said that the keel-mounted

transducer was also experiencing the attenuation problem at those wind speeds. Comparisons to general air bubble acoustic literature, Novarani & Bruno (1982) shows that the results are well within the expected region for transducers at 5 and 8 meters depth, operating at 38 kHz (Figure 6.1). The comparisons prove that this study does not in any way underestimating the bubble effects, hence set a low air bubble acoustic attenuation correction factor.

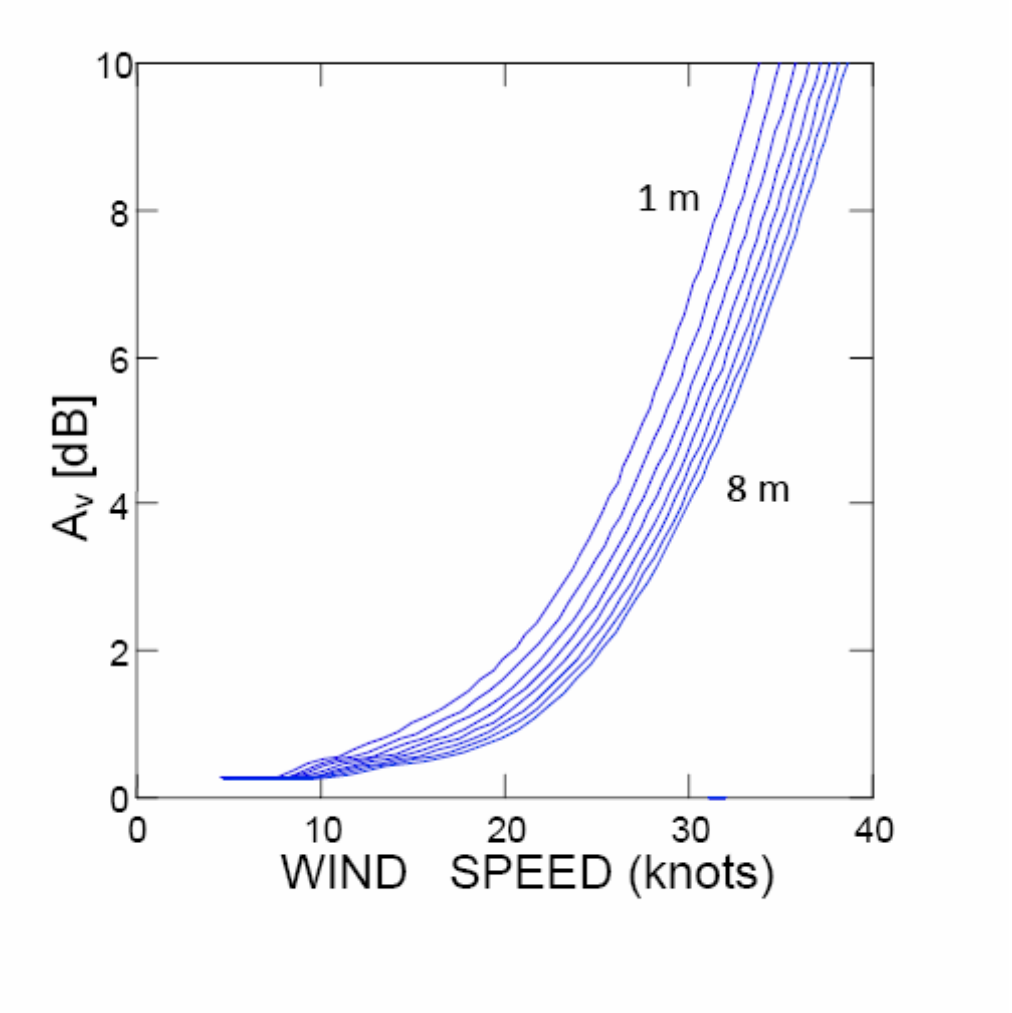

Figure 6.1. The estimated air bubble acoustic attenuation (dB) from Novarani & Bruno (1982), 38 kHz for transducers mounted at 1 to 8 meters depth from the surface. The attenuation is estimated using Equation 23.

In order for the correction factor established in this study to be considered valid and relevant, comparisons to previous established correction factors were undertaken to confirm its accuracy and precision. A paper by Berg *et al.* (1983) was reviewed and compared to; in this study they semi-empirically methods to establish an air bubble attenuation correction factor using data collected at 38 kHz onboard the RVs "G.O. Sars" and "Johan Ruud". No detailed comparison to Dalen and Løvik (1981) will be done since it is believed that they used the

same data from RV "G.O. Sars" as that later in Berg *et al.* (1983) and equivalent method for establishing their correction factors. The transducer onboard RV "G.O Sars" was stabilized while onboard RV "Johan Ruud" was not. First a comparison between the established correction factors from the stabilized transducer onboard old RV "G.O Sars" and stabilized transducers onboard new RV "Johan Hjort" was made. The results in Figure 6.2, shows that the correction factors established in this study are lower at all wind speed compared to Berg *et al.* (1983). The maximum recommended correction factor for normal practical surveying conditions is 1.5. A lower correction factor was also found by Ona and Mamylov (1988).

For absolute and precise abundance estimations, the stop condition for "G.O. Sars" is set at about 17 knots (red box in Figure 6.2), while set at about 25-30 knots (yellow box in Figure 6.2) for the RV "Johan Hjort" hull-mounted system. The correction factors set for RV "Johan Hjort" survey 1 and 2 are well below the threshold 1.5 in all wind speeds except at 50 knots or 25 m/s where they exceed the limit. The survey 3 from RV "Johan Hjort" is exceedingly above the threshold, therefore echo integrator values from that survey should not be used for fish abundance estimations. It can be seen from Figure 6.2 that the stop condition for Berg *et al.* RV "G.O. Sars" is considerably before the recommended stop wind speed of 20 knots (10 m/s); vessel of this kind should be used with high precaution to avoid errors since the stop condition is also dependent on vessel features like size and hull design. Air bubble attenuation correction factors established with different frequencies in both hull and keel systems are advised for multi-species characterisation surveys to determine frequency dependent attenuation at various wind speeds.

Secondly, comparisons of the correction factor from this study to those of Berg *et al.* stabilized transducer onboard RV "G.O. Sars" and non-stabilised transducer onboard RV "Johan Ruud" was conducted. The comparison also clearly shows that correction factors established in this study are considerably lower than those established before (Figure 6.3). The non-stabilized transducer onboard RV "Johan Ruud" had the lowest correction factor than the stabilized transducer onboard RV "G.O. Sars"; there may be many explanations to their observation, for example calibration errors. In either way, whether compared to stabilized or non-stabilized transducers the correction factors from this study are still outstanding low.

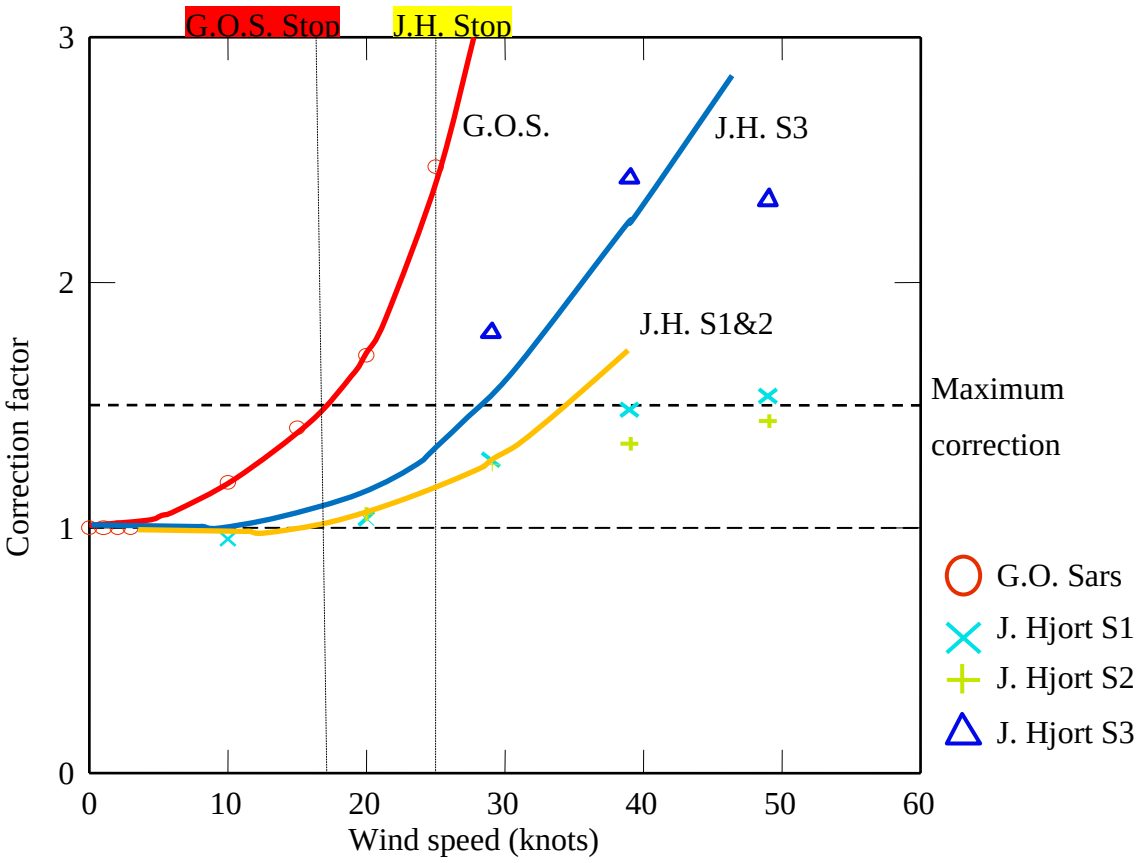

Figure 6.2. The comparison of current established correction factor for air bubble attenuation to previous established by Berg *et al.* (1983). For the current study the RV "Johan Hjort" (J.H. or J. Hjort) was used data collection while Berg *et al.* (1983) used RV "G.O. Sars" (G.O.S.). The letter S in the figure refers to the survey mean correction factor values, e.g. S1 for survey 1 correction factors. The vertical dashed lines indicate the stop conditions while the horizontal represent the minimum and maximum correction factors.

After 30 knots, the keel mounted transducer also experience air bubble attenuation (Ona and Traynor, 1990), hence the correction factor set by the s_A ratio stabilizes instead of exponentially increasing like in previous studies. This indicates that the method of setting the correction factor by using the mean s_A ratio is very resistant to attenuation effects even at high wind speeds. When the correction factors start to stabilize it is recommended that the survey be suspended or the data collected from such surveys will be prone to the error of underestimating the fish abundance. Since attempting to correct the backscattered strength when the effect of attenuation is very high is hazardous (Foote, 1990). The overall objective in correcting the recorded backscattering strength estimates for attenuation is to derive the best possible abundance estimates.

The comparison of the two stabilized transducers indicates that the correction established here in this study is incomparably lower, easy calculated and extremely suitable for everyday sea going surveys. The correction factor results from RV "Johan Hjort" hull-mounted transducer indicate that there is high potential in good-to-moderate weather conditions to use commercial vessels which are only equipped with hull-mounted transducers for collections of acoustic data. But at wind speeds above 15 m/s (30 knots) data from such vessel should be used with high precaution.

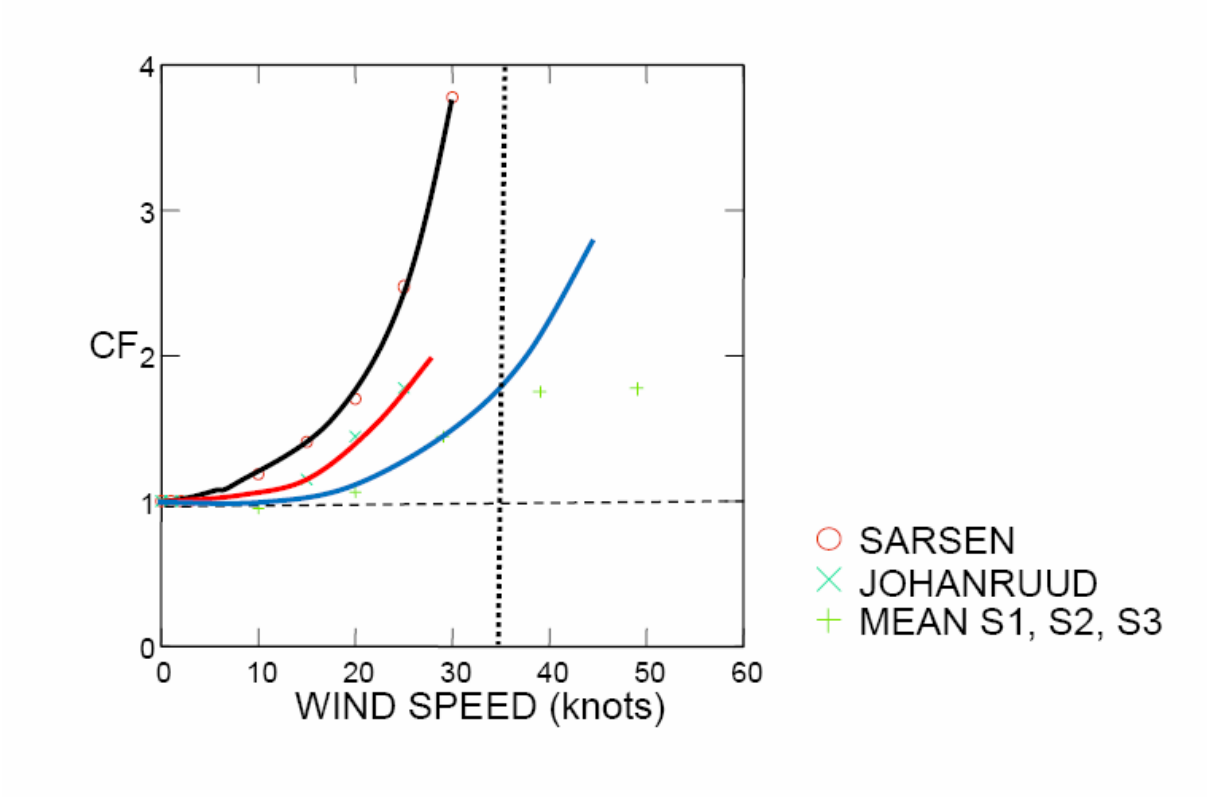

Figure 6.3. Correction factor (CF) for air bubble acoustic attenuation. Earlier results from RV "G.O. Sars" (Sarsen), black, and "Johan Ruud", red, compared with "Johan Hjort" (blue) mean data from survey 1, 2 and 3 from this investigation. Approximate wind speed for when the keel transducer also experience air bubble attenuation is shown by the vertical dashed line.

The use of commercial fishing vessel can also be considered as another approach towards ecosystem approach to fisheries (EAF) (Garcia *et al.*, 2003). The use of commercial vessels can be alternative way of reducing the number of vessels at sea, hence reducing air and water pollutions, and many other associated hazards. However, the installation of drop keels and other modern technologies to build commercial vessels as scientific vessels are highly recommended to improve the quality of data collected from these vessels (ICES, 2007). It is also recommended that more investigation should be simultaneously conducted in both the

fishing and research vessels at the same weather conditions to confirm this suggestion. Recent investigations like those by ICES (2007) and Peña (2009) are highly encouraged in finding a more rightful way of using commercial vessel for acoustic data collections.

CONCLUSIONS

- The sea bed can be used as a reliable reference target in investigations of air bubble acoustic attenuation. The bottom echo intensity is strongly affected by the weather conditions, the highest mean bottom echo intensities are found in good weather conditions.

- There is a strong correlation between the heave movement and the resultant bottom echo intensities, but since the ratio is used, the established correction factor is unaffected.

- The heave movement is highly influenced by the wind speed and sailing direction relative to the wind direction.

- The keel-mounted transducer is proved to perform better in bad weather conditions than the hull-mounted transducer.

- The ratio between the backscattering coefficients of the hull- and keel-mounted transducers could be used for measuring the attenuation for wind speeds up to about 17 m/s, before bubble attenuation also occurred on the reference transducer.

- A new and modern technique of establishing an absolute correction factor by computing the ratio of the backscattering from the bottom at various wind speeds is implemented.

REFERENCES

Aglen, A. 1989. Reliability of acoustic fish abundance estimates. Dissertation for the degree of philosophiae doctor (PhD), University of Bergen, Norway. 106 p.

Aglen, A. 1994. Sources of error in estimation of fish abundance. *In* Marine fish behaviour in capture and abundance estimation. *Edited by* A. Fernö and S. Olsen. Fishing News Books, Oxford. 107-133 p.

Armstrong, F., Simmonds, E.J., and MacLennan, D.N. 1989. Sound losses through aggregations of fish. Proceedings of the institute of acoustics 11 (3): 35-43.

Berg, T., Løvik, A., and Dalen, J. 1983. Increased precision of echo integration recordings under various weather conditions. FAO Fish. Rev. 300: 45-51.

Calise, L. 2009. Short range performances of a scientific echosounder with emphasis on accurate calibration. *In* Multifrequency acoustic target strength of Northern krill. Dissertation for the degree of philosophiae doctor (PhD), University of Bergen, Norway, ISBN 978-82-308-0768-2. (Available on online at: https://bora.uib.no/)

Dalen, J., and Løvik, A. 1981. The influence of wind induced bubbles on echo integration. Journal of the Acoustical Society of America, 69 (3): 1653-1659.

Dalen, J., Nedreaas, K., and Pedersen, R. 2003. A comparative acoustic-abundance estimation of pelagic redfish (*Sebastes mentella*) from hull-mounted and deep-towed acoustic systems. ICES Journal of Marine Science 60: 472-479.

Dragesund, O., and Olsen, S. 1965. On the possibility of estimating year-class strength for measuring echo-abundance of 0-group fish. Fisheridirektoratets Skrifter Serie Havundersokelser 13: 47-75.

Garcia, S.M.; Zerbi, A.; Aliaume, C.; Do Chi, T.; Lasserre, G. 2003. The ecosystem approach to fisheries. Issues, terminology, principles, institutional foundations, implementation and outlook. FAO Fisheries Technical Paper No. 443. Rome, FAO. 2003. 71 p.

Foote, K.G. 1983. Linearity of fisheries acoustics, with addition theorems. Journal of the Acoustical Society of America 73 (6): 1934-1940.

Foote, K.G., Knudsen, H.P., Vestnes, G., MacLennan, D.N., and Simmonds, E.J. 1987. Calibration of acoustic instruments for fish density estimation: a practical guide. Int. Coun. Explor. Sea Coop. Res. Rep. no. 144. 57 p.

Foote, K.G. 1990. Correcting acoustic measurements of scatterer density for extinction. Journal of the Acoustical Society of America 88 (3): 1543-1546.

Foote, K.G., Ona, E., and Toresen, R. 1992. Determining the extinction cross-section of aggregating fish. Journal of the Acoustical Society of America 91 (4): 1983-1989.

Foote, K.G. 1999. Extinction cross-section of Norwegian spring-spawning herring. ICES Journal of Marine Science 56: 606-612.

Francis, R.I.C.C., and Shotton, R. 1997. "Risk" in fisheries management: a review. Canadian Journal of Fisheries and Aquatic Sciences 54: 1699-1715.

Fréon, P., Soria, M., Mullon, C., and Gerlotto, F. 1993. Diurnal variation in fish density estimate during acoustic surveys in relation to spatial distribution and avoidance reaction. Aquatic Living Resources 6: 221-234.

Furusawa, M., Ishii, K., and Miyanohana, Y. 1992. Attenuation of sound by schooling fish. Journal of the Acoustical Society of America 89 (2): 987-994.

Godø, O.R. 2004. First fishing vessel to be built as a research platform. IMR Internal Marine Research News, No. 7. 2 p.

Hampton, I., and Soule, M.A., 2003. Acoustic survey of the orange roughy spawning plume on the northeast Chatham Rise, New Zealand: *San Waitaki* July 2003. Document presented to the New Zealand Deep Water Fisheries Assessment Working Group, 26 November 2003. 59 p.

Hilborn, R. 2007. Defining success in fisheries and conflicts in objectives. Marine Policy 31: 153-158.

ICES. 2007. Collection of acoustic data from fishing vessels. ICES Cooperative Research Report No. 287. 83 p.

ICES. 2008. Report of the Study Group on Fish Avoidance to Research Vessels (SGFARV), 22-23 June 2008, Bergen, Norway. ICES CM 2008/FTC: 07. 13 p.

Johannesson, K.A., and Mitson, R.B. 1983. Fisheries acoustics. A practical manual for aquatic biomass estimation. FAO Fisheries Technical Paper 240: 249 p.

Jørgensen, R., Handegard, N.O., Gjøsæter, H., and Slotte, A. 2004. Possible vessel avoidance behaviour of capelin in a feeding area and on a spawning ground. Fisheries Research 69: 251-261.

Kinsler, L.E., Frey, A.R., Coppens, A.B., and Sanders, J.V. 1982. Fundamentals of Acoustics, 3rd edn. John Wiley & Sons, Inc. Canada. 480 p.

Kloser, R.J. 1996. Improved precision of acoustic surveys of benthopelagic fish by means of a deep-towed transducer. ICES Journal of Marine Science 53: 407-413.

Knudsen, H.P. 1990. The Bergen Echo Integrator: an introduction. J. Cons. Int. Explor. Mer. 47: 167-174.

Knudsen, H.P. 2006a. Design criteria for improved hydro acoustic performance on fisheries research vessels. *In* Modernization of Fisheries Technology to Cope with Challenges and Profitability Proceedings, Nor-Fishing Technology Conference 2006 Trondheim, Norway, 7-8 August. 43-49 p.

Knudsen, H.P. 2006b. Gauging the reliability of acoustic instruments for fisheries surveys. Proceedings of the MTS/IEEE Oceans'06 Conference, Boston, Massachusetts USA, 18-21 September 2006. 6 p.

Knudsen, H.P. 2009. Long-term evaluation of scientific-echosounder performance. ICES Journal of Marine Science 66: 000-000.

Korneliussen, R.J., Ona, E., Eliassen, I., Heggelund, Y., Patel, R., Godø, O.R., Giertsen, C., Patel, D., Nornes, E., Bekkvik, T., Knudsen, H.P., and Lien, G. 2006. The Large Scale Survey System - LSSS. Proceedings of the 29th Scandinavian Symposium on Physical Acoustics, Ustaoset 29 January-1 February 2006.

Løvik, A. 1980. Acoustic measurements of the gas bubble spectrum in water. *In* Cavitation and inhomogeneities in underwater acoustics, proceedings of the first international conference. *Edited by* W. Lauterborn. Springer-Verlag, Berlin, 211-218 p.

MacLennan, D.N. 1990. Acoustical measurement of fish abundance. Journal of the Acoustical Society of America 89 (1): 1-15.

MacLennan, D.N., Armstrong, F., and Simmonds, E.J. 1990. Further observations of the attenuation of sound by aggregations of fish. Proceedings of the Institute of Acoustics 12: 99-106.

MacLennan, D.N., Fernandes, P.G., and Dalen, J. 2002. A consistent approach to definitions and symbols in fisheries acoustics. ICES Journal of Marine Science 59: 365-369.

Medwin, H., and Clay, C.S. 1998. Fundamentals of acoustical oceanography. Academic Press, London. 712 p.

Mitson, R.B. 1995. Underwater noise of research vessels: review and recommendations. ICES Coop. Res. Rep. No. 209: 65 p.

Mitson, R.B., and Knudsen, H.P. 2003. Causes and effects of underwater noise on fish abundance estimation. Aquatic Living Resources 16: 255-263.

Novarini, J.C., and Bruno, D.R. 1982. Effects of the sub-surface bubble layer on sound propagation. Journal of Acoustical Society of America 72 (2): 510-514.

Ona, E., and Mamylov, V. 1988. Scientific report on cooperative work between Norwegian and Soviet specialists, May 19 - June 2, 1988, PINRO, Murmansk, USSR., 1-22.

Ona, E., and Traynor, J. 1990. Hull-mounted, protruding transducer for improving echo integration in bad weather. ICES Document CM 1990/B: 31, 1-10.

Ona, E. 1991. Vessel heave, an index for air bubble attenuation corrections. ICES Document C.M. 1991/B: 37.

Ona, E., Mazauric, V., and Andersen, L.N. 2009. Calibration methods for two scientific multibeam systems. ICES Journal of Marine Science 69: 000-000.

Parker-Stetter, S.L., Rudstam, L.G., Sullivan, P.J., and Warner, D.M. 2009. Standard operating procedures for fisheries acoustic surveys in the Great Lakes. Great Lakes Fishery Commission Special Publication 09-01. 180 p.

Peña, H.A. 2005. Intercalibration of three commercial vessels equipped with scientific echosounders in the Norwegian Sea (MV Libas, MV Hardhaus and MV Møgsterbas). Unpublished Institute of Marine Research Internal Cruise Report, Bergen.

Peña, H.A. 2009. Comparison of scientific echo sounder data from commercial vessels in the Norwegian Sea. *In* Improving acoustic abundance estimates of pelagic fish using commercial fishing vessels. Dissertation for the degree of philosophiae doctor (PhD), University of Bergen, Norway.

Simmonds, E.J., and MacLennan, D.N. 2005. Fisheries Acoustics: Theory and Practice, 2nd edn. Blackwell Publishing, Oxford. 437 p.

Simrad, 2008. Simrad ER60 Scientific echo sounder. A reference manual. Simrad AS, Horten, Norway. 221 p.

Stanton, T.K. 1982. Effects of transducer motion on echo-integration techniques. Journal of the Acoustical Society of America 72 (3): 947-949.

Toresen, R. 1990. Absorption of acoustic energy in dense herring schools studied by the attenuation in the bottom echo signal. Fisheries Research 10: 317-327.

Urick, R.J. 1983. Principles of Underwater Sound, 3rd edn. McGraw Hill, New York. 423 p.

Venables, W.N., and Smith, D.M. 2002. An Introduction to R. Network Theory Limited, Bristol, United Kingdom. 156 p.

Ye, Z. 1996. Acoustic scattering from fish swimbladders. Journal of the Acoustical Society of America 99 (2): 785-792.

Zhao, X., and Ona, E. 2003. Estimation and compensation models for the shadowing effect in dense fish aggregations. ICES Journal of Marine Science 60: 155-163.

APPENDIX

Appendix A. Pictures and figures

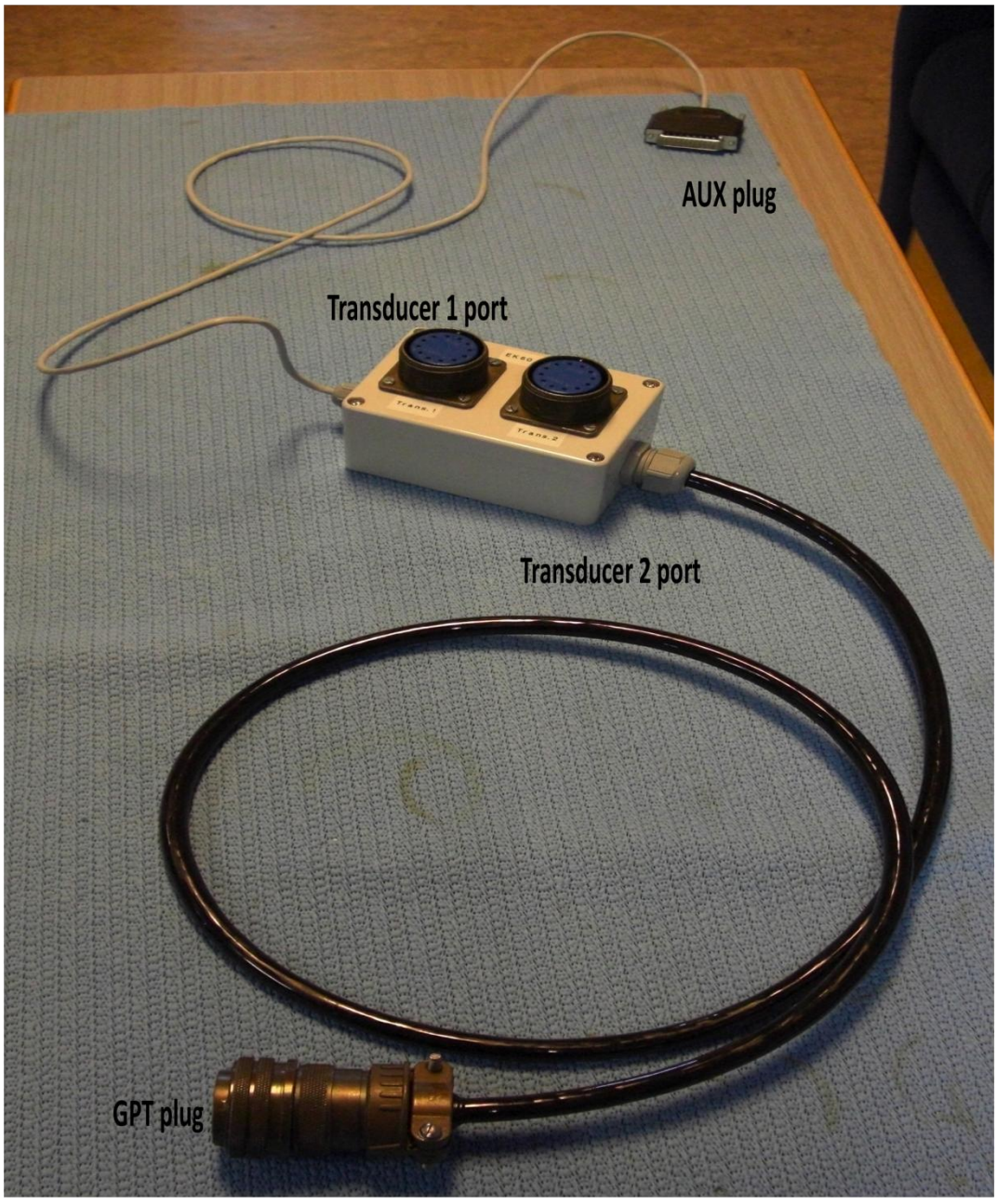

Figure A.1. A photographic picture with labels of parts of the multiplexer equipment onboard RV "Johan Hjort".

Figure A.2. Picture of the calm sea surface in good weather conditions in the Barents Sea.

Figure A.3. Sea waveforms and white foams of the sea surface in bad weather conditions in the Barents Sea.

Figure A.4. Picture of the RV "Johan Hjort" used for data collection in this thesis.

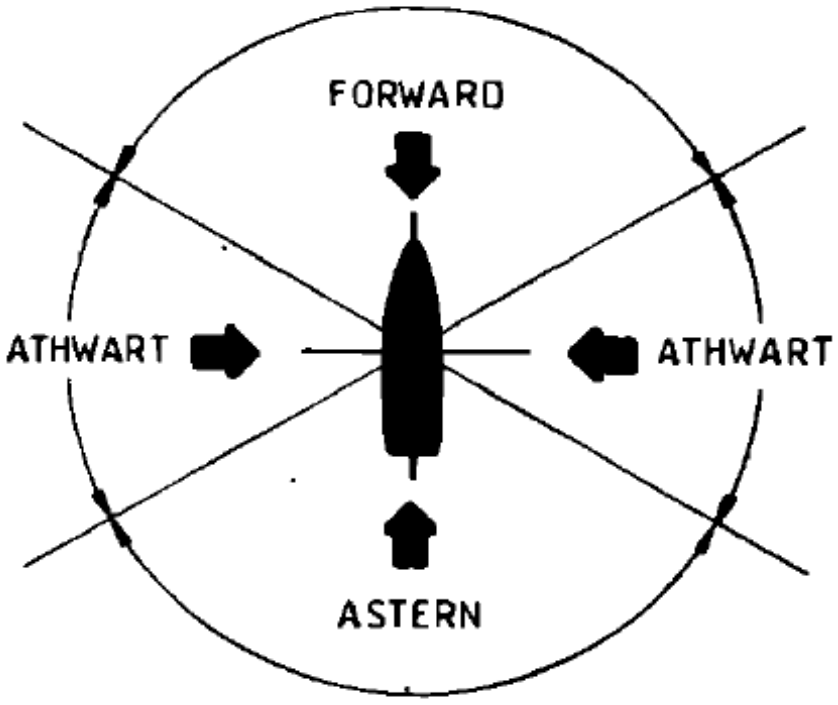

Figure A.5. The illustration of the influence of wind direction or vessel heading on acoustic attenuation. Drawing from Dalen and Løvik (1981), used by permission.

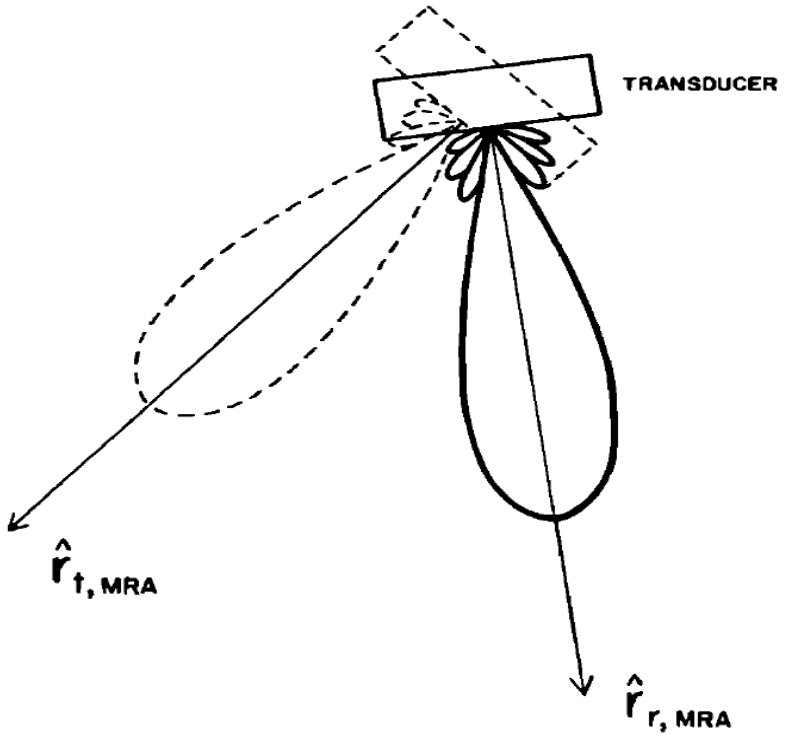

Figure A.6. The above diagram shows the effect of vessel roll on the transmitted and received pulse. The dashed lines show the transmission beam pattern while solid lines are the reception beam pattern. $\hat{r}_{t,MRA}$ is the transmission maximum response axis direction and $\hat{r}_{r,MRA}$ is the reception maximum response axis direction. (Diagram from Stanton, 1982.)

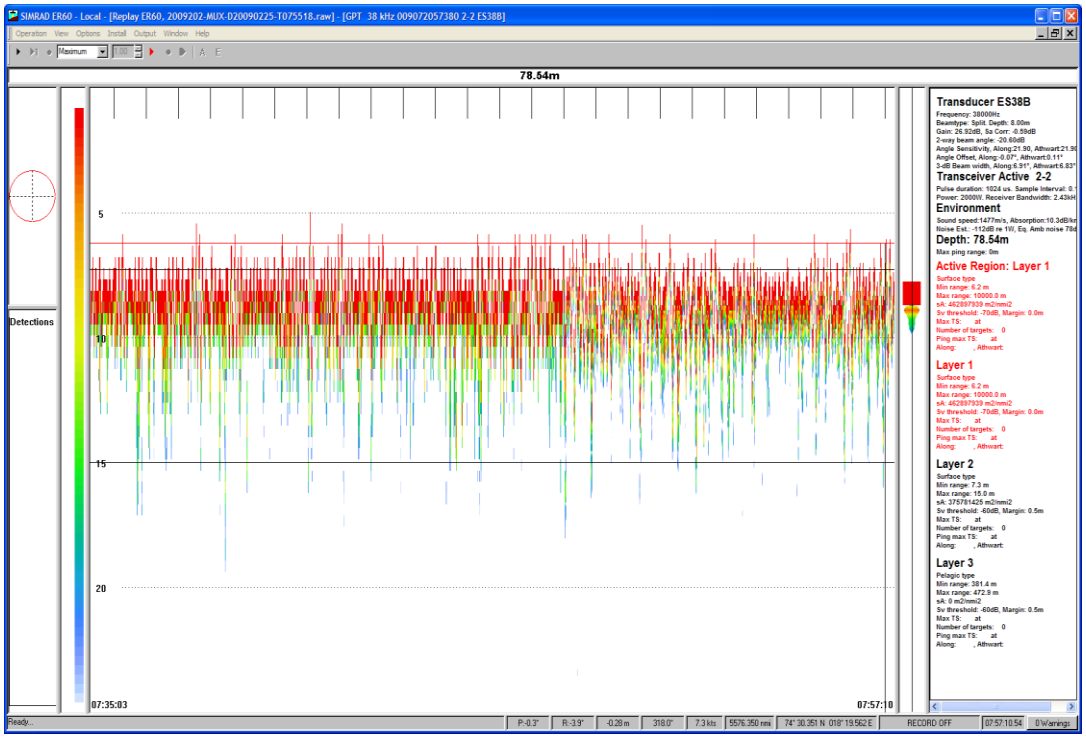

Figure A.7. The pelagic echogram showing fluctuation of the transmission pulse range from the transducer in the data collected with the vessel heave sensor activated.

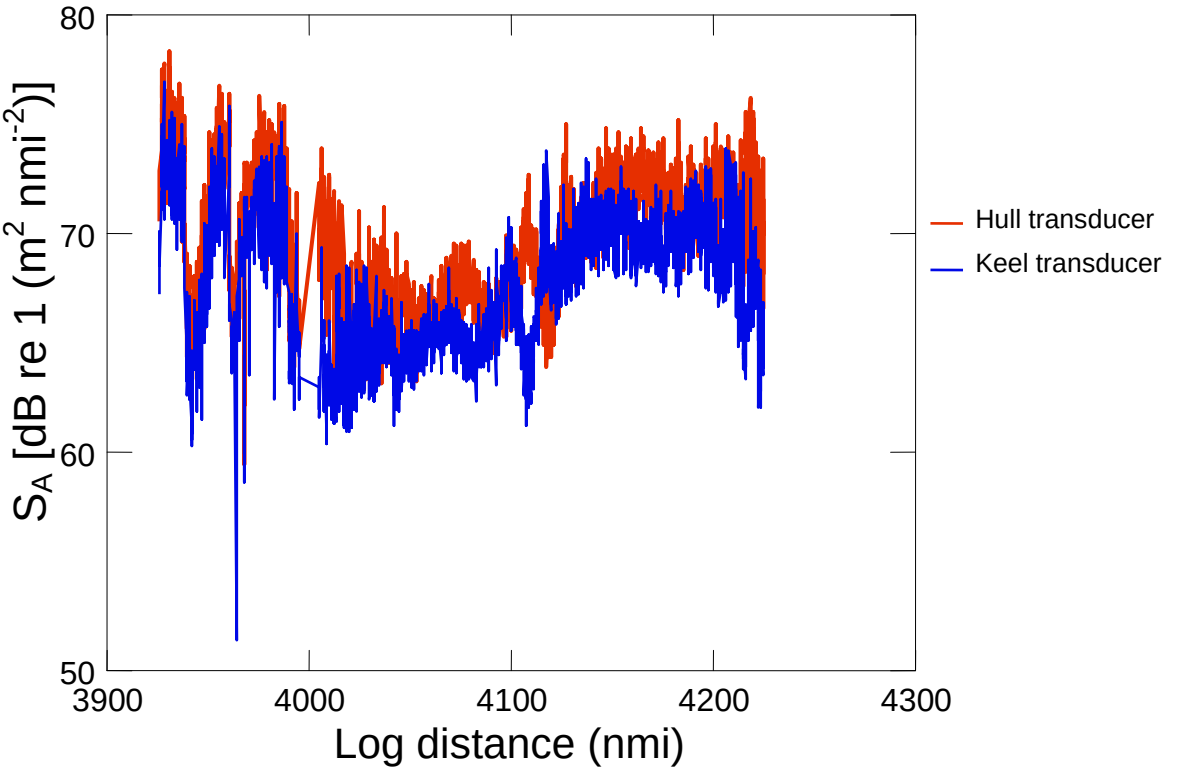

Figure A.8. The observed S_A of the hull and keel transducers plotted against cruised distance in period 1 of survey 1.

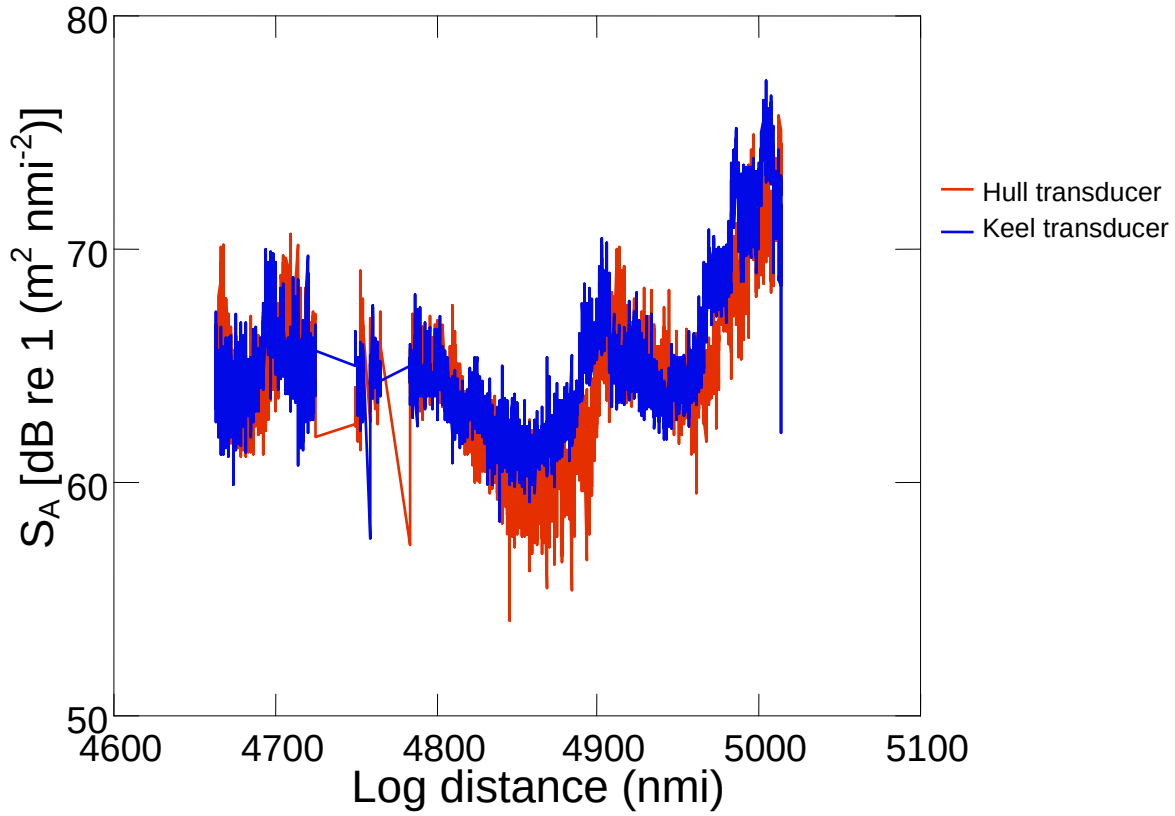

Figure A.9. The observed S_A of the hull and keel transducers plotted against cruised distance in period 2 of survey 1.

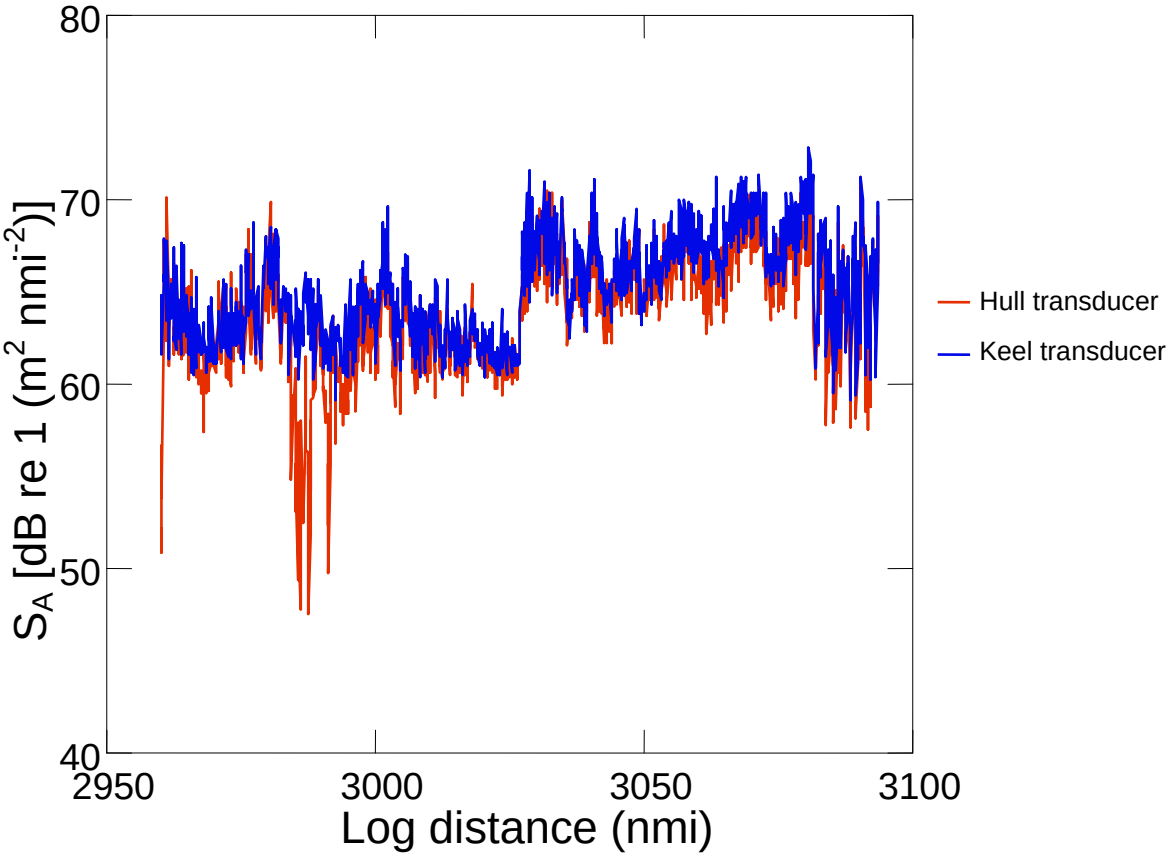

Figure A.10. The recorded S_A values recorded over the travelled distance in survey 2.

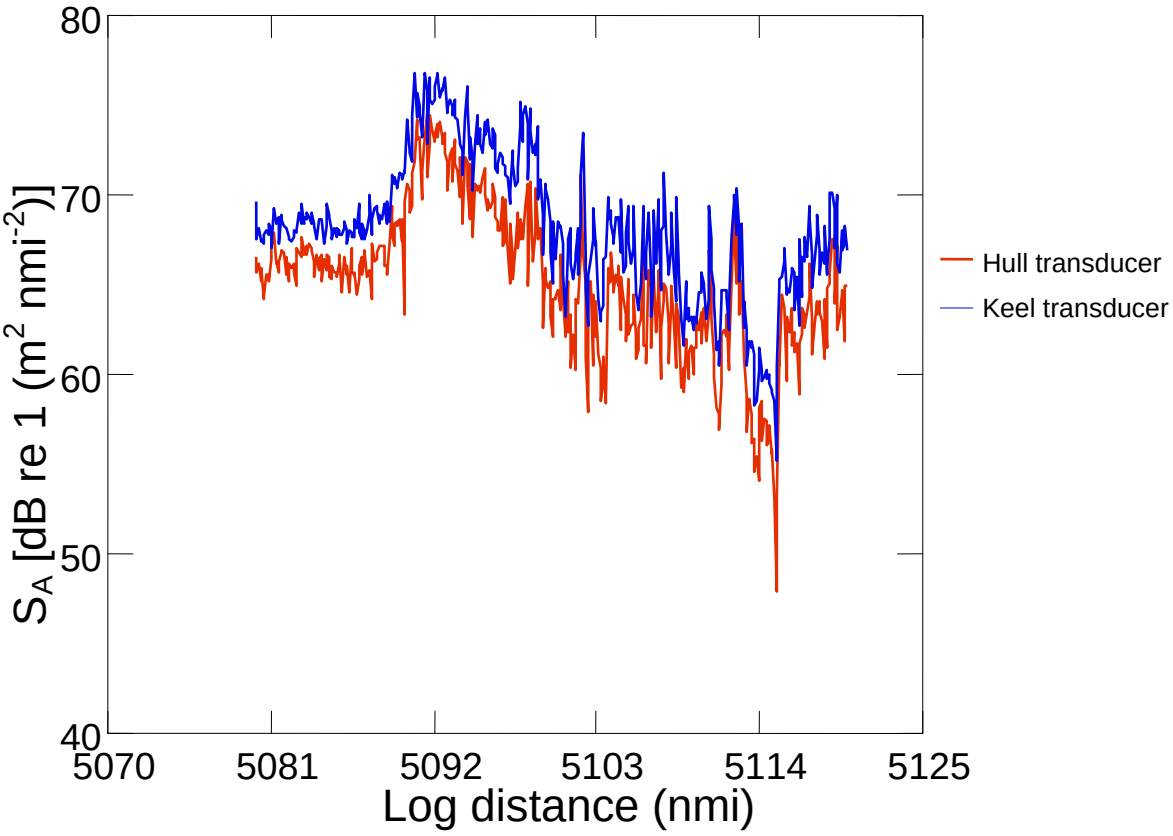

Figure A11. The recorded S_A values for the two-transducer systems in period 1 of survey 3.

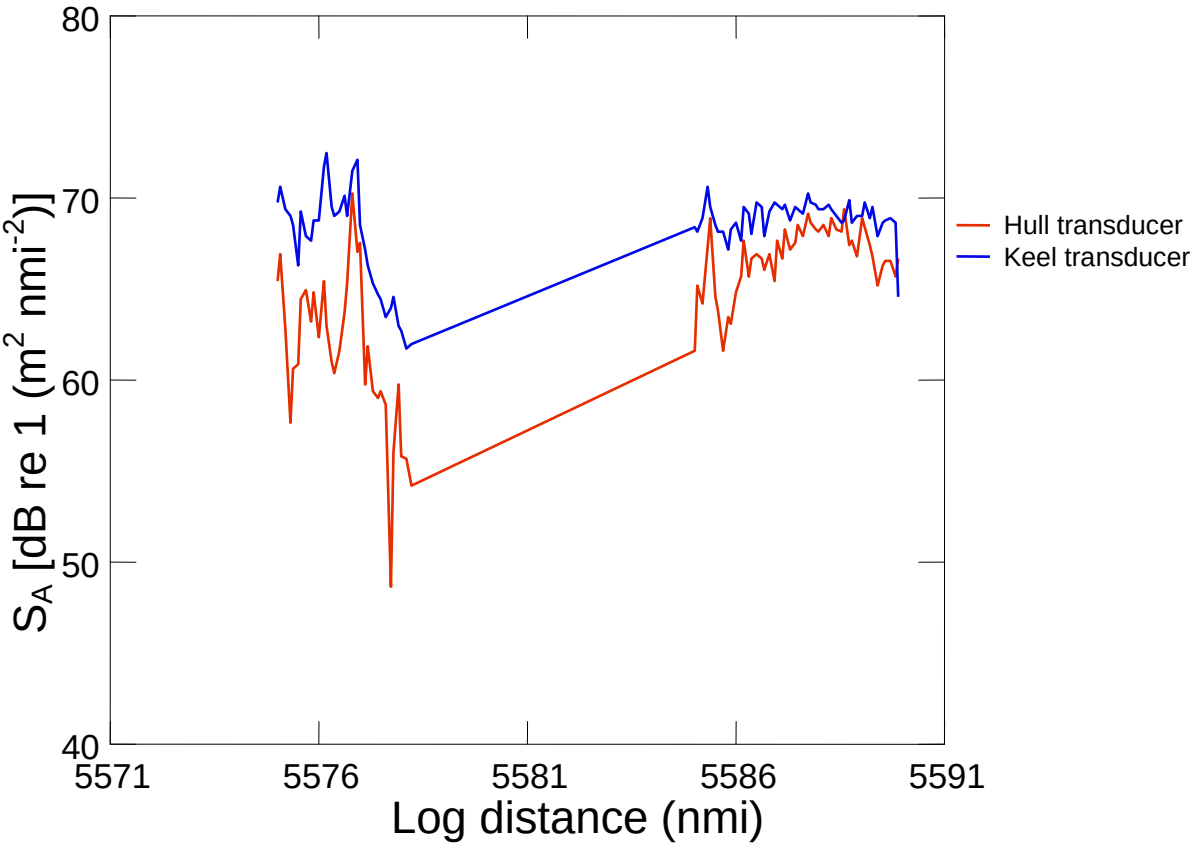

Figure A.12. The observed S_A values versus the logged distance in period 2 of survey 3.

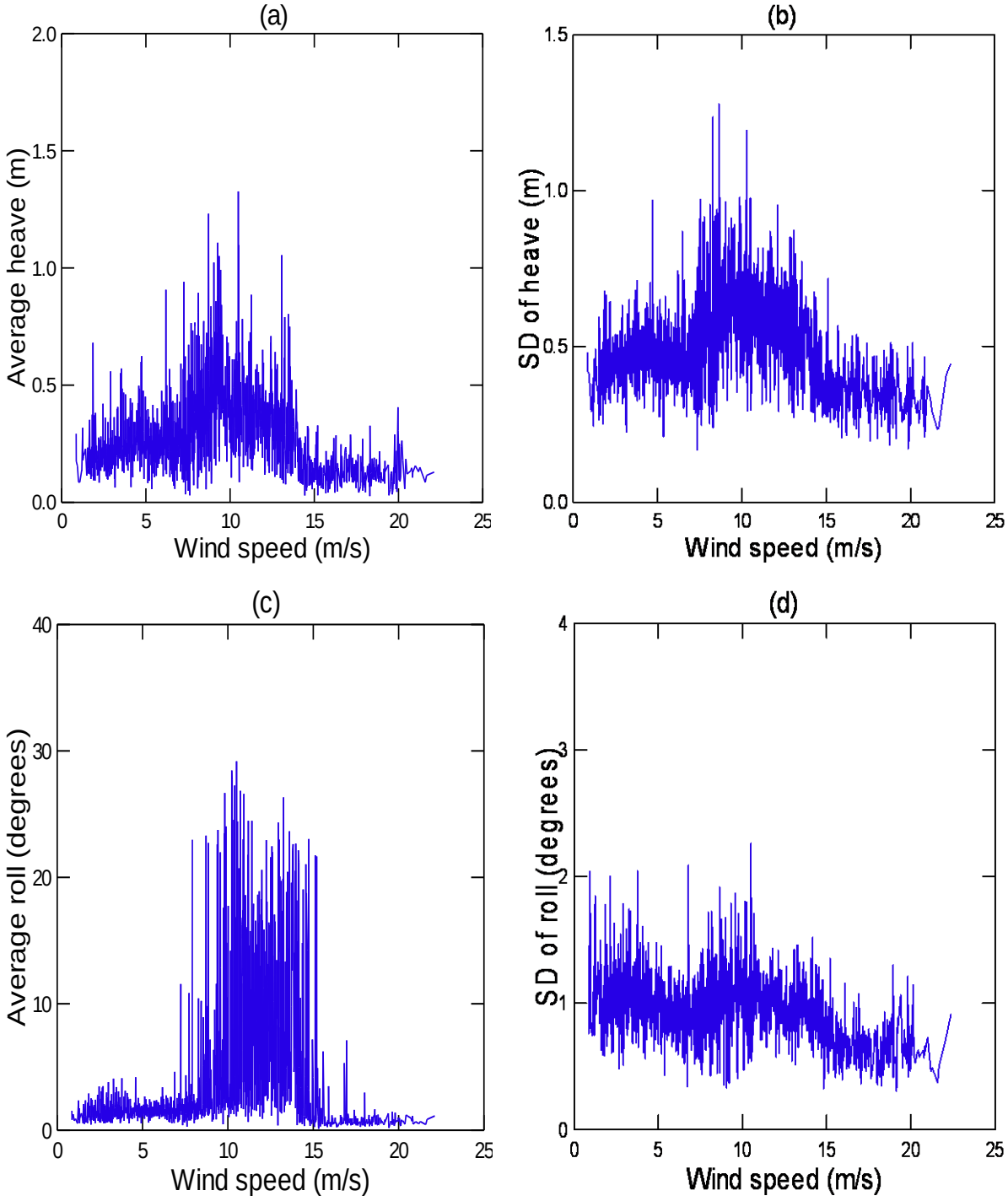

Figure A.13. The average 0.1 nmi heave (a and b) and roll (c and d) response in various wind speeds plotted with standard deviation (SD) during survey 1.

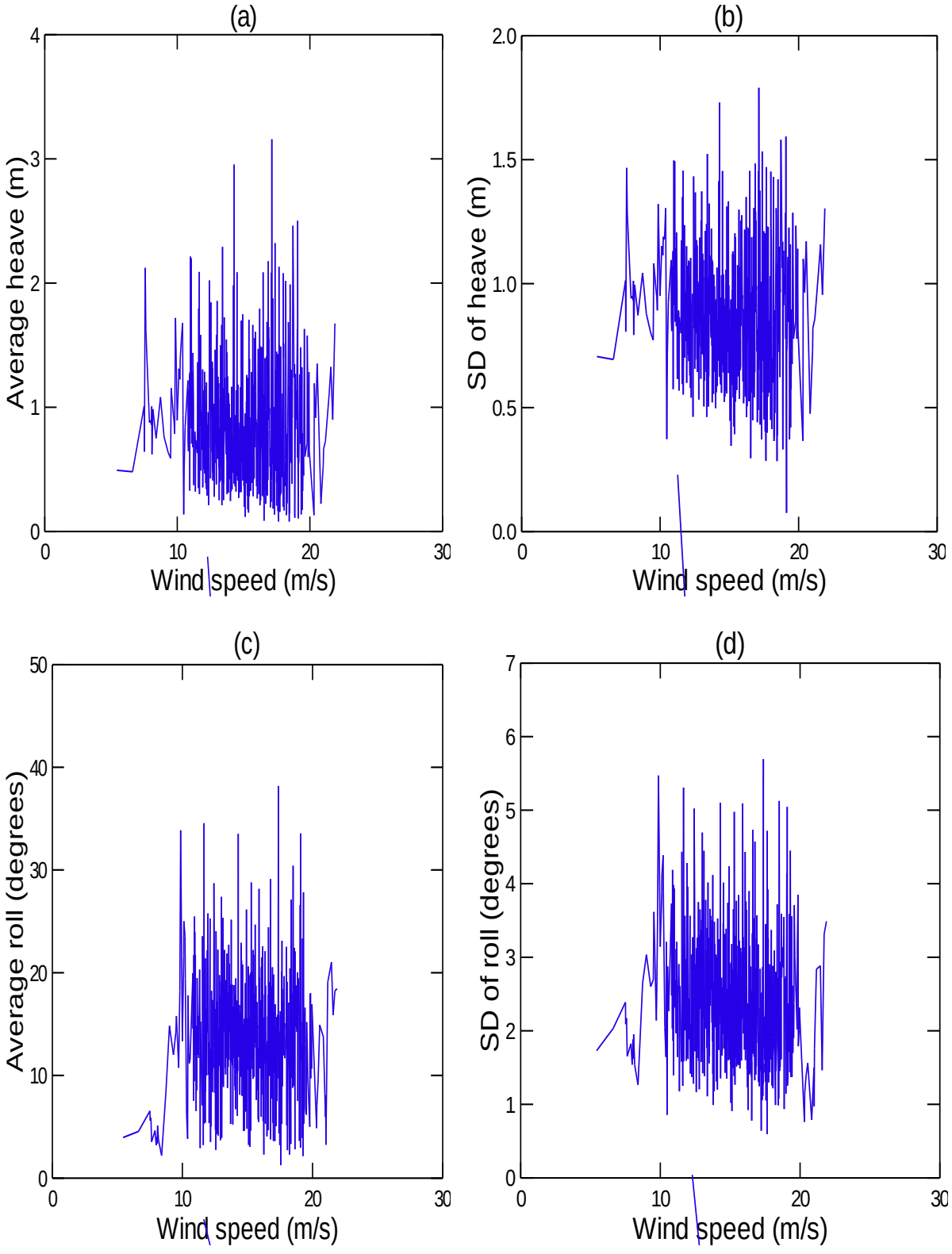

Figure A.14. The average 0.1 nmi heave (a and b) and roll (c and d) response in various wind speeds plotted with standard deviation (SD) during survey 2.

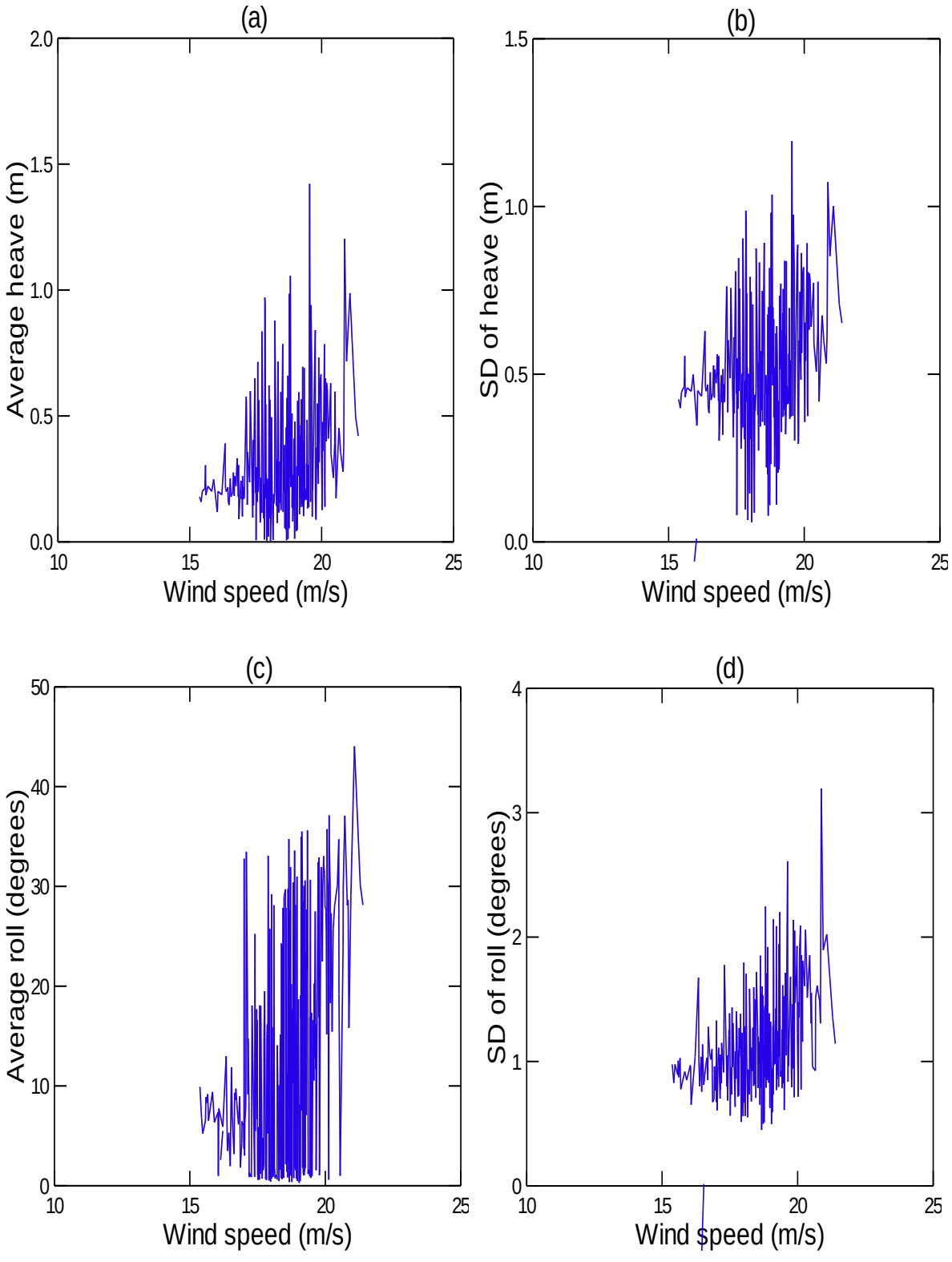

Figure A.15. The average 0.1 nmi heave (a and b) and roll (c and d) response in various wind speeds plotted with standard deviation (SD) during survey 3.

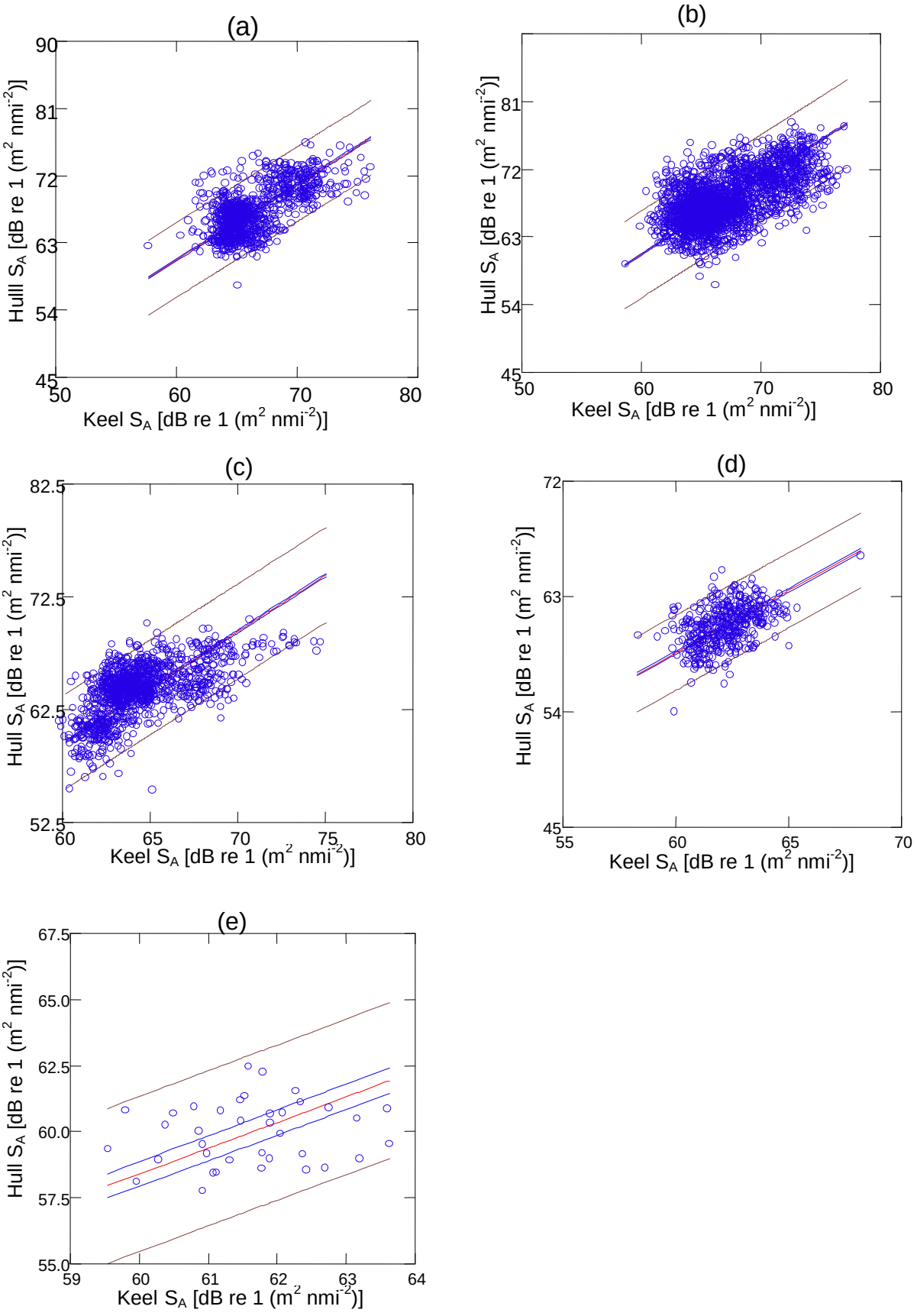

Figure A.16. Regression lines according to wind speeds from survey 1. Wind speeds are as (a) 0-5 m/s, (b) 5-10 m/s, (c) 10-15 m/s, (d) 15-20 m/s, and (e) 20-25 m/s.

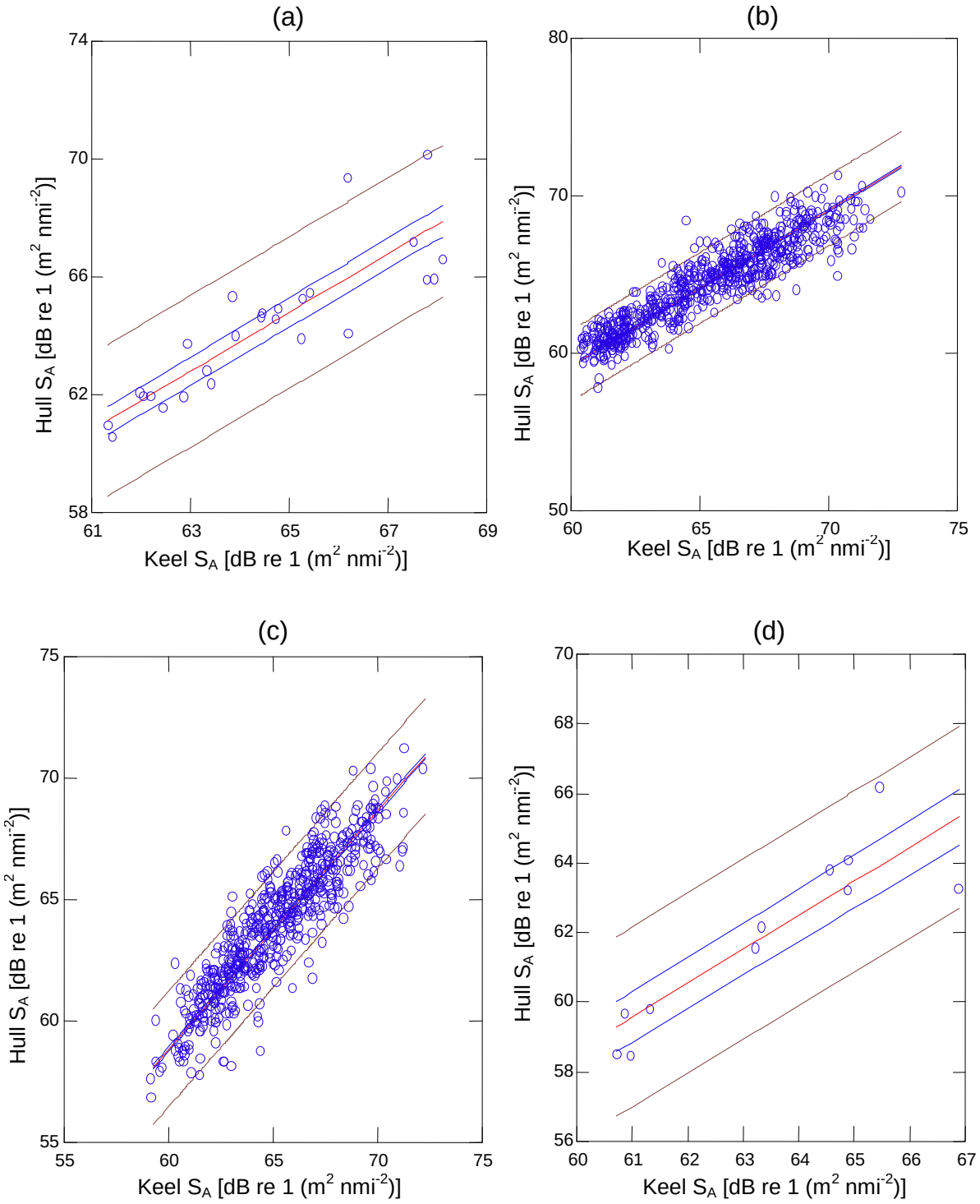

Figure A.17. Regression lines according to wind speeds from survey 2. Wind speeds are as (a) 5-10 m/s, (b) 10-15 m/s, (c) 15-20 m/s, and (d) 20-25 m/s.

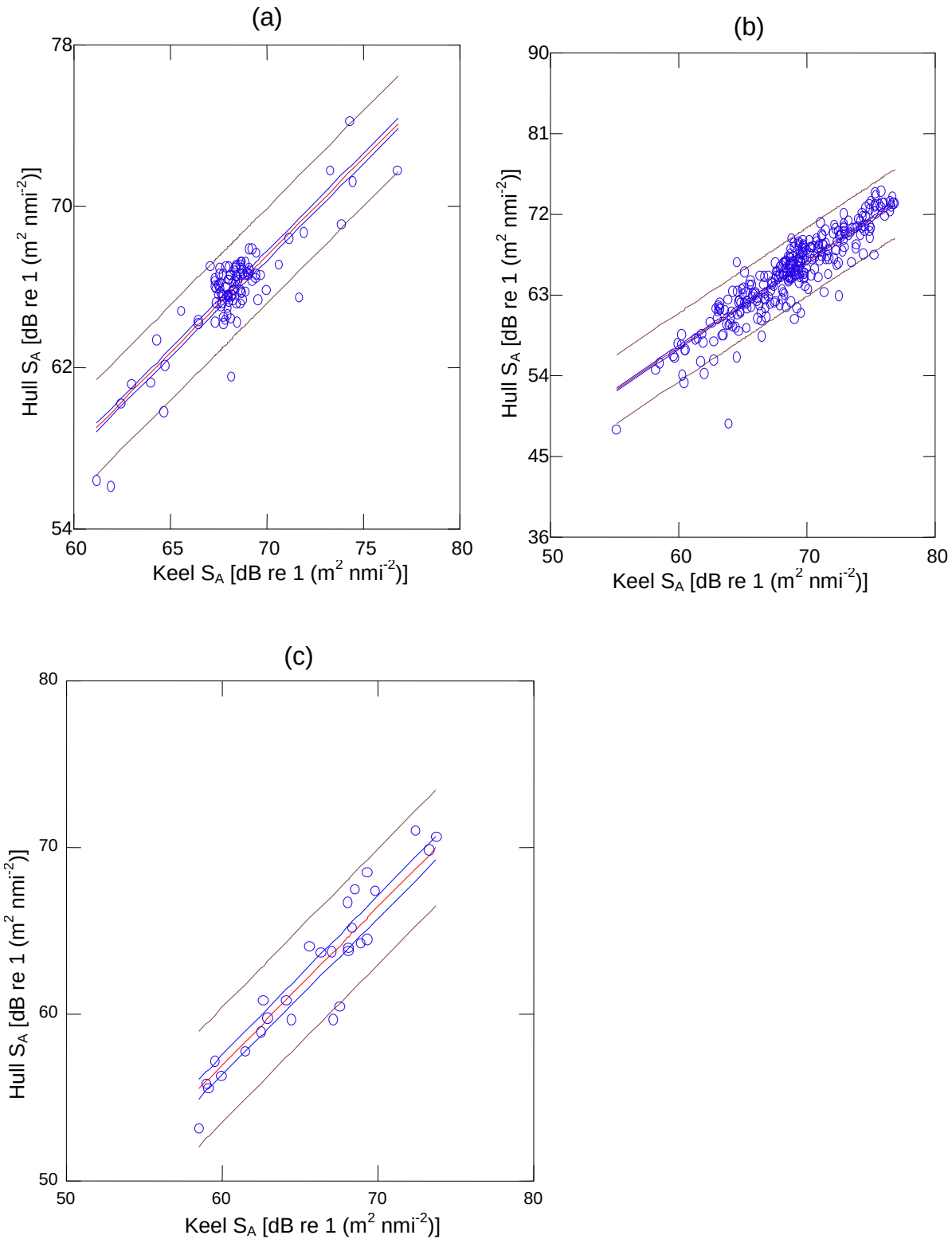

Figure A.18. Regression lines according to wind speeds from survey 3. Wind speeds are as (a) 10-15 m/s, (b) 15-20 m/s, and (c) 20-25 m/s.

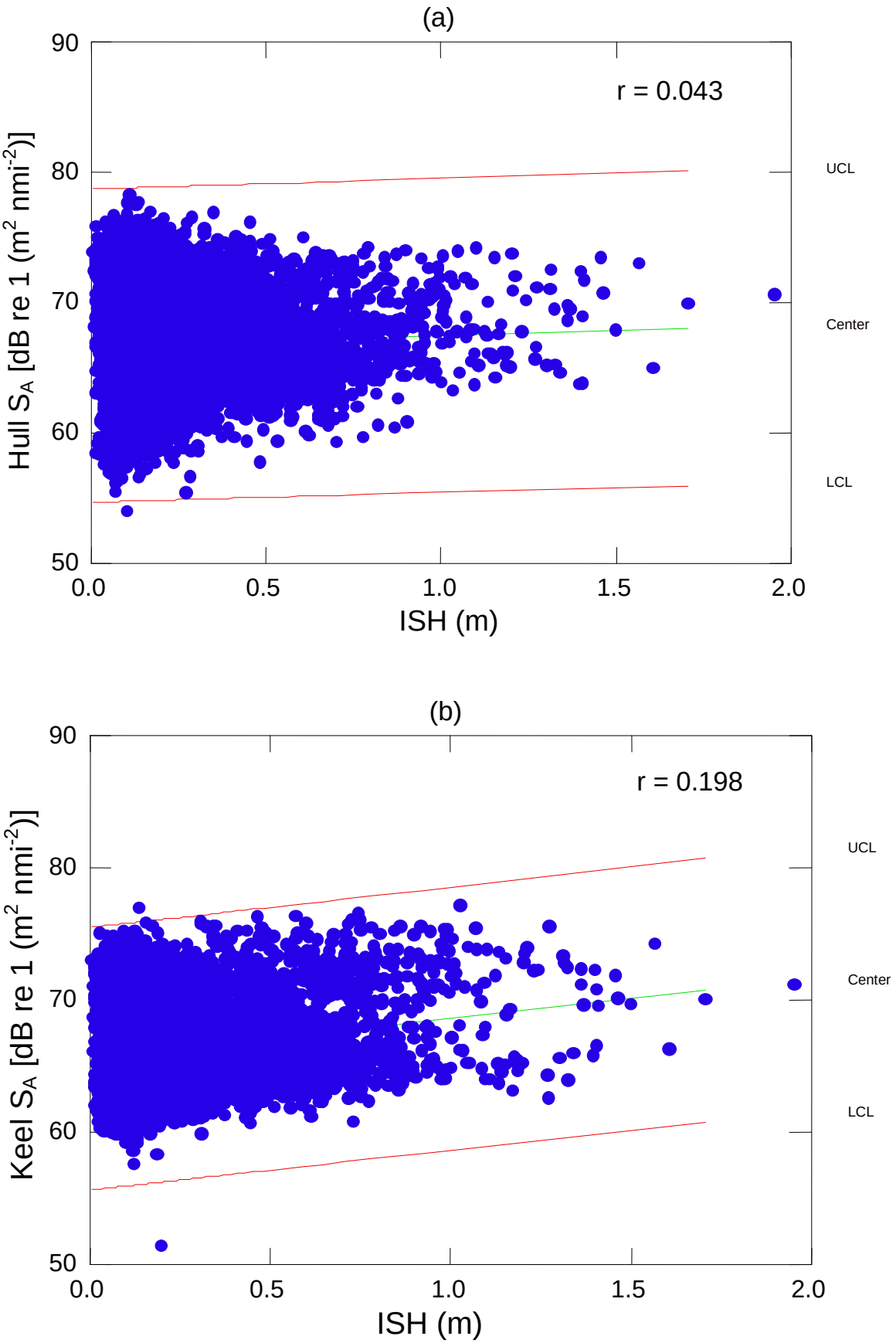

Figure A.19. Correlation between the backscattering strength of the hull (a) and keel (b) versus the integrated squared heave (ISH) in survey 1.

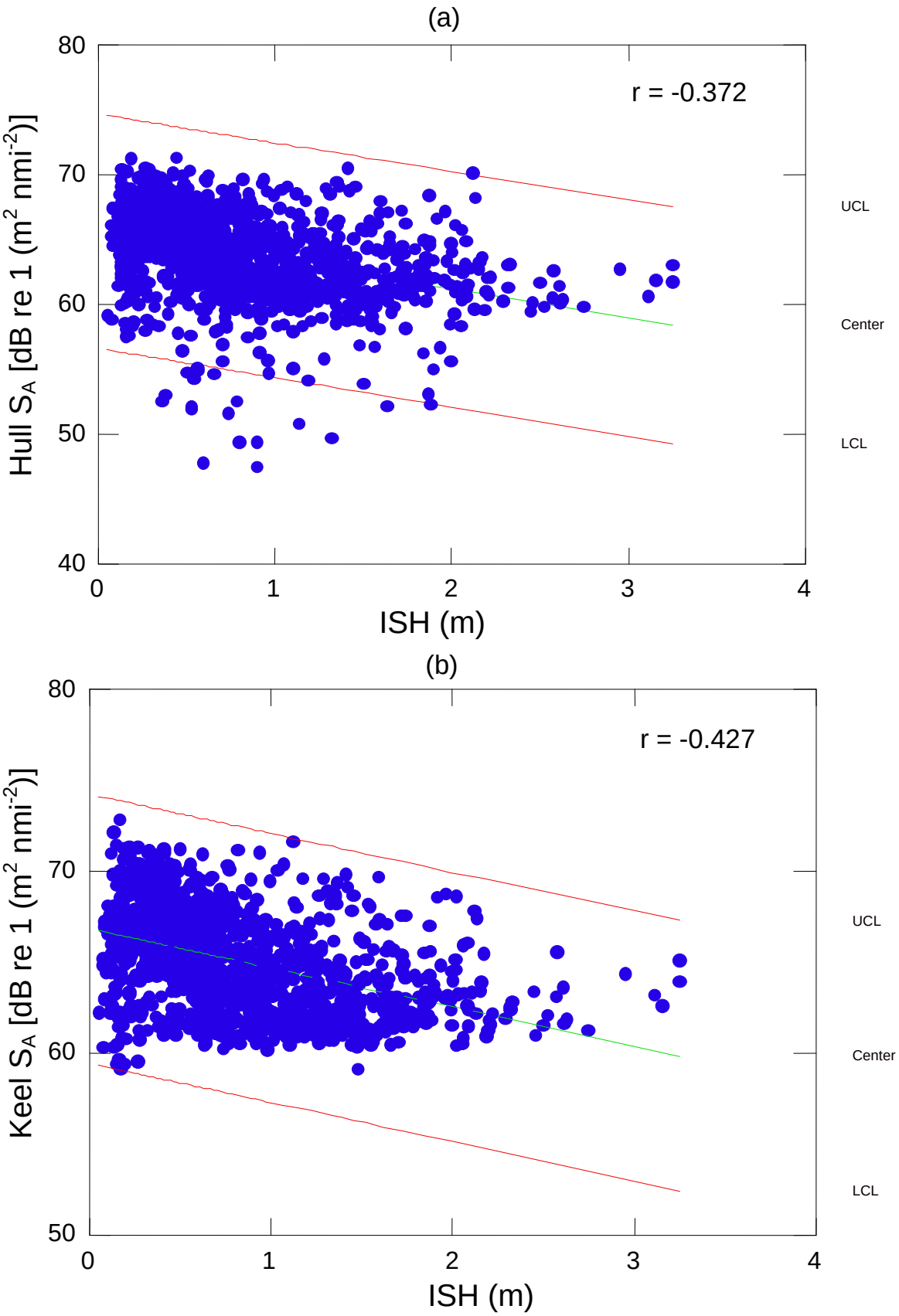

Figure A.20. Correlation between the backscattering strength of the hull (a) and keel (b) versus the integrated squared heave (ISH) in survey 2.

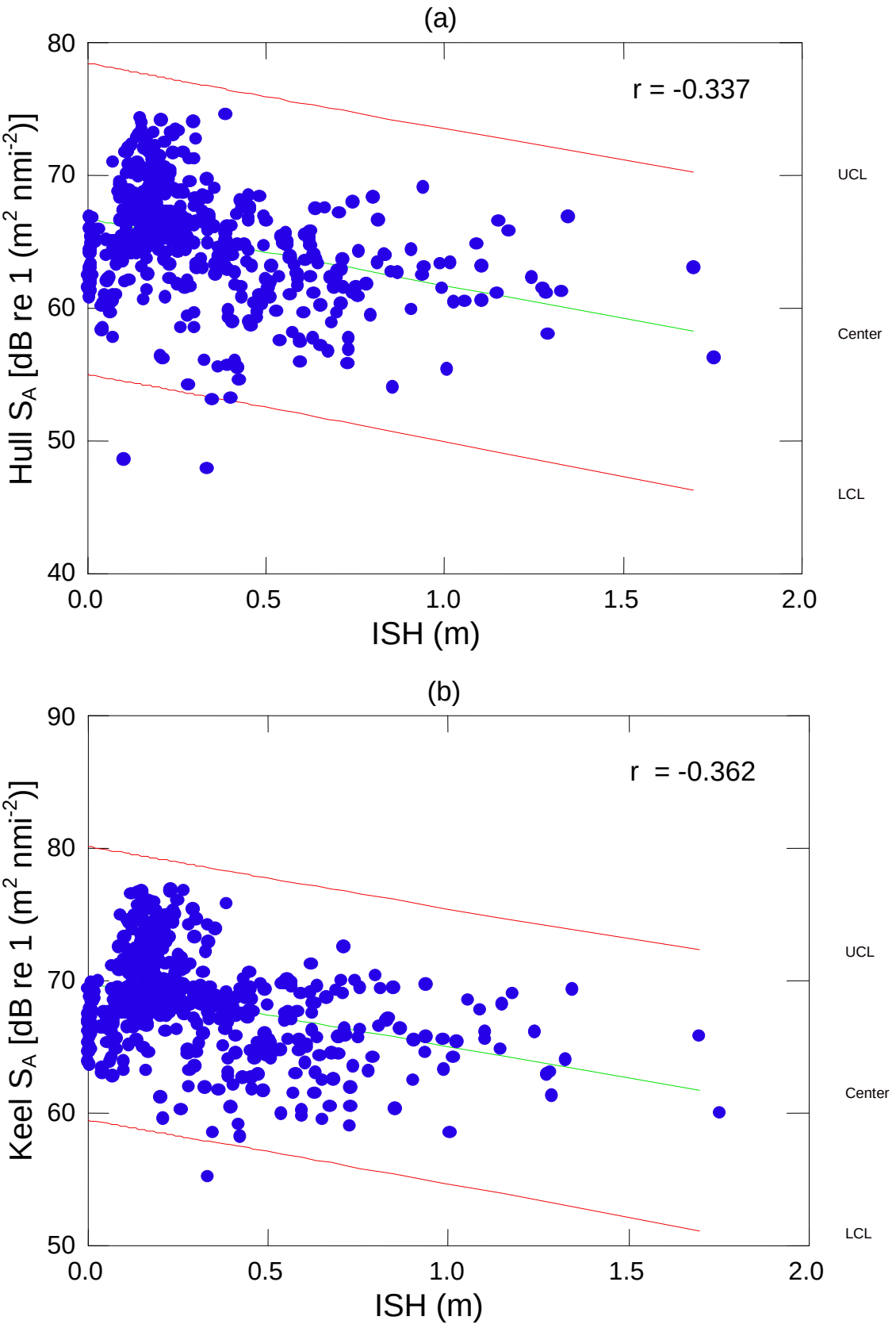

Figure A.21. Correlation between the backscattering strength of the hull (a) and keel (b) versus the integrated squared heave (ISH) in survey 3.

Appendix B. Commands used in R to merge the three different data sets

Step 1. Importing data to the directory

```
>library(RODBC)
>filename <- "../Data/AcousticData.xls"
>channel <- odbcConnectExcel2007(filename)
>acu <- sqlFetch(channel, "Sheet1$")
>close(channel)
>filename <- "../Data/WeatherData.xls"
>channel <- odbcConnectExcel2007(filename)
>weather <- sqlFetch(channel, "Sheet1$")
>close(channel)
>filename <- "../Data/TiltData.txt"
>tilt <- read.table(filename,header=T)
```

Step 2. Merging acoustic with weather data

```
>acu$logLink <- 0.5*(acu$LogStart + acu$LogStop)
>id <- numeric(nrow(acu))
>for(i in 1: nrow(acu)){
 id[i] <- sort(abs(weather$Logg - acu$logLink[i]), index=T)$ix[1]
}
>out <- cbind(acu,weather[id,])
>write.table(out,
"../Data/AcuWeather.txt",quote=FALSE,col.names=TRUE,row.names=FALSE,append=FALSE)
```

Writing out the output

Step 3. Merging AcuWeather with heave data

```
>round.gr <- function(x,gr=2) round(x/gr)*gr
>tilt1 <- tilt[is.na(tilt$Log),]
>tilt1$DateTime <- paste(tilt1$Date,tilt1$Time)
>out$DateTime <- paste(out$DATE,substr(out$Time,12,20))
>tilt1$DateNum     <-     as.numeric(as.POSIXct(tilt1$DateTime,     format="%y.%m.%d
%H:%M:%OS"))
>out$DateNum <- as.numeric(as.POSIXct(out$DateTime, format="%Y.%m.%d %H:%M:%OS"))
>id <- numeric(nrow(out))
>for(i in 1: nrow(out)){
  id[i] <- (1:nrow(tilt1))[(tilt1$DateNum - out$DateNum[i]) == 0][1]
}
>final <- cbind(out,tilt1[id,])
>final$LogNM <- floor(final$LogStart)
>heave1 <- tapply(abs(final$Heave),final$LogNM, mean)
>heave2 <- tapply(abs(final$Heave),final$LogNM, max)
>wind1 <- tapply(final$Wind,final$LogNM, mean)
>write.table(final,  "../Data/AcuWeatherTilt.txt",  quote=FALSE,  col.names  =TRUE,
row.names=FALSE,append=FALSE)
```

Writing out the output

Appendix C. Tables

Table C.1. Hull-mounted transducer calibration

Hull-mounted Transducer Calibration with Reference Sphere

Vessel:	RV Johan Hjort	Date:	2/7/2009
Echo sounder:	JHER60-2	Location:	Skogsfjord, Ringvassøy, Norway
Sphere:	CU-60	**TS-sphere:** -33.68 dB (correction for lydhastighet eller t,S	Depth: 40 m
Calibration Version 2.1.0.12			

Comments: Hull-mounted transducer Kal 1ms

Reference Target:

TS	-33.70 dB	Min. Distance	17.00
TS Deviation	5.0 dB	Max. Distance	22.00

Transducer: ES38B Serial No. 1000

Frequency	38000 Hz	Beamtype	Split
Gain	26.92 dB	Two Way Beam Angle	-20.6 dB
Athw. Angle Sens.	21.90	Along. Angle Sens.	21.90
Athw. Beam Angle	6.90 deg	Along. Beam Angle	7.00 deg
Athw. Offset Angle	-0.04 deg	Along. Offset Angl	0.03 deg
SaCorrection	-0.59 dB	Depth	5.00 m

Transceiver: GPT 38 kHz 009072057380 2-1 ES38B

Pulse Duration	1.024 ms	Sample Interval	0.187 m
Power	2000 W	Receiver Bandwidth	2.43 kHz

Sounder Type: EK60 Version 2.2.0

TS Detection:

Min. Value	-50.0 dB	Min. Spacing	100 %
Max. Beam Comp.	6.0 dB	Min. Echolength	80 %
Max. Phase Dev.	8.0	Max. Echolength	180 %

Environment:

Absorption Coeff.	10.4 dB/km	Sound Velocity	1464.2 m/s

Beam Model results:

Transducer Gain =	26.24 dB	SaCorrection =	-0.83 dB
Athw. Beam Angle =	7.03 deg	Along. Beam Angle =	6.99 deg
Athw. Offset Angle =	0.07 deg	Along. Offset Angle=	-0.04 deg

Data deviation from beam model:

RMS = 0.12 dB
Max = 0.38 dB No. = 197 Athw. = -3.7 deg Along = -2.5 deg
Min = -0.40 dB No. = 191 Athw. = -1.2 deg Along = -2.3 deg

Data deviation from polynomial model:

RMS = 0.11 dB
Max = 0.30 dB No. = 188 Athw. = -0.2 deg Along = -2.0deg
Min = -0.41 dB No. = 191 Athw. = -1.2 deg Along = -2.3 deg

Remarks:

Wind speed: 12 kn. **Wind direction:** 090 deg
Raw data file: G:\ER60\Kalibrering\2009\38khz, BUNNMONTERT 1ms
File name: G:\ER60\Kalibrering\2009\38khz 1ms-BM

Table C.2. Keel-mounted transducer calibration output

Keel-mounted Transducer Calibration with Reference Sphere

Vessel:	F/F Johan Hjort	Date :	2/7/2009
Echo sounder:	JHER60-2	Location :	Skogsfjord, Ringvassøy, Norway
Sphere:	CU-60	**TS-sphere:** -33.68 dB (Correction for lydhastighet eller t,S)	Depth: 40 m

Calibration Version 2.1.0.12

Comments: Kal 1ms

Reference Target:

TS	-33.70 dB	Min. Distance	18.00
TS Deviation	5.0 dB	Max. Distance	23.00

Transducer: ES38B Serial No. 2009

Frequency	38000 Hz	Beamtype	Split
Gain	27.03 dB	Two Way Beam Angle	-20.6 dB
Athw. Angle Sens.	21.90	Along. Angle Sens.	21.90
Athw. Beam Angle	6.78 deg	Along. Beam Angle	6.84 deg
Athw. Offset Angle	-0.13 deg	Along. Offset Angl	-0.09 deg
SaCorrection	-0.61 dB	Depth	5.00 m

Transceiver: GPT 38 kHz 009072057380 2-1 ES38B

Pulse Duration	1.024 ms	Sample Interval	0.189 m
Power	2000 W	Receiver Bandwidth	2.43 kHz

Sounder Type: EK60 Version 2.2.0

TS Detection:

Min. Value	-50.0 dB	Min. Spacing	100 %
Max. Beam Comp.	6.0 dB	Min. Echolength	80 %
Max. Phase Dev.	8.0	Max. Echolength	180 %

Environment:

Absorption Coeff.	10.3 dB/km	Sound Velocity	1479 m/s

Beam Model results:

Transducer Gain =	26.92 dB	SaCorrection =	-0.59 dB
Athw. Beam Angle =	6.83 deg	Along. Beam Angle =	6.91 deg
Athw. Offset Angle =	0.11 deg	Along. Offset Angle=	-0.07 deg

Data deviation from beam model:

RMS = 0.14 dB
Max = 0.36 dB No. = 11 Athw. = 2.3 deg Along = 3.3 deg
Min = -0.80 dB No. = 281 Athw. = 4.2 deg Along = -0.2 deg

Data deviation from polynomial model:

RMS = 0.11 dB
Max = 0.20 dB No. = 214 Athw. = 3.4 deg Along = -1.8deg
Min = -0.71 dB No. = 281 Athw. = 4.2 deg Along = -0.2 deg

Remarks :

Wind Speed: 12 kn. **Wind Direction:** 090 deg
RawdataFile: G:\ER60\Kalibrering\2009\38khz-1ms SK
Filename: G:\ER60\Kalibrering\2009\38khz 1ms-Sk

Table C.3. The representative example from the first period of survey 1 of the weather data used in this study.

Date	Time	Logg	Lattitude	Longitude	Depth	Heading	Velocity	Water temp	Wind	Wind dir	Weather	Seastate
18.10.2008	06:15:13	3925,995	7051.5619 N	01830.9314 E	190,74	281	11,06	7,8	5,49	45,35	4	3
18.10.2008	06:15:38	3926,182	7051.5999 N	01830.3704 E	189,13	281	10,99	7,8	5,75	48,43	4	3
18.10.2008	06:16:03	3926,367	7051.6373 N	01829.8305 E	188,07	281	10,96	7,8	6,77	36,39	4	3
18.10.2008	06:17:55	3926,548	7051.6738 N	01829.2852 E	186,5	281	11,01	7,8	5,7	29,76	4	3
18.10.2008	06:18:20	3926,732	7051.7108 N	01828.7306 E	184,6	281	11	7,8	5,53	29,53	4	3
18.10.2008	06:20:14	3926,923	7051.7462 N	01828.1740 E	182,15	281	11,08	7,9	6,12	31,29	4	3
18.10.2008	06:20:39	3927,107	7051.7828 N	01827.6346 E	179,56	281	11,01	7,9	5,86	49,66	4	3
18.10.2008	06:21:04	3927,298	7051.8209 N	01827.0615 E	179,17	281	11,17	7,7	5,85	31,22	4	3
18.10.2008	06:22:59	3927,485	7051.8593 N	01826.5056 E	179,21	281	11,23	7,9	6,38	42,03	4	3
18.10.2008	06:23:24	3927,675	7051.8954 N	01825.9419 E	178,18	281	11,09	7,8	7,53	35,08	4	3
18.10.2008	06:25:17	3927,865	7051.9347 N	01825.3709 E	176,47	281	11,21	7,8	6,38	38,14	4	3
18.10.2008	06:25:43	3928,063	7051.9751 N	01824.8020 E	176,05	282	11,3	7,9	6,95	50,85	4	3
18.10.2008	06:26:08	3928,248	7052.0154 N	01824.2385 E	174,67	282	11,3	7,9	7,94	27,86	4	3
18.10.2008	06:28:01	3928,44	7052.0565 N	01823.6824 E	174,26	283	11,17	8	5,61	29,39	4	3
18.10.2008	06:28:26	3928,628	7052.0984 N	01823.1244 E	174,37	282	11,21	7,9	5,72	40,99	4	3
18.10.2008	06:30:19	3928,815	7052.1397 N	01822.5768 E	172,58	283	11,29	7,8	5,95	32,49	4	3
18.10.2008	06:30:44	3929,005	7052.1840 N	01822.0035 E	170,5	283	11,23	7,9	5,58	29,77	4	3
18.10.2008	06:31:09	3929,195	7052.2266 N	01821.4403 E	169,08	282	11,24	7,8	6,78	32,5	4	3
18.10.2008	06:33:03	3929,385	7052.2682 N	01820.8874 E	170,13	283	11,13	7,9	6,81	43,81	4	3
18.10.2008	06:33:28	3929,573	7052.3121 N	01820.3260 E	171,66	283	11,2	8	5,77	42,19	4	3
18.10.2008	06:35:22	3929,765	7052.3551 N	01819.7740 E	175,6	283	11,27	8	6,86	28,52	4	3
18.10.2008	06:35:47	3929,958	7052.3988 N	01819.2047 E	170	282	11,34	7,9	6,5	39,65	4	3
18.10.2008	06:36:13	3930,148	7052.4406 N	01818.6243 E	172,75	282	11,37	7,9	6,37	38,53	4	3
18.10.2008	06:38:07	3930,338	7052.4802 N	01818.0710 E	173,87	282	11,34	7,9	5,51	41,73	4	3
18.10.2008	06:38:32	3930,528	7052.5214 N	01817.5064 E	173,46	282	11,29	7,9	5,47	44,96	4	3
18.10.2008	06:40:24	3930,723	7052.5633 N	01816.9264 E	174,09	282	11,32	7,9	5,96	45,9	4	3
18.10.2008	06:40:49	3930,913	7052.6072 N	01816.3674 E	173,59	282	11,27	7,9	5,28	37,87	4	3
18.10.2008	06:41:14	3931,098	7052.6479 N	01815.8124 E	173,03	282	11,2	7,9	5,99	30,18	4	3
18.10.2008	06:43:09	3931,285	7052.6871 N	01815.2531 E	171,33	281	11,36	7,9	5,45	26,87	4	3
18.10.2008	06:43:35	3931,475	7052.7257 N	01814.6878 E	171,25	282	11,48	7,9	4,99	28,19	4	3
18.10.2008	06:45:26	3931,673	7052.7670 N	01814.1141 E	172,25	282	11,34	8	4,78	37,96	4	3
18.10.2008	06:45:51	3931,865	7052.8079 N	01813.5377 E	173,08	282	11,41	7,9	6,75	30,76	4	3
18.10.2008	06:46:17	3932,055	7052.8486 N	01812.9718 E	174,52	282	11,27	7,9	5,69	39,72	4	3
18.10.2008	06:48:11	3932,248	7052.8893 N	01812.4106 E	174,51	281	11,3	7,8	6,32	38,36	4	3
18.10.2008	06:48:36	3932,438	7052.9298 N	01811.8238 E	176,77	282	11,4	7,8	4,89	48,91	4	3
18.10.2008	06:50:29	3932,632	7052.9692 N	01811.2552 E	178,29	282	11,41	7,8	7,85	45,58	4	3
18.10.2008	06:50:55	3932,825	7053.0105 N	01810.6826 E	177,12	282	11,31	7,8	7,39	36,71	4	3
18.10.2008	06:51:20	3933,018	7053.0522 N	01810.1066 E	178,54	282	11,43	7,8	6,38	34,98	4	3
18.10.2008	06:53:15	3933,208	7053.0907 N	01809.5361 E	176,53	281	11,53	7,7	5,46	37,12	4	3
18.10.2008	06:53:40	3933,405	7053.1326 N	01808.9559 E	178,52	282	11,44	7,7	5,34	38,19	4	3
18.10.2008	06:55:34	3933,605	7053.1729 N	01808.3625 E	174,51	281	11,58	7,8	5,58	27,03	4	3
18.10.2008	06:55:59	3933,798	7053.2146 N	01807.8001 E	174,66	282	11,51	7,7	6,18	32,48	4	3
18.10.2008	06:56:24	3933,995	7053.2564 N	01807.2088 E	175,86	282	11,55	7,7	6,45	39,12	4	3
18.10.2008	06:58:16	3934,185	7053.2960 N	01806.6501 E	174,25	282	11,45	7,8	6,36	39,55	4	3
18.10.2008	06:58:41	3934,375	7053.3385 N	01806.0758 E	180,43	282	11,44	7,8	5,48	35,93	4	3
18.10.2008	07:00:35	3934,573	7053.3810 N	01805.5099 E	183,14	283	11,44	7,7	5,47	47,4	4	3
18.10.2008	07:01:00	3934,765	7053.4259 N	01804.9366 E	184,01	283	11,45	7,8	5,85	47,27	4	3

Date	Time	Logg	Lattitude	Longitude	Depth	Heading	Velocity	Water temp	Wind	Wind dir	Weather	Seastate
18.10.2008	07:01:24	3934,953	7053.4679 N	01804.3811 E	184,55	282	11,37	7,8	6,96	49,52	4	3
18.10.2008	07:03:19	3935,148	7053.5148 N	01803.7952 E	186,23	283	11,5	7,8	6,96	52,43	4	3
18.10.2008	07:03:44	3935,348	7053.5580 N	01803.2163 E	187,61	283	11,53	7,8	5,6	35,15	4	3
18.10.2008	07:05:38	3935,543	7053.6026 N	01802.6384 E	187,91	283	11,47	7,8	5,59	45,33	4	3
18.10.2008	07:06:03	3935,738	7053.6454 N	01802.0500 E	188,86	282	11,48	7,8	6,28	33,19	4	3
18.10.2008	07:06:28	3935,938	7053.6896 N	01801.4713 E	189,61	283	11,51	7,9	6,29	47,68	4	3
18.10.2008	07:08:22	3936,128	7053.7358 N	01800.8993 E	190,47	284	11,64	7,8	5,47	40,45	4	3
18.10.2008	07:08:46	3936,323	7053.7822 N	01800.3405 E	190,32	284	11,6	7,9	6,54	53,14	4	3
18.10.2008	07:10:40	3936,518	7053.8292 N	01759.7531 E	191,95	284	11,69	7,8	7,27	50,62	4	3
18.10.2008	07:11:05	3936,718	7053.8757 N	01759.1721 E	193,59	283	11,75	7,8	5,89	59,24	4	3
18.10.2008	07:11:30	3936,918	7053.9244 N	01758.5707 E	191,87	283	11,83	7,8	6,38	38,26	4	3
18.10.2008	07:13:23	3937,118	7053.9707 N	01757.9877 E	192,68	283	11,74	7,9	6,05	45,33	4	3
18.10.2008	07:13:48	3937,318	7054.0164 N	01757.4007 E	192,21	283	11,64	7,8	6,42	44,5	4	3
18.10.2008	07:15:42	3937,515	7054.0640 N	01756.8138 E	193,2	283	11,71	7,7	5,62	47,86	4	3
18.10.2008	07:16:07	3937,708	7054.1103 N	01756.2466 E	193,84	283	11,74	7,7	6,5	52,58	4	3
18.10.2008	07:16:32	3937,908	7054.1608 N	01755.6494 E	188,94	284	11,73	7,8	6,27	55,31	4	3
18.10.2008	07:18:28	3938,113	7054.2083 N	01755.0482 E	189,46	283	11,79	7,8	6,82	50,86	4	3
18.10.2008	07:18:53	3938,315	7054.2554 N	01754.4494 E	191,3	283	11,88	7,8	5,59	56,97	4	3
18.10.2008	07:20:44	3938,513	7054.3001 N	01753.8844 E	191,75	283	11,82	7,8	5,29	51,11	4	3
18.10.2008	07:21:09	3938,705	7054.3475 N	01753.2914 E	200,55	283	11,62	7,8	5,4	43,84	4	3
18.10.2008	07:21:35	3938,905	7054.3945 N	01752.7085 E	204,32	284	11,63	7,8	5,31	54,16	4	3
18.10.2008	07:23:28	3939,098	7054.4408 N	01752.1392 E	205,34	283	11,55	7,9	6,28	48,12	4	3
18.10.2008	07:23:53	3939,288	7054.4875 N	01751.5771 E	207,23	284	11,43	7,8	6,13	60,96	4	3
18.10.2008	07:25:47	3939,475	7054.5318 N	01751.0340 E	211,25	284	11,41	7,9	5,67	56,53	4	3
18.10.2008	07:26:12	3939,668	7054.5808 N	01750.4627 E	211,57	284	11,47	7,9	6,15	56,5	4	3
18.10.2008	07:26:39	3939,862	7054.6463 N	01749.9011 E	209	291	11,15	7,9	6,23	32,77	4	3
18.10.2008	07:28:30	3940,052	7054.7338 N	01749.3836 E	213,85	296	11,29	7,9	7,03	41,27	4	3
18.10.2008	07:28:56	3940,245	7054.8187 N	01748.8563 E	215,24	296	11,34	7,9	6,64	52	4	3
18.10.2008	07:30:50	3940,443	7054.9034 N	01748.3278 E	217,47	295	11,4	7,9	6,67	57,49	4	3
18.10.2008	07:31:16	3940,635	7054.9883 N	01747.7952 E	216,62	296	11,49	7,9	6,2	38,44	4	3
18.10.2008	07:31:41	3940,833	7055.0697 N	01747.2476 E	219,73	294	11,66	7,9	4,66	50,56	4	3
18.10.2008	07:33:35	3941,023	7055.1473 N	01746.7247 E	220,87	294	11,56	7,9	5,49	43,98	4	3
18.10.2008	07:34:00	3941,215	7055.2275 N	01746.1822 E	224,56	294	11,48	7,9	6,67	49,14	4	3
18.10.2008	07:35:52	3941,408	7055.3102 N	01745.6571 E	225,49	295	11,51	7,9	6,8	41,09	4	3
18.10.2008	07:36:17	3941,603	7055.3906 N	01745.1276 E	228,01	294	11,55	8	5,8	50,16	4	3
18.10.2008	07:36:42	3941,795	7055.4722 N	01744.5839 E	231,1	294	11,57	8	4,77	43,89	4	3
18.10.2008	07:38:35	3941,985	7055.5514 N	01744.0587 E	232,87	294	11,59	8,1	5,22	53,64	4	3
18.10.2008	07:39:00	3942,178	7055.6357 N	01743.5239 E	232,52	295	11,68	8	6,27	42,35	4	3
18.10.2008	07:40:54	3942,375	7055.7196 N	01742.9848 E	233,79	295	11,76	7,9	6,56	52,36	4	3
18.10.2008	07:41:20	3942,575	7055.8069 N	01742.4395 E	234	295	11,74	8	6,42	49,65	4	3
18.10.2008	07:41:45	3942,775	7055.8952 N	01741.8952 E	235,91	296	11,76	8,1	7,63	40,92	4	3
18.10.2008	07:43:39	3942,949	7055.9634 N	01741.4587 E	234,89	294	9,51	8	5,68	62,62	4	3
18.10.2008	07:44:04	3943,073	7056.0136 N	01741.1121 E	236,27	293	7,32	8	7,81	62,03	4	3
18.10.2008	07:45:55	3943,18	7056.0523 N	01740.8197 E	236,27	292	6,26	8	6,42	33,04	4	3
18.10.2008	07:46:20	3943,278	7056.0873 N	01740.5527 E	237,98	291	5,61	7,9	8,08	37,39	4	3
18.10.2008	07:46:46	3943,366	7056.1174 N	01740.3127 E	237,36	290	4,87	8	6,78	43	4	3
18.10.2008	07:48:40	3943,437	7056.1403 N	01740.1133 E	238,69	287	4,08	8	4,99	59,66	4	3
18.10.2008	07:49:05	3943,495	7056.1568 N	01739.9428 E	237,05	286	3,38	8	5,17	57,57	4	3
18.10.2008	07:51:00	3943,548	7056.1688 N	01739.7863 E	238,56	282	3,17	8,1	5,69	27,02	4	3
18.10.2008	07:51:25	3943,624	7056.2001 N	01739.5272 E	235,77	292	5,73	8,1	6,89	33	4	3

Table C.4. Main linear regression results of the backscattering strength for the hull and keel systems. Included are the Arithmetic Mean (AM), Standard Error of Arithmetic Mean (SEAM), 95 % Lower and Upper Confidence Limits (LCL and UCL), Standard deviation (SD), and the Coefficient of Variance (CV).

Measure	Survey 1		Survey 2		Survey 3	
	Hull	Keel	Hull	Keel	Hull	Keel
No. of cases	5645	5645	1219	1219	433	433
Minimum	60.0	51.4	60.0	59.4	60.2	61.6
Maximum	78.3	77.2	71.3	72.8	74.6	76.8
Range	18.3	25.8	11.3	13. 5	14.4	15.2
Sum	379596	375807	78584	79708	28583	29861
Median	66.7	65.7	64.6	65.4	65.8	68.6
AM	67.3	66.6	64.5	65.4	66.0	68.9
SEAM	0.05	0.04	0.07	0.07	0.15	0.15
95 % LCL	67.2	66.5	64.3	65.2	65.7	68.7
95 % UCL	67.3	66.7	64.6	65.5	66.3	69.3
SD	3.73	3.31	2.49	2.64	3.16	3.05
Variance	13.9	10.9	6.23	6.95	10.0	9.30
CV	0.06	0.05	0.04	0.04	0.05	0.04

Table C.5. Main regression results of the backscattering strength grouped according to wind speeds between 0 and 10 m/s for Survey 1 and 2.

Measure	Survey 1: 0 - 5 m/s		Survey 1: 5 - 10 m/s		Survey 2: 5 - 10 m/s	
	Hull	Keel	Hull	Keel	Hull	Keel
No. of cases	953	953	2437	2437	21	21
Minimum	57.4	57.6	56.6	58.6	60.6	61.4
Maximum	76.5	76.0	78.3	77.2	70.2	67.8
Range	19.1	18.4	21.7	18.6	9.58	6.46
Sum	64115	63245	165207	163192	1346	1348
Median	66.9	65.5	67.2	66.1	63.9	63.9
AM	67.3	66.4	67.8	67.0	64.1	64.2
SEAM	0.10	0.09	0.07	0.07	0.57	0.45
95 % LCL	67.1	66.2	67.7	66.8	63.9	63.2
95 % UCL	67.5	66.5	67.9	67.1	65.3	65.1
SD	3.11	2.71	3.30	3.3	2.59	2.07
Variance	9.69	7.36	10.9	10.9	6.72	4.28
CV	0.05	0.04	0.05	0.05	0.04	0.03

Table C.6. Main regression results of the backscattering strength grouped according to wind speeds between 10 and 15 m/s.

Measure	Survey 1		Survey 2		Survey 3	
	Hull	**Keel**	**Hull**	**Keel**	**Hull**	**Keel**
No. of cases	1146	1146	605	605	104	104
Minimum	55.4	60.2	57.8	60.4	56.13	61.2
Maximum	70.5	75.1	71.3	72.8	74.2	76.8
Range	15.1	14.9	13.5	12.5	18.1	15.6
Sum	73571	74144	39055	39561	6849	7098
Median	64.4	64.2	64.8	65.6	66.1	68.2
AM	64.2	64.8	64.6	65.4	65.7	68.3
SEAM	0.07	0.07	0.11	0.12	0.24	0.22
95 % LCL	64.1	64.6	64.3	65.16	65.4	67.8
95 % UCL	64.3	64.8	64.8	65.6	66.3	68.7
SD	2.36	2.40	2.66	2.83	2.41	2.21
Variance	5.57	5.76	7.08	8.03	5.81	4.87
CV	0.04	0.04	0.04	0.04	0.04	0.03

Table C.7. Main regression results of the backscattering strength grouped according to wind speeds between 15 and 20 m/s.

Measure	Survey 1		Survey 2		Survey 3	
	Hull	**Keel**	**Hull**	**Keel**	**Hull**	**Keel**
No. of cases	441	441	514	514	284	284
Minimum	54.0	58.3	56.8	59.1	47.9	55.2
Maximum	66.2	68.2	71.2	72.1	74.6	76.8
Range	12.2	9.9	14.4	13.0	26.7	21.7
Sum	26786	27427	32955	33520	18604	19540
Median	60.8	62.2	64.3	65.2	65.9	68.9
AM	60.7	62.2	64.2	65.2	65.5	68.8
SEAM	0.08	0.06	0.12	0.12	0.27	0.24
95 % LCL	60.6	62.1	63.9	65.0	64.9	68.3
95 % UCL	60.9	62.3	64.4	65.5	66.1	69.3
SD	1.60	1.18	2.68	2.66	4.64	4.12
Variance	2.57	139	7.21	7.09	21.5	16.86
CV	0.03	0.02	0.04	0.04	0.07	0.06

Table C.8. Main regression results of the backscattering strength grouped according wind speeds between 20 and 25 m/s.

Measure	Survey 1		Survey 2		Survey 3	
	Hull	**Keel**	**Hull**	**Keel**	**Hull**	**Keel**
No. of cases	37	37	9	9	28	28
Minimum	57.8	59.5	58.5	60.8	53.2	58.5
Maximum	62.5	63.6	66.2	66.9	71.0	73.7
Range	4.70	4.08	7.71	6.02	17.9	15.2
Sum	2218	2279	562	575	1751	1846
Median	60.0	61.6	63.2	64.6	63.7	67.1
AM	59.9	61.6	62.5	63.9	62.5	65.9
SEAM	0.19	0.17	0.78	0.67	0.92	0.83
95 % LCL	59.6	61.3	60.7	62.4	60.7	64.2
95 % UCL	60.4	61.9	64.3	65.4	64.4	67.6
SD	1.18	1.01	2.35	2.01	4.85	4.39
Variance	1.39	1.02	5.51	4.04	23.5	19.251
CV	0.02	0.02	0.04	0.04	0.08	0.07

Table C.9. The description and categorization of Beaufort Sea state scale

Force (Beaufort)	Wind speed		Wave height (m)	Description	Sea conditions
	Knots	$m \cdot s^{-1}$			
0	0 - 1	0 – 0.2	0	Calm	Sea like a mirror.
1	1 - 3	0.3 – 1.5	0 - 0.2	Light Air	Ripples with the appearance of scales are formed, but without foam crests.
2	4 - 6	1.6 – 3.3	0.2 - 0.5	Light Breeze	Small wavelets, crests glassy, no breaking.
3	7 - 10	3.4 – 5.4	0.5 - 1	Gentle Breeze	Large wavelets, crests begin to break, scattered whitecaps.
4	11 - 16	5.5 – 7.9	1 - 2	Moderate Breeze	Small waves 1-4 ft. becoming longer, numerous whitecaps.
5	17 - 21	8.0 – 10.7	2 - 3	Fresh Breeze	Moderate waves 4-8 ft taking longer form, many whitecaps, some spray.
6	22 - 27	10.8 – 13.8	3 - 4	Strong Breeze	Larger waves 8-13 ft, whitecaps common, more spray.
7	28 - 33	13.9 – 17.1	4 - 5.5	Near Gale	Sea heaps up, waves 13-20 ft, white foam streaks off breakers.
8	34 - 40	17.2 – 20.7	5.5 - 7.5	Gale	Moderately high (13-20 ft) waves of greater length, edges of crests begin to break into spindrift, foam blown in streaks.
9	41 - 47	20.8 – 24.4	7 - 10	Strong Gale	High waves (20 ft), sea begins to roll, dense streaks of foam, spray may reduce visibility.
10	48 - 55	24.5 – 28.4	9 - 12.5	Storm	Very high waves (20-30 ft) with overhanging crests, sea white with densely blown foam, heavy rolling, and lowered visibility.
11	56 - 63	28.5 – 32.6	11.5 - 16	Violent Storm	Exceptionally high (30-45 ft) waves, foam patches cover sea, visibility more reduced.
12	64 - 72	32.7 – 36.9	≥ 14	Hurricane	Air filled with foam, waves over 45 ft, sea completely white with driving spray, visibility greatly reduces.

Table adopted from: City of Stuttgart, Office for Environmental Protection, Section of Urban Climatology

Brief description of the Beaufort scale:

"Beaufort wind scale" or "Beaufort wind force scale" was created by British Admiral Sir Francis Beaufort in 1805. The individual wind stage is called the Beaufort number or level. At that time, ships included fishing boats and warships, where canvas sails were deployed to ride the waves using wind power. Anemometer was not yet available. Wind and waves are inter-related. The stronger the winds, the higher will be the waves. The wind strength has direct influence on the state of the sea. Beaufort developed the scale based on experience and observations on board a warship (called "44 gun man-of-war"). The scale is in form of a table (above) grading the wind strength from force 0 to force 12 (totally 13 categories).

The Beaufort wind scale was originally drawn up to relate the number of canvas sails required to each category of the wind forces. The higher the wind force, the less canvas sails would be required. The Beaufort wind scale was revised several times. In 1906, the description was extended from sea state to land observations of objects being blown by winds. In 1926, a set of equivalent wind speeds corresponding to the Beaufort wind force scale was adopted. In 1947, the International Meteorological Organization agreed reporting of wind velocity in knots. Beaufort's original scale was later correlated to wind speed in two different ways. The U.S. and British scale is for winds measured at a 36-ft elevation, while the international scale requires only a 20-ft elevation. The Beaufort scale is the oldest method of judging wind force. Separate scales for tornadoes and hurricanes did not come until the 1970s.

Appendix D. Statistical Formulations

Appendix D.1. Definition of the variance and the standard deviation

A variance is the measure of the dispersion of a set of values around the sample mean. It is the mean of the sum of the squares of the differences between the values and the mean of the sample. While the standard deviation is the measure of the variability or dispersion of a data set around the population mean. The standard deviation is in simple terms the square root of the variance that indicates the precision of the investigation. The standard deviation has a confidence interval of 95%, compared to 68% confidence interval by the standard error. Below are the formulas used for computing the variance and standard deviation of the population and sample for the pitch and roll movements data. The sample variance and standard deviation formula have the term *n*-1 to indicate the degree of freedom of a particular sample.

Appendix D.2. Formulas

Sample variance formula:

$$S^2 = \frac{1}{n-1}\sum_{i=1}^{n}(x-\bar{x})^2 \tag{D.1}$$

Population variance formula:

$$\sigma^2 = \frac{1}{N}\sum_{i=1}^{N}(x-\mu)^2 \tag{D.2}$$

Sample standard deviation formula:

$$S = \sqrt{\frac{1}{n-1}\sum_{i=1}^{n}(x-\bar{x})^2} \tag{D.3}$$

Population standard deviation formula:

$$\sigma = \sqrt{\frac{1}{N}\sum_{i=1}^{N}(x-\mu)^2} \tag{D.4}$$